Transmission Line Modelling Techniques for Hybrid Systems

(*400kV Cables Installed Inside a Ventilated Concrete Tunnel*)

تقنيات نمذجة خط النقل للأنظمة المختلطة

(400 كيلو فولت كابلات ممدودة داخل قناة اسمنتية مزودة بنظام تهوية)

By:

Haifa Ali Mubarak Busamra

Dissertation submitted in partial fulfilment of the requirements

for the Degree of MSc Systems Engineering

Faculty of Engineering

Dissertation Supervisor

Dr. Alaa Abdul-Ameer

May - 2012

DISSERTATION RELEASE FORM

Student Name	Student ID	Programme	Date
Haifa Busamra	80155	MSc System Engineering	21 May 2012

Title:
Transmission Line Modelling Techniques for Hybrid Systems (*400kV Cables Installed Inside a Ventilated Concrete Tunnel*)

I warrant that the content of this dissertation is the direct result of my own work and that any use made in it of published or unpublished copyright material falls within the limits permitted by international copyright conventions.

I understand that one copy of my dissertation will be deposited in the University Library for permanent retention.

I hereby agree that the material mentioned above for which I am author and copyright holder may be copied and distributed by The British University in Dubai for the purposes of research, private study or education and that The British University in Dubai may recover from purchasers the costs incurred in such copying and distribution, where appropriate.

I understand that The British University in Dubai may make that copy available in digital format if appropriate.

I understand that I may apply to the University to retain the right to withhold or to restrict access to my dissertation for a period which shall not normally exceed four calendar years from the congregation at which the degree is conferred, the length of the period to be specified in the application, together which the precise reasons for making that application.

Signature

Abstract

The study in this research focuses on modelling a long, 400kV cable transmission line and the forced ventilation system employed. Emphasises is placed on exploring the most appropriate modelling techniques available to deal with transmission line systems. The projected benefits are to reduce the computational time, the errors in the mathematical derivation and achieve an accurate numerical simulation as a final result.

The first portion of this research provides an introduction to the discoveries of electromagnetism and the development of modelling techniques from inception to the current known forms of structured adopted for various engineering system applications.

The problem identified investigates the possibility of modelling the 400kV electrical cable, with its four line parameters for no line losses. The objectives set are to model the system by using two modelling methods, to verify the capability of the 400kV cable to transmit its full rated power and the effect of the ventilation system to enhance performance under loss and lossless operating conditions.

The modelling process uses the Finite Element Method and the Distributed-Lumped Modelling Method. Results from both methods are compared and the research is concluded with a final recommendation of using the Distributed-Lumped Transmission Line Modelling Method for this, and similar applications.

خلاصة البحث

تتركز الدراسة في هذا البحث على تصميم نموذج لكابلات كهربائية طويلة ذات فئة جهدية تصل إلى 400 كيلوفولت، ولنظام التهوية. الدراسة تسلط الضوء على أنسب تقنية رقمية موجودة ويمكن تطبيقها لتصميم نموذج لخطوط النقل الطويلة، بهدف تقليل الوقت اللازم لإعداد التصاميم، تقليص الأخطاء المصاحبة للإشتقاقات الحسابية، والحصول على حلول دقيقة من المحاكاة الرقمية للأنظمة المصممة.

الجزء الأول من أطروحة هذا البحث يقدم مدخلا إلى اكتشاف الكهرومغناطيسية، وتقنيات النمذجة التي تم تطويرها منذ بداياتها ووصولا إلى شكلها الحالي المتعارف عليه والمعتمدة في مختلف التطبيقات الهندسية، إذ تعد الكهرومغناطيسية أساس عمل تقنيات التصميم المطبقة في هذا البحث.

المشكلة التي تم تحديدها والتركيز عليها في هذه الدراسة هي التحقق من إمكانية نمذجة الكابلات الكهربائية ذات الفئة الجهدية 400 كيلوفولت دون تجاهل الفقد في الطاقة الكهربائية نتيجة تسرب التيار عبر المقاومات المتوالية والمتوازية لخط النقل. وقد تم وضع أهداف محددة للتحقق من حل هذه المشكلة، وذلك من خلال إعداد تصاميم نمذجة للكابل الكهربائي باستخدام أسلوبين من أساليب النمذجة، ثم التحقق من قدرة الكابل على نقل الطاقة الكلية له مع دراسة تأثير نظام التهوية المزود به لتحسين أدائه.

تم عقد مقارنة بين نتائج الأسلوبين المعتمدين في البحث، والخروج بتوصية فاعلية نمذجة خطوط النقل الطويلة باستخدام تقنية نمذجة خطوط النقل على تقنية نمذجة العناصر المتناهية.

Acknowledgements

The author would like to thank Dr. Alaa Abdul-Ameer for his continuous support and directions provided during the period of this research. It was a pleasure to work with him as one of his students.

The author would like also to extend her thanks to Professor R. Whalley for his assistance and knowledge shared with respect to his vast experience and the researches carried out in the same field.

Special thanks to Dubai Electricity and Water Authority – DEWA for providing the required data needed to model the transmission line system analysed in this research. Specifically, the engineers who assisted in data collection from Engineering and Site Supervision (Transmission) Department are acknowledged.

Dedication

To H.H. Sheikh Mohammed Bin Rashid Al Maktoum, Vice President and Prime Minister of UAE and Ruler of Dubai for his boosted support and encouragement to all UAE nationals, to enhance their skills and knowledge by continual education. This is in order to serve their community and to contribute in developing their country toward being a world class and a model followed by others.

List of Notations

C_1, C_2, C_3, C_4	:	Shunt Capacitance per unit length
C_d	:	Distributed Capacitance
C_m	:	Membrane Capacitance
d	:	Diameter
F	:	Cutting Force
$\Gamma(s)$	:	Wave Propagation Function
G_1, G_2, G_3, G_4	:	Shunt Leakage Conductance per unit length
G_m	:	Membrane Conductance
I, I_1, I_2, I_3, I_4	:	Phase Current
I_a	:	Longitudinal (axial) Current
$I_f(s)$	:	Motor Field Current
I_L	:	Terminal Load Current
$I_{Ls.s}$	:	Steady State Terminal Load Current
I_{LM}	:	The magnitude of the Terminal Load Current
I_m	:	Membrane Current
I_s	:	Supply Current
$I_a(x,t)$	:	Longitudinal (axial) Current function of distance and time
$I(x,t)$	:	Phase Current function of distance and time
K_m	:	Motor Torque Constant
l	:	Length
L_1, L_2, L_3, L_4	:	Series Inductance per unit length

L_L	:	Terminal Load Inductance
L_{ac}	:	AC Inductance
L_d	:	Distributed Inductance
σ_i	:	Input end Stress
σ_o	:	Output end Stress
R_1, R_2, R_3, R_4	:	Series Resistance per unit length
R_L	:	Terminal Load Resistance
R_d	:	Distributed Resistance
R_f	:	Motor Field Resistance
R_i	:	Intracellular (axial) Resistivity
t	:	Time
T, $T_1(s)$, $T_i(s)$	:	Motor Torque
$p_1(s)$	:	Pressure at Entrance
$q_1(s)$	:	Airflow Rate at Entrance
$q_2(s)$		Airflow Rate at Exit
Φ	:	Function
ζ	:	Characteristic Impedance
$w(s)$	:	Function
wL	:	Resistance and Inductance Reactance
V	:	Phase Voltage
V_L	:	Terminal Load Voltage
Vs	:	Supply Voltage
V(t)	:	Voltage function of time

$\upsilon_{\circ}$, υ_{i}	:	Longitudinal Velocity
ω_{i}, $\omega_{\circ}$, ω_{1}, ω_{2}	:	Angular Velocity
x	:	Distance in axial direction along the transmission line
x-y-z axes	:	x axes, y axes, and z axes directions
$\chi(s)$	:	Function
α	:	Coefficient
$\bar{\alpha}$	:	Coefficient
Y	:	Admittance Matrix
Z	:	Impedance Matrix

List of Terminologies

2-D	:	Two-Dimensional
3-D	:	Three-Dimensional
AC	:	Alternative Current
ADINA	:	A commercial software
ANN	:	Artificial Neural Networks
ASCN	:	Adaptable Symmetrical Condensed Node
CAD	:	Computational Aided Design
CEM	:	Computational tools for Electromagnetic
C Language	:	A software Programming Language
CV	:	Continuous Vulcanization
DC	:	Direct Current
DD-TLM	:	Domain Decomposition Transmission Line Modelling
$^{\circ}$C	:	Degree Celsius
DLPM	:	Distributed Lumped Parameter Modelling
DLMPT	:	Distributed Lumped Parameter Modelling Technique
DSCT	:	Discrete Space Continuous Time
ECT	:	Electric Capacitance Tomography
EHV	:	Extremely High Voltage
EM	:	Electromagnetic
EMTP	:	Electromagnetic Transients Program
FDTD	:	Finite Difference Time Domain

FE	:	Finite Element
FE-TLM	:	Finite Element – Transmission Line Modelling
FEM	:	Finite Element Method
FORTRAN	:	A software Programming Language
GIL	:	Gas Insulated Line
HDPE	:	High Density Poly Ethylene
HV	:	High Voltage
IEC	:	International Electro-technical Commission
KCC	:	Kimberley Communications Consultants
LHS	:	Left Hand Side
MOM	:	Method of Moments
ODE	:	Ordinary Differential Equation
OHL	:	Over Head Lines
PDE	:	Partial Differential Equation
RC	:	Resistance and Conductance network
RHS	:	Right Hand Side
RLC	:	Resistance Inductance and Capacitance network
SC	:	Simi Conductor
SCN	:	Symmetrical Condensed Node
SPICE	:	A software Simulation Program
TLM	:	Transmission Line Modelling or Transmission Line Matrix
TMM	:	Transfer Matrix Method
UG/C	:	Underground/Cable

XLPE	:	Cross-Linked Polyethylene

List of Figures

Contents

Chapter-I

Introduction

1.1. Research Background

The Transmission Line Modelling – TLM technique is a computational tool used to model many significant applications. It was initially introduced to tackle and study, problems related to electromagnetic wave propagation application (Pomeroy, 1991). It has been also extensively used to evaluate the weakness of aircraft when subjected to lightning (Christopoulos, et.al 1988).

Historically, the detection of the electromagnetic waves was classified as a supreme accomplishment of mankind together with the discovery of electricity. This, happened in nineteen hundreds when the, envisaged possibility of electromagnetic travelled waves were detected (Giancoli, 1988).

For example, one of the famous recognized scientists named 'Christian Huygens' presented in 1690 a newly proposal demonstrating light wave propagation. His principle basically stated that each wave can be treated as a source of new waves. Accordingly, one wave can produce a number of spherical waves when it is advancing (Johns, 1974) and (Hansen and Kaiser, 2011).

The interest in this issue is that Huygens did not know that his principle would be used three hundred years later as a base by Johns and Beurle to develop

Transmission Line Modelling techniques in order to solve electromagnetic problems, numerically.

Going back to the original point, the ancient relationship between electricity and magnetism was well known; perhaps from the time of confirming that light is an electromagnetic wave. Yet, the understanding of the nature of this was the main concern of the scientists and researchers at that time. This concern raised their curiosity to perform continuous researches and studies to form a relationship between electricity and magnetism, particularly when demonstrating electrical phenomena through lightening shrikes (Christopoulos, 2003).

Benjamin Franklin (1706-1790), Luigi Galvani (1737-1798), Alessandro Volta (1745-1827), Andre-Marie Ampere (1775-1836), Hans Christian Oersted (1777-1851), Georg Simon Ohm (1787-1854), Michael Faraday (1791-1867) and Joseph Henry (1797-1878) are some of the famous scientists and physicists who dedicated their research in eighteenth and nineteenth centuries to achieve an appropriate explanation and understanding of electromagnetic phenomena. However, despite their accomplishments, which added to the world's knowledge of electricity and magnetism, and despite their enormous attempts to establish a foundation for electromagnetic phenomena, the first valuable and effective addition in this field was made by James Clerk Maxwell in 1860 (Giancoli, 1988).

James Clerk Maxwell (1831-1879) combined the entire electricity and magnetism phenomena within a single outstanding principal. He formed all the related rules of

electricity and magnetism and the relation between them in four main differential equations known as "Maxwell Equations" (Giancoli, 1988).

Experimentally, the availability of electromagnetic waves was later verified and proved by Heinrich Hertz (1857-1894) in 1887 (Giancoli, 1988).

The discovery of electromagnetic waves and the formation of all related rules of electricity and magnetism opened the doors toward transmitting various types of data through free space.

Additionally, it inspired innovations, which rapidly started to introduce a variety of inventions that serve the life style of mankind. For instant, one of the main development areas where the electromagnetic wave phenomena was used as a basis was in modelling antenna, microwaves, and transmission lines.

The next section will briefly describe the principles involved in modelling electromagnetic waves.

1.1.1. Electromagnetic Modelling Principles

Electromagnetic wave modelling was originally, based on electrical circuit elements (Chistopoulos, 1991) and it was simply categorized as a one dimensional field problem (Chistopoulos, 1991).

This was based on the well-known relationship between voltage and current and electromagnetic fields travelling in transmission lines (Gothard and German, 1997).

By utilizing this similarity, it was easy to describe wave propagations in space by means of voltage and current pulse propagation in a grid consisting of transmission line segments (Chistopoulos, 1993) and (Johns, 1971).

The advantages achieved while modelling electromagnetic applications using electrical circuit models is being a simple way to assess the errors in most of cases (Chistopoulos, 1991).

Further, in view of the fact that the electrical circuit model, with passive circuit elements, are inherently stable. As such, there was no necessity to study stability in these applications (Chistopoulos, 1991).

On the contrary, the main disadvantage faced while modelling electromagnetic applications while using the electrical circuit models, was the limitation of the calculation tools needed to solve these models. This gave another trend of development pertaining TLM techniques towards newly aided computational tools introduced to assist in overcoming these obstacles.

1.1.2. Transmission Line Modelling and Computational Tools

The complexity of studying and modelling electromagnetic problems required computational tools such as digital computers and supportive software. However, these kinds of tools cannot be considered as superseding or a relieving method from understanding the mathematical formulations and conceptual idea of electromagnetic which from the core knowledge for the design engineer (Christopoulos, 2003).

Generally, these computational tools for electromagnetic problems – CEM are defined as computational algorithms which are able to solve Maxwell's equations depending on selecting the most suitable initial and boundary conditions.

Such famous computational tools for solving electromagnetic problems are but not limited to Finite Element Method (FEM), Finite Difference Time-Domain (FDTD), Method of Moments (MOM), and Transmission Line Modelling (TLM) (Christopoulos, 2003).

It is important to mention here before exploring some of these followed methods, which are of research interest here that the drawbacks in these methods do not indicate weakness. Each method has its main suitability and applicability of usage based on the application to be modelled. In some cases; one method is complemented the other method rather than competing with each other. This is at the end decided by the researcher, and the method to be used, based on the chosen application.

1.1.2.1. Finite Element Method - FEM

The concept of Finite Element Method (FEM), in the case of using it as a method to model a long transmission line, is based on dividing the line into n number of sections. Each section has its own properties and is treated as a lumped.

Further, these divided sections or finite elements can be connected in series or in parallel in order to provide the overall model of the system.

By adopting the finite element approach, a simple, rational function models is extracted, which can be easily analysed either by using well tried numerical techniques or any commercially available software.

There are unavoidable weaknesses with this approach. Some of them are, for example, the non availability of a guideline addressing the number of elements that need to be employed for appropriate design. As the numbers of sections increases, the mathematical complexity also increases leading to long computation time and large memory requirements for data storage. There is no guarantee of the accuracy of the results obtained.

Moreover, the concept of travelling wave propagation cannot be proven as the model does not have any dimensional information. This will obviously create difficulties in assessing the dynamics modelled transmission lines.

As an example of using FEM, Nelson (1976) used this method to analyze the dynamic phenomena of a rotor bearing system. His contribution in this regard ended by having a large number of eigenvalues, which increases as the n number of sections increases. Not only that, but also the complexity in carrying out the mathematical calculations increases (Aleyaasin and Ebrahimi).

Watton and Tadmori (1988) stated that instability of finite element technique maybe observed in the case that the time step size is not appropriately selected. Additionally, increasing node numbers may not show improvement in the comparison with the results achieved. On contrary, it would be, advisable to choose a lesser number of nodes in such cases (Watton and Tadmori, 1988).

The above statement will be further examined and proven by the author in this research when applying the finite element method.

1.1.2.2. Finite Difference Time Domain - FDTD

The Finite Difference Time-Domain (FDTD) was first formulated by Yee (Choi and Hoefer, 1986) in 1966 (Xu, Chen, and Chuang, 1997) and became one of the most famous time-domain numerical methods used in analysing electromagnetic problems (Sadiku and Obiozor, 2000) in the time domain, based on Maxwell's equations (Chen, Ney and Hoefer, 1991).

FDTD uses differencing to set the mathematical model (Johns, 1987) and from a similarity point of view, it is equivalent to SCN –TLM modelling (Chen, Ney and Hoefer, 1991).

FDTD main advantages are in being a robust, flexible, efficient and a versatile method. Further, it is easy and simple to be understood and implement it to solve Maxwell's equations in the time domain (Sadiku and Obiozor, 2000).

Moreover, this method is a preferable and extensively used for computing various application and circuit modelling problems. Some of the examples where this method is used are in modelling radiation, open region scattering, absorption or penetration, electromagnetic compatibility, electromagnetic interference, transient, diffusion, microwave, and bio-electromagnetic applications (Sadiku and Obiozor, 2000).

Nevertheless, FDTD despite its advantages has significant problems.

FDTD has slow convergence pertaining to working out a solution for resonant structures. Not only that, but it requires a huge data storage area for inhomogeneous, waveguide structures to carryout the analysis of a full wave (Sadiku and Obiozor, 2000).

Besides, the method shows its incapability to appropriately handle curved boundaries. This is owing to its low accuracy unless using an optimised mesh for, low stability, and orthogonally nature (Sadiku and Obiozor, 2000).

Finally, FDTD exhibits an increase in the computational time needed to model, for example, a thin wire (Sadiku and Obiozor, 2000).

1.1.2.3. Transmission Line Modelling - TLM

Recalling Nelson's (1976) contribution, in analyzing the dynamic phenomena of a rotor bearing system by using FEM, this was one of the reasons for developing other methods to assist in reducing the substantial numbers of eigenvalues introduced by FEM.

Another modelling way used additionally to FEM is Transmission Line Modelling – TLM or Transfer Matrix Method (Aleyaasin and Ebrahimi).

Basically, the TLM analysis technique is based on utilizing the impulse technique in order to contain all the analytical equations within a set of boundary conditions and at the same time. However, as a consequence, a huge number of simultaneous

equations are introduced. Alternatively, it is a preferable to work in the time domain as it will assure that the information at all frequencies while using infinitely narrow impulses, will be achieved. This will avoid the prolonged computational time needed from the original excitation to solve for the steady state case. Normally, after excitation, impulses are propagate outward. At the start, the boundaries will not affect the impulse propagation, but later, after a sufficient time, the reflections at the boundaries will ultimately occur. At that time, the field pattern setup will be entirely defined (Rowbotham and John, 1972). The repetition of this course of action is adequately repeated several times in order to obtain the desired precision of solution (Akhtarzad and Johns, 1974).

In short, the Transmission Line Modelling technique can be considered as a modelling method more than a numerical method. It is used to solve differential equations of the modelled system, simulate it and to examine its performance or behaviour (Sadiku and Obiozor, 2000).

It can be also said that, the Transmission Line Modelling is an electric circuit analogue technique, applied on systems comprising transmission lines, based on Maxwell's electromagnetic equations. The beauty of it is that, it can deal directly with the issues without going through the deferential equations (Rak, Gui, and Cogan, 1999).

Hence, it can be said that TLM is a simple method from a programming and adoption point of view (Mimouni, Saidane, and Feradji, 2008).

As an example, applying TLM on self heating devices enables an accurate view of the temperature distribution generated on the device. This has an advantage in giving a comprehensive view of the heat behaviour generated by the device, with an appropriate controlling and monitoring of it, at each layer (Mimouni, Saidane, and Feradji, 2008).

When comparing the TLM method with other numerical techniques, it has a significant advantage, which distinguishes. It is a method which can be applied easily to analyse a structure (Sadiku and Obiozor, 2000).

Stability is one of the added values of TLM with reference to other well-known numerical techniques. It is stable with no conditions and can be applied easily among complicated structures (Mimouni, Saidane, and Feradji, 2008).

For instant, S. Mimouni, A. Saidane and A. Feradji stated that solving analytically, heat flow equation in three dimensions for a real structure maybe extremely complicated without the aiding tools. FDTD and FEM methods are generally used in such situation. Alternatively, TLM can be effectively selected as a modelling technique to model thermal behaviour. It will also enables steady-state and transient thermal analysis related to typical microwave power devices, manufactured from various types of materials, as in, (Mimouni, Saidane and Feradji, 2008).

Further, with the TLM, the properties of electromagnetic fields along with interaction with the material media and boundaries can be incorporated. The advantage gained from this feature is that, the electromagnetic field problem will remain invariant whenever a new geometry is introduced. The general purpose

program in this situation will be established in this regard. Only the parameters of the structure need to be updated to obtain a solution (Sadiku and Obiozor, 2000). Moreover, TLM is purely a numerical solution. Therefore, it can furnish the design engineers with a conceptual model possible to be simulated precisely by using well developed, computer software (Johns, 1987).

Furthermore, it is an appropriate method for modelling inhomogeneous or nonlinear problems. Only, the time step needs to be adjusted when any variation in the material properties occurs (Sadiku and Obiozor, 2000).

On contrary, there are negative points taken on TLM technique. One of the main disadvantages is its limitation with respect of the memory storage area needed while modelling. This varies according to the complexity of the Transmission Line Modelling mesh (Sadiku and Obiozor, 2000).

In summary, it can be noted that despite its disadvantage, TLM is a famous and widely used modelling method in respect of its advantages over other numerical methods. This led to introduction of various applications on which this method was applied. Such applications on which the TLM is applied are cut off frequencies in fin lines, diffusion and propagation problems, linear and nonlinear lumped networks, transient analysis of strip-lines micro-strip lines and resonators, antenna problems, electromagnetic compatibility problems, cylindrical and spherical waves, induced currents in biological bodies exposed to EM fields etc, (Sadiku and Obiozor, 2000).

1.2. Research Problem Statement

This research is focused on investigating the possibility of modelling a 400kV electrical cable transmission line considering in terms of the four line parameters for lossless and loss conditions.

1.3. Research aims and Objectives

The main purpose of this research is to utilize the mathematical hybrid modelling technique developed by R. Whalley in 1988 for modelling a spatially dispensed system model while considering all four line, per meter length parameters of L, C, R and G.

A comparison between the Distributed Lumped Parameter Modelling technique and the Finite Element Method will be presented compare the results achieved.

The outcome of this research will cover of the following main objectives: -

1. Model mathematically a hybrid system comprising of electrical and mechanical elements using Finite Element and Distributed – Lumped Parameter techniques. Modelling a line considering no line resistance losses (R and G = 0) and with line losses (R and G ≠ 0).

2. Simulate the modelled system and validate the results for: -

2.1. the effectiveness of the ventilation system inside the tunnel and detail the effect on the cable performance.

2.2. compare the system responses achieved from Finite Element and Transmission Line Modelling techniques.

2.3. check system time domain responses considering no resistance line losses and compare these with the results of line losses.

2.4. verify the capability of 400kV cables to transmit full rated power for the cable rating capacity specified.

1.4. Research Dissertation Organization

Chapter two in general, will cover the literature review of previous work carried out pertaining to Transmission Line Modelling, and how this method was introduced and developed to the present time.

It will be demonstrated that the various system engineering applications in which Transmission Line Modelling techniques are applied. This will illustrate the different methods followed while modelling the selected system, in terms of the two modelling methods, on which this research will focus.

Chapter three will conclude the modelling methodologies applied for the selected system.

A brief introduction to the electric power system in Dubai and the description of the selected hybrid system will be presented.

Thereafter, the mathematical derivation and analysis using the Finite Element Method and the Transmission Line Modelling will be demonstrated in detail. There will be two mathematical models derived for each method; one with no line losses and the other one with line losses modelled.

Chapter four will deal with the simulation and discussions of the achieved results and the responses of the system model.

Chapter five will provide a summary of the outcome of this research and list the recommendations and conclusion from it.

Chapter-II

Literature Review

2.1. Transmission Line Modelling Background

The TLM technique is more than forty years old, but its roots date back to the 1940s (Duffy, 1995).

In the early forties, specifically in 1944, Kron along with Whinney and Ramo noticed the similarity between circuit concepts and Maxwell equations. Accordingly, they worked to model electromagnetic free space by an equivalent transmission line circuit (Gothard and German, 1997).

Conventionally, from the time of Maxwell's or Helmholtz's equations, the majority of the electromagnetic field work remains on the basis of this analytical models. These were solved mainly by solving the integral equations or differential equations subjected to specific constitutive parameters and boundary conditions. Then, the model derived was treated, analytically. At the end, it is programmed to obtain a numerical solution. Refer Figures - 2.1 and 2.2 (Hoefer, 1991).

The main problem faced while adopting this method was the limitation in computational tools uses to solve the model equations as it became increasingly complicated.

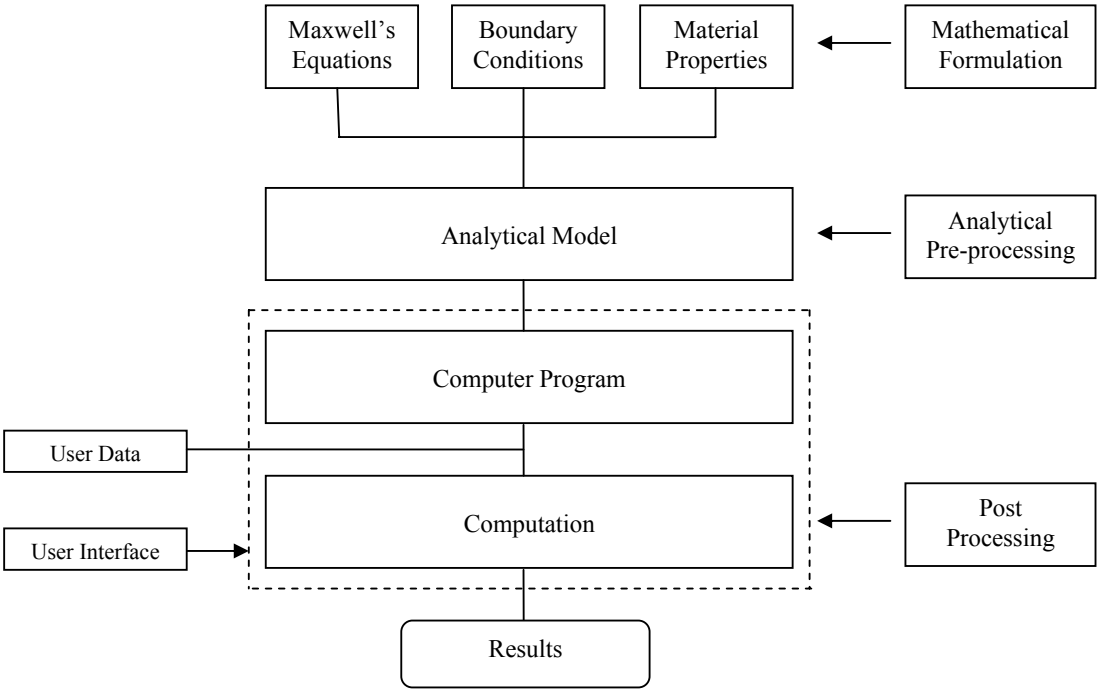

Figure-2.1: Traditional Solution of Electromagnetic Problem (Hoefer, 1991)

Accordingly, in the early 1970s researchers were describing the homogeneous and inhomogeneous transmission line models by means of numerical methods. This was in order to eliminate the inaccuracy in the system's mathematical model (Johns, 1986).

This was in fact, the trigger toward developing TLM method and refining this procedure (Johns, 1986).

However, despite all attempts in this regard, limited progress in developing TLM technique were made as there was no significant development to be mentioned with respect to this, until the seventies, specifically in 1971.

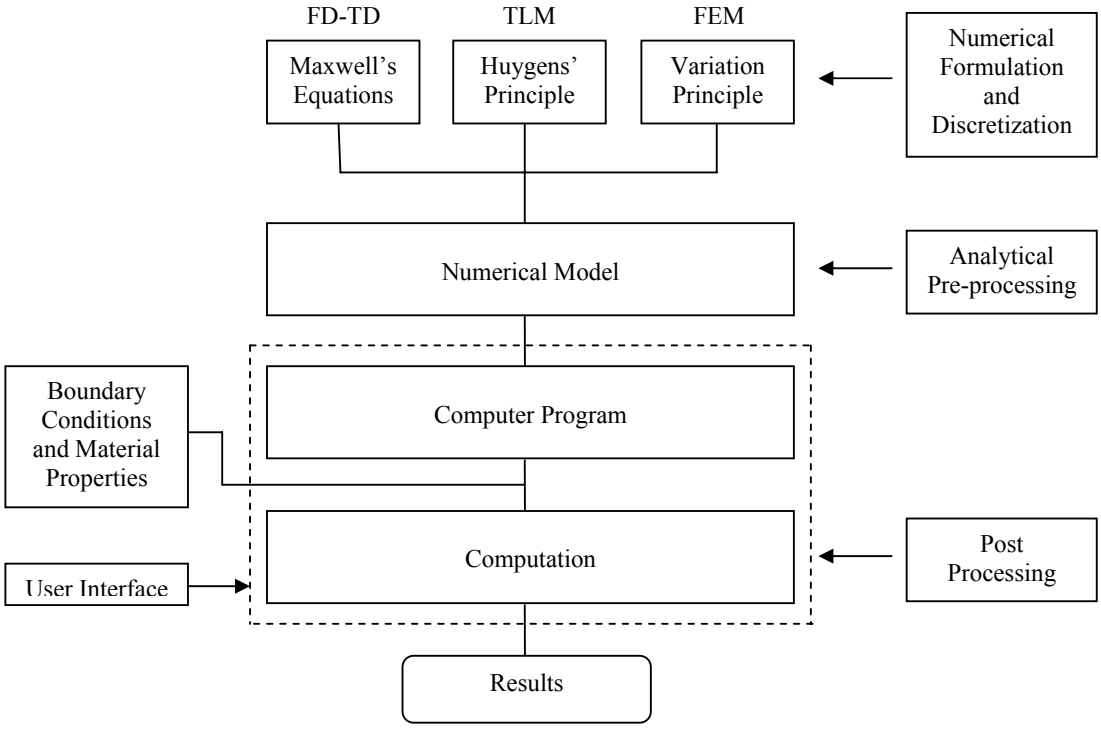

Figure-2.2: Numerical Solution of Electromagnetic Problem
(Hoefer, 1991)

2.1.1. Development of Two – Dimensional Transmission Line Modelling

In 1971, Johns and Beurle published a paper named as "Numerical solution of the 2-dimensional scattering problems using a transmission-line matrix", which made advanced the TLM history. It can be said that this paper was the first worthy paper to mention the numerical development of the TLM technique (Chistopoulos, 1993) as shown in Figure-2.3, which was based on Christian Huygens's model of wave propagation introduced in 1690 (Hoefer, 1990). In addition, it contains the concepts required to understand the TLM technique (Pomeroy, 1991).

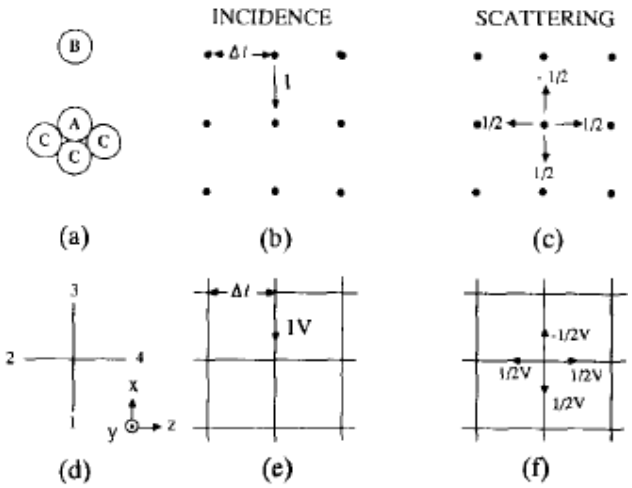

Figure-2.3: (a) and (b) Huygens's model of light propagation. (c) Its formalized version in discretized two-dimensional space. (d), (e) and (f) together with its equivalent transmission line model.
(Hoefer, 1991)

In detail, the paper offered a computer based solution, to the equivalent transmission line circuit, carried out by Kron, Whinney and Ramo in early forties (Duffy, 1995).

Both, Johns and Beurle used the electric and magnetic field philosophy described earlier to derive a new numerical technique, equivalent to the computational technique, for the purpose of solving 2-D scattering problems related to electromagnetic waves (Gothard and German, 1997) and (Johns and Beurle, 1971).

This newly developed method was named the "Transmission Line Matrix" and at present is known also as "Transmission Line Modelling – TLM" (Gothard and German, 1997).

The method is basically used, to represent the propagation space but without counting the losses in the space. This was achieved by assuming the transmission lines lossy. On the other side, the Lossy boundaries were simulated by inadequate boundary reflections on the transmission lines. FORTRAN program was used at that time as software to do the simulation for the modelled system (Akhtarzad and Johns, 1974).

As a matter of fact, the simulation of electromagnetic wave interactions by using transmission line modelling was later, comprehensively detailed, by Johns in 1988 (Johns, 1988).

Referring back to the two-dimensional – 2D TLM, the design concept of this is briefly formulated based on a basic structural model named as "shunt node". The propagation wave was represented by connecting these nodes together (Akhtarzad and Johns, 1975), which act as dispersal centres for short voltage impulses (Hoefer, 1990). Refer Figure-2.4.

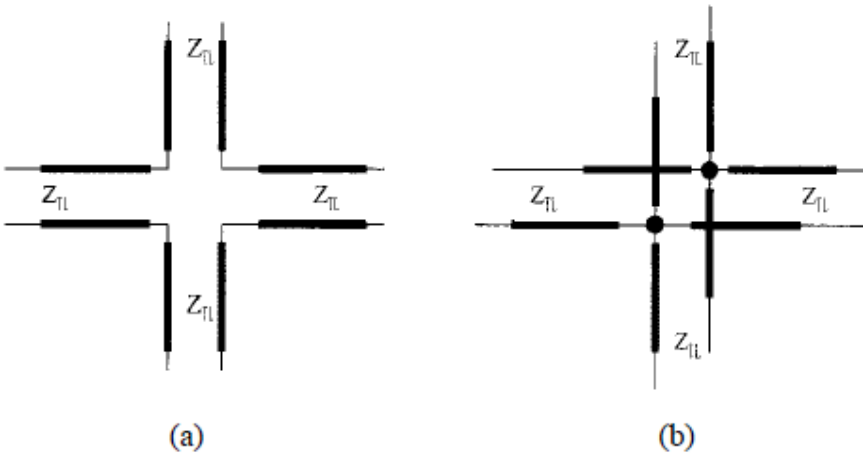

Figure-2.4: Structure of 2-D Nodes. (a) Series Node and (b) Shunt Node (Li and Liu, 2000).

The 2-D TLM was subsequently used extensively in number of papers by various researchers aiming in solving general 2-D loss free and lossy inhomogeneous field problems (Akhtarzad and Johns, 1975). P.B. Johns for example, used this method in 1972 to present a new approach for obtaining the solution of modal, cut off frequencies, in homogeneous waveguides (Johns, 1972).

Subsequently, S. Akhtarzad and P.B. Johns proved in 1973 with the support of UK Ministry of Defence that the TLM can provide a solution for 2-D space wave equation. In this regard, they divided the propagation space between boundaries and nodes, each spaced at a distance Δl within Cartesian mesh. The comparison between the numerical results was made on loss-free waveguide (Akhtarzad and Johns, 1973).

Moreover, P.B. Johns described, in the same year (1973), the usage of Transmission Line Matrix to find out the solution for inhomogeneous waveguide problems, specifically, when a stud or additional length of a line is added to the mesh (Johns, 1973).

Furthermore, Shih and Hoefer were also able to obtain the scattering characteristics of fin line by deploying the developed 2-D Transmission Line Model (Johns, 1986).

There where also other researchers such as Hoefer, who worked out in developing and enhancing the TLM method developed by Johns (Jin and Vahldieck, 1993) and presented the same in various published papers.

2.1.2. Development of Three – Dimensional Transmission Line Modelling

Upon success of 2-D TLM, the method was further expanded and developed by Johns and Akhtarzad to cover inhomogeneous media and to include the effectiveness of losses (Hoefer, 1990). Furthermore, to be able to utilize the Transmission Line Modelling in characterizing a structure over the whole frequency ranges (Johns, 1986).

Due to this necessity, three dimensional Transmission Line Modelling (3-D TLM) was presented in 1974 by using shunt nodes connected together in conjunction with series nodes (Akhtarzad and Johns, 1975). However, prior to this, Sina Akhtarzad and P.B. Johns examined the use of the series nodes establishing thereby the foundation for the development of the three-dimensional transmission line technique (Akhtarzad and Johns, 1975). Refer Figure-2.5 (Akhtarzad and Johns, 1975).

In details, Sina Akhtarzad and P.B. Johns demonstrated the possibility of representing a simple model for the three dimensional transmission lines extracted from the 2-D nodes. After that, they applied the numerical solution on the basis of magnetic and electric vector fields inside a medium. The beauty in their presented work is that it was carried out without the needs of any mathematical formulation pertaining to the problem. As an outcome, they achieved outstanding conformity in each and every case, in which comparisons are applicable (Akhtarzad and Johns, 1975).

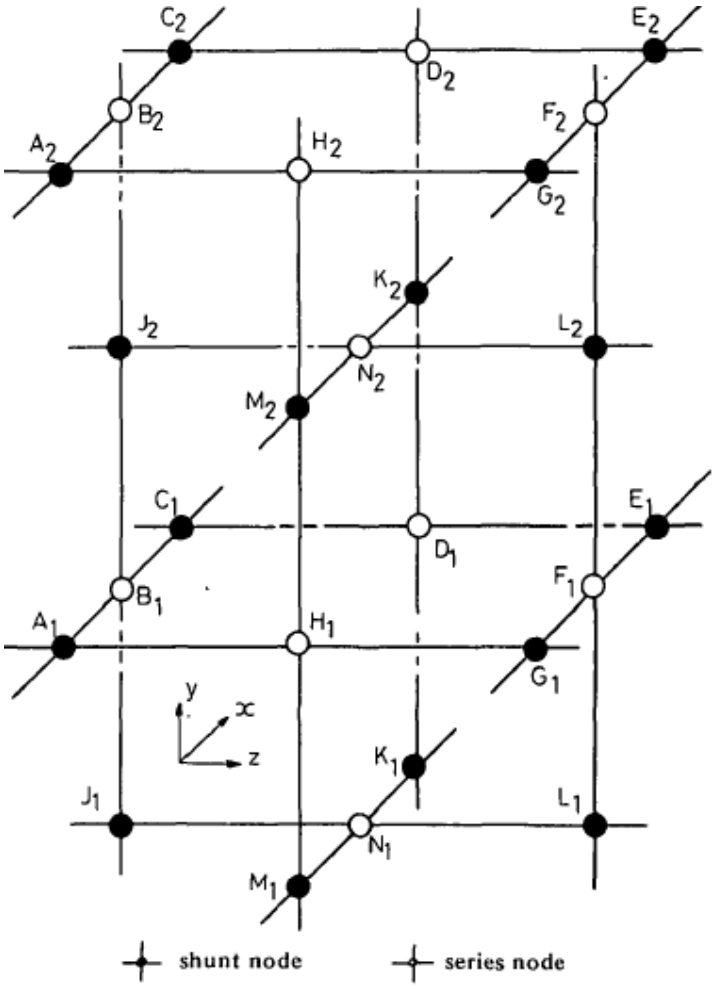

Figure-2.5: 3-D Network Model
(Akhtarzad and Johns, 1975)

Consequently, the successful establishment of 3-D TLM was initially used for modelling electromagnetic problems and the diffusion phenomenon (Christopoulos, 1991), (Hoefer, 1990), (Johns, 1986) and (Akhtarzad and Johns, 1975).

Xiang Gui, Paul W. Webb and Guang-bo Gao used it in the early 1990's in the thermal simulation and design of semiconductor devices (Gui, Webb and Gao, 1992). Also, apart of verification, Sina Akhtarzad and P.B. Johns successfully

demonstrated in 1975, the accuracy of 3-D TLM via applying it on a range of cavity lengths in order to compute the scattering curves (Akhtarzad and Johns, 1975).

Nevertheless, despite such success, there was a difficulty faced in introducing 3-D TLM. It was in the expansion of the number of nodes, which became more and more complex, based on the complexity of the application on which the method was applied (Christopoulos, 1991) and (Hoefer, 1990).

It was also found unnecessary and wastage in such cases where the frequency is low but high numbers of 3-D TLM nodes are applied in the direction of propagation (Johns, 1986).

To overcome the occurrence of this complexity in modelling, a stepped impedance approach was introduced (Johns, 1986).

2.1.3. Diakoptics Technique

Diakoptics or Johns Matrix as also named can be defined as a technique used originally in the steady state network theory by Kron (Hoefer, 1991) for the purpose of solving networks (Johns, 1986). Then, it was used in the power systems to analyze transient stability (Venkatramana and Jenkins, 1978).

As a matter of fact, this technique opened the possibilities in modelling the dispersive boundaries in the time domain. Also, it is to allow dividing large networks or electromagnetic structures and execute them numerically (Hoefer, 1991).

For more clarity, Diakoptics technique is based on breaking the network in to substructures, where each substructure is required to be solved separately. Later, the individual solved substructures are reconnected together to form the overall solution, of the modelled system (Johns, 1986).

Diakoptics is classified as one of the most significant developments in the Transmission Line Modelling. The reason behind this is that it reduces the time needed to obtain a solution, specifically when frequent analysis is required (Johns, 1986).

As stated earlier, this technique was initially used for modelling steady state networks. Then, Sina Akhtarzad and P.B. Johns worked an extending it to operate in the time domain, inline with the TLM, which is a time domain method (Johns, 1986).

In continuation to Sina Akhtarzad and P.B. John's work done earlier, Hoefer with his team developed further the Diakoptics technique. Their efforts successfully enabled them to achieve a developed form for Diakoptics technique called a Generalized Discrete Green's Function Technique. This technique was called also "Johns Matrix Technique" (Hoefer, 1991) and (Eswarappa, Costache and Hoefer, 1990).

2.1.4. Asymmetrical and Symmetrical Condensed Nodes

The Transmission Line Modelling nodes were further expanded apart of studies carriedout to model microwave circuits. The most 3-D expanded node extensively

used consists of 2-D shunt and series nodes segregated by a transmission line having half the length of the mesh. However, the expansion of the nodes was not so easy in addition to setting the boundary conditions, as it was inconvenient leading to modelling inaccuracy, specifically in the line. Obviously, the modelling inaccuracy considered was serious and needed to be enhanced to achieve better modelling results (Johns, 1986).

Accordingly, Asymmetrical Condensed Node - ACN was introduced in three dimensional transmission lines modelling for electromagnetic simulation to overcome modelling inaccuracy. However, the main drawback, which can be noticed from its name, is that it is being asymmetrical. This effect can cause movement of the boundaries and apparent positions (Johns, 1986).

To overcome this issue, “Symmetrical Condensed Node - SCN” was developed by P.B Johns in 1987 and used for modelling three dimensional TLM electromagnetic problems. SCN has an advantage of having all the three shunt and series nodes referencing to the centre of the node. Refer Figure-2.6 (Christopoulos, 1991), (Leonard and Hoefer, 1991) and (Johns, 2010).

In general, the Symmetrical Condensed Node is the main modelling tools in 3-D TLM (Trenkic, Christopoulos, and Benson, 1997) and it deals with modelling homogeneous material with a standard mesh. From a structure point of view, SCN consists of six lines used to form the models and a node (Trenkic, Christopoulos, and Benson, 1994). In addition, SCN show high accuracy, working efficiency and require uncomplicated pre-processing procedures (Johns, 1986). In short,

Symmetrical Condensed Node accumulates all the advantages possessed by the condensed node, in addition of being symmetrical (Johns, 1986).

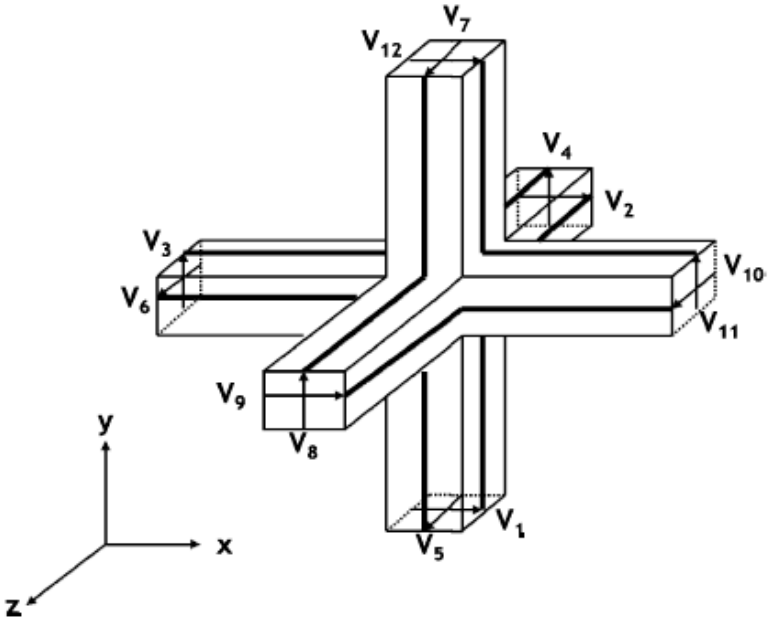

Figure-2.6: Symmetrical Condensed TLM Node SCN
(Johns, 2010)

On the other hand, with respect to inhomogeneous material with nonstandard mesh, additions of three more capacitive and inductive stubs are required to be considered. This addition in the number of stubs is for the purpose of increasing the storage area needed to store the pulses. However, it leads to setting a very small time-step in order to avoid the instability introduced, due to negative impedance created by the additional stubs (Trenkic, Christopoulos, and Benson, 1994).

Trenkic, Christopoulos and Benson in 1994 described a novel node, which can be used to simulate the transmission line modelling and overcome the above problems (Trenkic, Christopoulos, and Benson, 1994).

Inline with the three dimensional SCN transmission line modelling established by P.B Johns in 1987, Kimberley Communications Consultants - KCC worked out in 1993 in developing a Computational Aided Design Tool – CAD customized for aspects related to microwave, lightning, and electromagnetic analysis. The program developed by them used a mix of C and FORTRAN languages and divided into three levels classified as post-processing, pre-processing and electromagnetic simulation (Johns, Wlodarczyk, Mallik and Scaramuua, 1993).

Despite the 3-D TLM was well developed, there were obstacles to face. This is due to the requirement to identify the scattering matrices, which were extremely specific and complicated due to a dependency on nonlinear simultaneous equations and the requested experience need to understand the solution (Naylor and Ait-Sadi, 1992).

P. Naylor and R.Ait-Sadi introduced in 1992 a procedure, from which it is possible to eliminate solving the scattering matrices and therefore, efficient algorithm was developed (Naylor and Ait-Sadi, 1992).

In continuity, C. J. Smart and C. Christopoulos successfully combined in 1998 the transmission line modelling method with the nonlinear discrete transform method. This is in order to model the nonlinear propagation problems in electromagnetic fields as well as the lumped element transmission lines. They were able to show through the test problems that the developed nonlinear model is stable and energy efficient (Smart and Christopoulos, 1998).

2.1.5. Adaptable Symmetrical Condensed Node

In addition to the "Symmetrical Condensed Node" structure used for modelling 3-D TLM electromagnetic problems, there were other ways introduced to model 3-D TLM. At the same time there were the usage of 3-D TLM techniques often uses expanded to solve problems other than electromagnetic problems (Christopoulos, 1991).

For instant, subsequent to the study carried out in 1994 by Trenkic, Christopoulos and Benson, they further continued their study to enhance the 3-D TLM (SNC) and introduced in 1996 the "Adaptable Symmetrical Condensed Node – ASCN" method (Trenkic, Christopoulos, and Benson, 1996).

The advantage of the newly developed concept is that the arbitrary weighting functions can customize the numerical properties. This is to improve the accuracy of the scheme and to minimize dispersion (Trenkic, Christopoulos, and Benson, 1996).

2.1.6. Hybrid and Super Symmetrical Condensed Nodes

In further development of SCN, hybrid node was introduced in the area, where the link-line impedance is different. Moreover, only one type of stubs; either capacitive or inductive is needed. This developed SCN, known as Hybrid Symmetrical Condensed Node – HSCN (Trenkic, Christopoulos, and Benson, 1997).

The advantage of HSCN is that it works with a longer time step in comparison to Symmetrical Condensed Node, in addition of having higher accuracy (Trenkic, Christopoulos, and Benson, 1997).

On the other side, another structure was developed named as Super Symmetrical Condensed Node – SSCN, which eliminating the stubs from the SCN (if all the effects created because of the grading and materials are included) into the link-line impedance (Trenkic, Christopoulos, and Benson, 1997).

In general, it is important to highlight that SSCN has many advantages when compared with the earlier mentioned structures (Trenkic, Christopoulos, and Benson, 1997).

2.1.7. General Symmetrical Condensed Node - GSCN

In the same year (1996), Trenkic, Christopoulos and Benson presented the General Symmetrical Condensed Node – GSCN apart of Transmission Line Modelling development. They worked on this new concept to unify all the existing condensed nodes into a single formulation. The purpose behind that is to provide a template to derive unlimited sets of new nodes with improved propagation properties. This will include also the nodes with enhanced numerical characteristic (Trenkic, Christopoulos, and Benson, 1996).

The work of the researchers was based on considering six lossy elements, six stubs and six different link-line characteristic impedances, demonstrated for the first time to achieve the above stated purpose (Trenkic, Christopoulos, and Benson, 1996).

Generally, the GSCN can be derived from Maxwell's equations directly or based on the equivalent network model, using averaging and central differencing (Trenkic, Christopoulos, and Benson, 1996).

Subsequently in 1997 the previous authors (Trenkic, Christopoulos and Benson) presented the derivation of General Symmetrical Condensed Node – GSCN. They established a mapping between field components and voltage pulses in the Transmission Line Modelling mesh by carrying out derivation of scattering equations. With this, they were able to reduce the scattering error and improve the numerical technique's accuracy (Trenkic, Christopoulos, and Benson, 1997).

2.1.8. Development of Three Dimensional Hybrid Systems TLM

In 1998, Lucia Cascio and Wolfgang J.R. Hoefer expanded the Transmission Line Modelling that can enable analyzing 3-D hybrid systems, which contains a lumped and distributed components (Cascio and Wolfgang, 1998).

The main purpose of carrying out such extension of TLM was for modelling media properties and arbitrary geometries. Not only that, but also to model nonlinear devices. An amendment of the stub-loaded Symmetrical Condensed Node scattering matrix was introduced for this purpose (Cascio and Wolfgang, 1998).

Further, they used SPICE simulation to validate the accuracy of their offered technique (Cascio and Wolfgang, 1998).

Despite the accuracy achieved by adopting the above described proposal, it is important to highlight that, a matrix of a size of 21x21 was required for modelling a hybrid system consist of a distributed and lumped components. Solving such a large size matrix from mathematical point of view will lead to long computation times and errors, unless a method is established to overcome such obstacle.

In summary, the TLM method firstly developed by Johns about forty decays ago, is usually utilized for numerical simulation pertaining to transport phenomena and wave propagation (Hein, 1997). It is currently the base of all the subsequent efforts taken up to model diffusion and acoustic systems, but its widely used in obtaining the full wave electromagnetic field solutions, in the time domain. (Herring and Hoefer, 1996).

Further, Transmission Line Modelling algorithm produces numerical solutions for Transmission Line Modelling networks as a response to impulsive excitations. Excitation impulses may be a single impulses or a sequence of impulses, which sample a continuous waveform within time and space (Hoefer, 1991).

2.2. Transmission Line Modelling Applications

The TLM technique is used nowadays, to model many significant applications, which either modelled as individual system or as hybrid systems. Such applications in which the TLM is employed are diffusion, electrical, mechanical, chemical, civil, radiation, thermal, hydraulic, marine or hybrid engineering systems.

In the same year (1998), Ruddle, Ward, Scaramuzza and Trenkic, stated the transmission line modelling, it became easy to demonstrate extremely complex problems pertaining to the metal surfaces, wires, dielectric and bulk metal easily. This has considered as an added value in analysing complicated structures (Ruddle, Ward, Scaramuzza and Trenkic, 1998).

Various applications with respect of engineering systems mentioned above will be briefly demonstrated in the below coming subsections.

2.2.1. Diffusion Engineering Systems

In year 1986 M. Hendrickx, C. Engels, P. Tobback and P. Johns used the transmission line modeling to describe the soaking behavior of the white rice. They built a white rice a Transmission Line Modelling mesh having a fixed size and compared the calculated outcomes achieved from TLM with FEM (Hendrickx, Engels, Tobback and P. Johns, 1986).

The pre-requisition of having a mathematical model to describe the soaking behavior of white rice was to envisage the moisture uptake of the rice while using variables which were easy to measure (Hendrickx, Engels, Tobback and P. Johns, 1986).

Earlier attempts in studying this scenario were carried out by various researchers such as Zhang et al., in 1984. He used the approximation of the FEM for short grain rice. Off course, this attempt was not successful because of the huge time needed by finite element method, to obtain a solution. The reason behind is that the various numerical values, which required to be considered were for different properties of

the rice. Such values are like Poisson's ratio, expansion coefficient in x, y and z directions, density and elastic modulus (Hendrickx, Engels, Tobback and P. Johns, 1986).

It is to be noted that, most of the studies presented through various papers to model the soaking behavior of the white rice considered short grain rice. The availability of information on the long grain rice was much less (Hendrickx, Engels, Tobback and P. Johns, 1986).

The attention of using transmission line modelling as a method to model diffusion problems by P.B. Johns in 1977, Graham and the previous said researchers in 1983, was used as a base in this paper to present the modelling of long grain white rice (Hendrickx, Engels, Tobback and P. Johns, 1986).

In this regard, the non-constant diffusion coefficient of the system was modelled by using FDTD or FEM. On the other hand, the diffusion problems in foodstuff were modelled by using the 2-D TLM and by considering no losses in the transmission line. In other word, only the distributed capacitance and inductance with a characteristic impedance of unity were considered apart of modelling the system. Furthermore, the system was connected to a lumped resistor (Hendrickx, Engels, Tobback and P. Johns, 1986).

Another application pertaining thermal diffusion was carried out by S. H. Pulko and C. P. Phizacklea in 1990. It is to be noted that, they did not describe the modelling of the thermal diffusion since the model was described earlier by S.H. Pulko, A. Mallik and P.B. Johns in 1986 and 1987 respectively. What they did is to

concentrate on proofing that modelling thermal diffusions can be done by using RC networks. This means that modelling the thermal diffusions can be limited to the line resistance and the capacitance per unit length (Pulko and Phizacklea, 1990).

The proof in this regard was concluded from the 2-D Transmission Line Modelling algorithms to solve the equations, which are stated as shown below (Pulko and Phizacklea, 1990): -

$$\frac{\partial^2 \Phi}{\partial x^2} + \frac{\partial^2 \Phi}{\partial y^2} = 4R_d C_d \frac{\partial \Phi}{\partial t} + 2L_d C_d \frac{\partial^2 \Phi}{\partial t^2} \qquad 2.1$$

L_d, C_d and R_d are the distributed inductance, capacitance and resistance respectively (Pulko and Phizacklea, 1990).

By looking to the above referred diffusion equation, it can be seen that the wave equation is lossy. In other word, if the RHS of the equation is small and therefore neglected, no loses is counted when waves propagate. On contrary, if the LHS treated similar to RHS but considering a short time-step, the equation will be similar to above diffusion equation (Pulko and Phizacklea, 1990).

2.2.2. Electrical Engineering Systems

In 1986, Adam Semlyca and Huang Wei-Gang presented a mathematical model for corona by using Transmission Line Modelling (Semlyca and Wei-Gang, 1986).

They modelled the corona by both, the space and surface charges to ensure having close results to reality, while calculating the transients of the transmission lines (Semlyca and Wei-Gang, 1986).

The line was modelled using Norton equivalent, whereas the components modelled by using the lumped parameter model. This is in order to ensure the compatibility of the model with the Electro-Magnetic Transients Program (EMTP) used as part of the modelling (Semlyca and Wei-Gang, 1986).

In addition, for corona modelling, two ways were considered to model longitudinal elements. One of the ways was by representing the line as an inductance, which means no losses are considered. The other way was to represent the line in impedance form, which means considering the resistance and the inductance elements. In short, the lumped parameter was approached for line modelling by dividing it into segments with state variable current, voltage and charges (Semlyca and Wei-Gang, 1986).

Unfortunately, the above study could not solve the modelling difficulties created due to the space charges drifting in the course of slow transients despite its precious lesson illustrated when models the corona on OHL as part of calculating the propagating transients (Semlyca and Wei-Gang, 1986).

In 1996, L Oprea and C Velicescu modelled nonlinear frequency dependent transmission line to study the electromagnetic transient in the Power Systems. They formulated the model in terms of PDE's, in the modal domain and used Laplace transforms to solve it, taking into consideration the line inductance and capacitance only. Switching surges and lightning were simulated on the basis of the transient response of the line and by means of the convolution integral. The terminal load connected at the end of the line was considered as linear, when represented as a

resistance and as nonlinear when represented as a surge arrester (Oprea and Velicescu, 1996).

As a consequence, the high voltage transmission line's mathematical model had the capability to anticipate the over-voltages generated from the lightning surges or from the system itself (Oprea and Velicescu, 1996).

It is important to highlight that at the line's sending end, a step function was counted as part of the model. This is in order to reduce the complexity, which may arise while determining the terminal voltages of the line, analytically (Oprea and Velicescu, 1996).

In 1998, Michael Fette, Juergen Voss, Liliana Oprea and Corneliu Velicescu modelled the high-voltage transmission lines with frequency dependent parameters by using the Laplace transform method. This is to solve the system partial differential equations, decoupled in modal domain (Fette, Voss, Oprea and Velicescu, 1998).

The mathematical model formulated for the system considered the four line parameters (series resistance per unit length (R), series inductance per unit length (L), shunt capacitance per unit length (C) and shunt leakage conductance per unit length (G) (Fette, Voss, Oprea and Velicescu, 1998).

In this regard, the single phase transmission line of length l is illustrated by PDE, for current I(x,t) and voltage V(x,t) passing through or across the transmission line as shown below (Fette, Voss, Oprea and Velicescu, 1998): -

$$\frac{\partial V}{\partial x}(x,t) + L\frac{\partial I}{\partial t}(x,t) + RI(x,t) = 0 \qquad 2.2$$

$$\frac{\partial^2 V}{\partial x^2} = LC\frac{\partial^2 V}{\partial t^2} + (RC + GL)\frac{\partial V}{\partial t} + RGV \qquad 2.3$$

$$\frac{\partial I}{\partial x}(x,t) + C\frac{\partial V}{\partial t}(x,t) + GV(x,t) = 0 \qquad 2.4$$

$$\frac{\partial^2 I}{\partial x^2} = LC\frac{\partial^2 I}{\partial t^2} + (RC + GL)\frac{\partial I}{\partial t} + RGI \qquad 2.5$$

The three phase transmission line of length l can be extended from above equations as follow (Fette, Voss, Oprea and Velicescu, 1998): -

$$\frac{\partial^2 V}{\partial x^2} = Z.Y.V; \text{ and } \frac{\partial^2 I}{\partial x^2} = Y.Z.I \qquad 2.6$$

where, Z and Y are system impedance and admittance matrices, and V and I are the phase voltage and phase current of the wires (Fette, Voss, Oprea and Velicescu, 1998).

The researchers stated that the "solution of equation (2.6) can be obtained **only** by decomposing the three-phase system into three decoupled single-phase lines" (Fette, Voss, Oprea and Velicescu, 1998).

In continuation to above, the author of this research will show in this study that the hybrid modelling system developed by Whalley in 1988 can be easily adopted to model a long transmission line considering all four line parameters without having major complications in mathematical derivation and system simulation.

In 2003 G. McClure and M. Lapointe studied the dynamic response of overhead transmission lines, when suffering from sudden failure or unbalanced loads. This

was experienced from the sudden failures of overhead line's components or breakage of conductor (McClure and Lapointe, 2003).

The Finite Element Method originally suggested by McClure was used to model the cable along with ADINA as commercial software. Other overhead line components such as masses and inertia were modelled as lumped, or by using modelling options available in ADINA (McClure and Lapointe, 2003).

G. McClure and M. Lapointe concluded that further improvement is required in modelling the post elastic response along with the strain rate effect on the material prosperities of the OHL components. However, the significant part, which needs enhancement, was the numerical models. This can be proven by carrying out physical testing and comparing the outcomes for adoption of further improvement (McClure and Lapointe, 2003).

2.2.3. Mechanical Engineering Systems

In 1995, H. Selhi, S. Y .R. Hui, C. Christopoulos and A. F. Howe, worked on modelling and simulation of an induction motor drive, by using Transmission Line Modelling Techniques (Selhi, Hui, Christopoulos and Howe, 1995).

For the purpose of modelling, the block diagram of the induction motor drive shown in Figure-2.7 was broken into three main sections named as Section-1: AC/DC converter, Section-2: inverter and Section-3: induction motor and each is modelled separately (Selhi, Hui, Christopoulos and Howe, 1995).

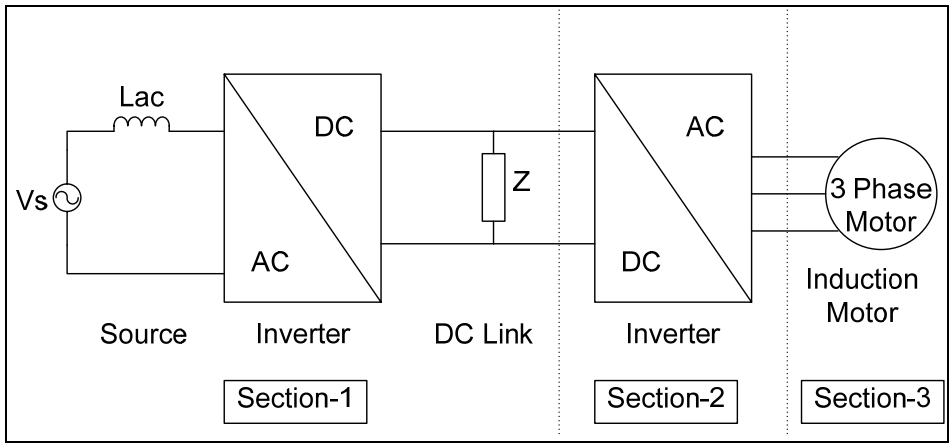

Figure-2.7: Block diagram of the induction motor drive broken into three main sections (Selhi, Hui, Christopoulos and Howe, 1995)

The achieved TLM of induction motor drive was further converted to Thevenin equivalent circuits of AC/DC converter section, inverter section and induction motor section. These three circuits were subsequently, solved using the standard circuit solvers (Selhi, Hui, Christopoulos and Howe, 1995).

As an outcome, the TLM method had shown its useful features when adopted with respect of ensuring the stability while dealing with rigid grids along with unambiguous algorithm nature that allows segmentation and effectual network solution (Selhi, Hui, Christopoulos and Howe, 1995).

From the author point of view, the finite element modelling adopted for above system was long until converting the model to Thevenin equivalent circuits, which needs further to be solved to obtain the system transfer function. It can also be noticed that, this depends on the number of segments and the complexity in computing the above mathematical model.

Similar to the worked carried out by H. Selhi, S. Y .R. Hui, C. Christopoulos and A. F. Howe in 1995 pertaining to modelling of a three-phase induction motor using TLM by the means of Finite Element Transmission Line Modelling method (FE-TLM), Tim J Flack and Rachel E Knight in 1999 predicted successfully the time domain, induction motor model's performance by using Domain Decomposition Transmission Line Modelling Method (DD-TLM). In other words, they demonstrated how the DD-TLM is employed to simulate the three-phase induction motors, considering the high computational cost of FE-TLM (Flack and Knight, 1999).

In this regard, the induction motor was divided into three types of sub-domains, named as rotor, stator and air gap. Even with a poor selection of the number of sub-domains for modelling purpose, Tim J Flack and Rachel E Knight proved that the computation time taken while applying DD-TLM is still better, when compared with FE-TLM (Flack and Knight, 1999).

In 1997 C. M. Ting and P. A. Jennings presented a paper describing the adoption of numerical electromagnetic while using transmission line modelling for vehicles. This is for the purpose showing how the electromagnetic field can be handled as apart of the design stage. However, the approach followed depends on common assumption, on which the most important assumption considered is no line losses (Ting and Jennings (1997).

2.2.4. Chemical Engineering Systems

J. K. Van Deen and S. R. Reintsema in 1983 model a high-pressure gas transmission line based on analogue computer systems, subjected to using a second-order truncation error, Discrete-Space Continuous-Time (DSCT) method (Van Deen and Reintsema, 1983).

They described the gas flow in the transmission line in the form of three coupled PDEs and worked out in solving them by using two ways. One of the techniques followed in solving them is the method of characteristics and the other one is the FDTD with a second order truncation error computed using analogue computers. The second approach enabled them to reduce the PDEs to ODEs function in time and then, integrate this directly on the analogue computer (Van Deen and Reintsema, 1983).

It is important to highlight that the gas transmission line described above was based on the RC or RLC models with the essential needs in deploying engineering judgment while modelling (Van Deen and Reintsema, 1983). This may have impact from the accuracy point of view as engineering judgment varies from one engineer's opinion to another.

In 1999, Miroslawa Rak, Xiang Gui, and Donard de Cogan used the Transmission Line Modelling technique to verify the results achieved when solving the system equations analytically, in order to examine the transient state of a crystal submersed in supersaturated solution. The results were satisfactory and promising of the

suitability of applying TLM as a method to verify the processes of the transient crystal growth (Rak, Gui, and Cogan, 1999).

Vanja Kosar, Zoran Gomzi and Kresimir Sintic in 2006, derived a mathematical model consist of a set of partial differential equations, describing the curing process in the Continuous Vulcanization tube (CV), apart of manufacturing process of power cables insulated with cross-linkable polyethylene (Kosar, Gomzi and Sintic, 2006).

The mathematical model was then, transformed into dimensionless form to solve it numerically by using the Finite Element Method. They further verified the capability of the continuous cross-linking process, inline, with the derived mathematical model by simulation (Kosar, Gomzi and Sintic, 2006).

The achieved results show that the implemented process parameters during manufacturing are practically valid and aligned with the derived mathematical model. These parameters are line speed, temperature in CV tube, nitrogen pressure, thermodynamic constant for insulation and conductor (Kosar, Gomzi and Sintic, 2006).

2.2.5. Civil Engineering Systems

In 2005, A.Y. Shehata, A.A. El Damatty, and E. Savory offered a detailed descriptions and procedure on how to model and anticipate the performance of the transmission line structure when exposed to downburst, wind loads. They adopted the Finite Element method to model the various components of the transmission

line, such as conductors, tower, guys, connections and ground wire. The modelling and discussion have taken into account the behaviour of the nonlinearity in some of the system items, which are mainly the ground wires and the conductors. This is because of the lengthy span of the ground wires and the conductors with respect to their small cross section, which subject them to large displacements as a consequence of wind loads (Shehata, Damatty and Savory, 2005).

Since, the Finite Element Method is based on dividing the system into subsections, each tower member is considered as one element, whereas, each cable span is modelled by ten consistent beam elements each stroud is divided into five elements (Shehata, Damatty and Savory, 2005).

The increases in the segments as stated earlier will definitely increase the level of complexity in deriving and solving the mathematical model.

2.2.6. Radiation Engineering Systems

In 2008, A. Vukovic, P. Sewell, C. Styan and T. M. Benson employed the TLM to model nonlinear Photonic Structures by extending the Kerr nonlinearity method proposed for one-dimensional TLM to two-dimensional TLM. The characteristic impedance of the transmission line is computed by adding a suitable admittance or stub impedance to nodal transmission networks (Vukovic, Sewell, Styan and Benson, 2008).

2.2.7. Thermal Engineering Systems

In 2008, J. A. Pilgrim, D. J. Swaffield, P. L. Lewint and D. Payne investigated the thermal ratings of the HV cable joints by using two-dimensional and three-dimensional Finite Element Analysis. They stated that most of the studies carried out so far, are not taking into consideration the temperature distribution within the cable joints while modeling. Hence, they took this in their study and proposed that the results on the joint bays are not a limiting factor on the circuit rating, subject that sufficient core to core spacing is provided (Pilgrim, Swaffield, Lewint and Payne, 2008).

Original attempts in modeling HV joint bays used the analytical methods, which deal with using the electrical analogue as a base toward thermal system. The representation of the materials of cable joints along with their thermal resistances was simply by admittance and capacitance networks (Pilgrim, Swaffield, Lewint and Payne, 2008).

Later on, the numerical methods introduced which permitted extending the modeling of the system of a third dimension. Again the representation of the cable joint's materials and their thermal resistances were by admittance and capacitance networks except in having a detailed lumped parameter approach (Pilgrim, Swaffield, Lewint and Payne, 2008).

The usefulness of the lumped parameter approach is that it can be consolidated with the generation tools of the FE mesh (Pilgrim, Swaffield, Lewint and Payne, 2008).

It is important also to indicate that these numerical techniques have shown some quality improvement in the produced solution with reference to the analytical techniques. However, there were some unavoidable limitations faced at that time pertaining to the capability of these numerical methods from computational point of view. These restrictions acted as a boundary in increasing the number of nodes needed to be allocated to problems during the development phases. Alternatively, it directed the researchers to adopt assumptions (Pilgrim, Swaffield, Lewint and Payne, 2008).

As indicated earlier, S. Mimouni, A. Saidane and A. Feradji used TLM to deal with the steady-state analysis and the transient thermal of a typical microwave power devices, manufactured using different materials. However, the modelling was based on consideration of three line parameters; inductance, capacitance and the resistance per unit of length. (Mimouni, Saidane and Feradji, 2008).

In case the resistance per unit of a length considered as zero, then the system equation will match the wave equation. On the other hand, in case the resistance per unit of a length was not considered as zero, system the equations will describe only the wave attenuation (Mimouni, Saidane and Feradji, 2008).

As a summary, it is to be noticed that, the majority of the contributions in modelling the transmission lines in the above referred various applications, were based on finite element method, method of characteristics and lumped, considering mainly in most cases the inductance and capacitance per unit length of the line parameters while computing the mathematical model of the system. This is adopted to avoid

complexity in driving the mathematical model, which resulted in generating irrational functions, on transformation, due to the combination of algebraic, ordinary and partial differential equations.

The next subsection will illustrate some of the applications on which the TLM adopted for hybrid systems to model the transmission lines used in engineering systems.

2.2.8. Hybrid Engineering Systems

From definition point of view, any system or scheme consists of a discrete time, described by difference equations and a continuous subsystem described by differential equations, is called a hybrid system (Close and Frederik, 1993).

There are many modern systems that are classified as hybrid systems due to containing both discrete time and continuous subsystems and are usually, classified with reference to the type of equations used in deriving the mathematical model (Close and Frederik, 1993).

Distributed systems for examples, are modelled by partial differential equations, whereas the lumped systems are modelled by ordinary differential equations (Close and Frederik, 1993).

Further, the distributed parameter model accounts for a situation, in which the scalar field related to the concentrated amounts is function of position and time (Dynamic Models, Chapter-7).

It is also important to indicate here that, changing distributed systems to lumped approximations is sometimes necessary, specifically, when solving the desired model is required taking into consideration the available resources (Close and Frederik, 1993).

Below are illustrations to some of the hybrid systems consists of distributed systems, lumped systems, or combination of both.

Prior to 1977, the dynamic simulation routine available at that time was limited to processes of a unit represented by lumped parameter model. Subsequently, in 1977 John C. Heydweiller, Richard F. Sincovec and Liangtseng Fan presented a paper, which gives an overall procedure that can describe the chemical processes of a respective unit by using both lumped and distributed parameter models (Heydweiller, Sincovec and Fan, 1977).

The mathematical distributed parameter model introduced by them was based on PDEs. These PDEs are subsequently, converted into a set of ODEs depending only on time. Further, it uses finite difference approximations for discretizing the spatial variable (Heydweiller, Sincovec and Fan, 1977). It can be observed here, that the distributed system was converted to lumped system in order to be able to solve it based on the available computational resources.

Boundary conditions, representing unit outlet and inlet were required to be identified while modelling to couple these sets of discretized equations derived from a lumped parameter model with other sets of discretized equations derived from a distributed parameter model of another unit. This combination resulted into a

large set of time dependent ODEs, which required to be solved. In this regard, A Gear type integrator was used to solve these sets of produced ordinary differential equations - ODEs (Heydweiller, Sincovec and Fan, 1977).

In the same year (1977), J. W. Bandler used transmission line matrix as a new modelling method to analyze the time domain of the lumped networks. The method showed its ability to give an exact solution to the model. Nevertheless, with regard to the error arises while modelling the elements of the network, this was compensated by adding extra components (Bandler, 1977).

In 1978, W. H. Ray carried out a survey on some of the recent applications on which the distributed parameter system theory is used. The survey pointed out to some of the applications such as heat transfer processes, chemical reactors, open loop stability problem, mechanical systems, resource recovery and the environment, environmental quality modelling, monitoring and control, physiological and sociological systems, and process control such as for polymer processing operations, in the control of plasmas, in nuclear reactor control, and for a scattered variety of other process control applications (Ray, 1978).

As a matter of fact, a number of above mentioned applications involved roughly lumped system models initially. After that, the lumped parameter theory was applied to the final constructed model. In fact, this method was well with the reported limitation in experimental results (Ray, 1978).

In 1988, Watton and Tadmori carried out a comparison using four different methods to analyze and solve numerically, the transmission line dynamics in the electro-

hydraulic control systems in time domain. They ended up that the modal analysis is the best method to be adopted in this regard (Watton and Tadmori, 1988).

As it is known, the modelling of the transmission line is normally defined based on distributed parameter method. This was considered while modelling the above electro-hydraulic control system, but with two line parameters; the series impedance and the shunt admittance per unit length (Watton and Tadmori, 1988).

Further, the researchers presented three models for the wave propagating in the electro-hydraulic transmission line while using the fundamental fluid equations. These models are lossless line models in which, only the inductance (fluid acceleration) and capacitance (fluid compressibility) were considered, average friction model in which, the effect of the laminar pipe friction (series reactor) was added, and the distributed friction model considering the effect of the heat transfer between the pipe and the fluid walls keeping the shunt admittance unchanged (Watton and Tadmori, 1988).

In 1988, R. Whalley presented a paper named as "The response of distributed-lumped parameter systems", to assist in overcoming one of the main drawbacks of finite element method, which is the prolonged computation time taken without improving the confidence in the results obtained, and to reflect the wave propagation concept.

He investigated modelling a system contains a distributed parameter dynamic components followed by lumped elements connected in series (Whalley, 1988).

The outcome achieved from this investigation, shows that mapping input signal into output signal is done over a rational function belonging to the related frequency domain and discrete time domain provided that the lumped parameter elements is presented by rational functions in both time and frequency domains (Whalley, 1988).

Ultimately, when adopting Whalley's hybrid modelling technique, for the long transmission lines can be presented by using distributed parameter modelling technique in the following format: -

$$\begin{bmatrix} Input_1(s) \\ Input_2(s) \end{bmatrix} = \begin{bmatrix} \zeta w(s) & -\zeta(w^2(s)-1)^{\frac{1}{2}} \\ \zeta(w^2(s)-1)^{\frac{1}{2}} & -\zeta w(s) \end{bmatrix} \times \begin{bmatrix} Output_1(s) \\ Output_2(s) \end{bmatrix} \qquad 2.7$$

where, the system matrix or impedance relates the output of the system to the input of the system.

The linearity of the system depends that the series and shunt impedances being rational functions (Whalley, 1988).

Further, it can be noticed from the above model, that the transfer function is a multi-dimensional matrix, which means, the system was more than one lumped element and one distributed parameter element, even if rational (Whalley, 1988).

Equivalent to voltage and current as input and output in electrical system, the input and output of the other systems such as mechanical, thermal, hydraulic, etc can be substituted in the above driven distributed model.

Subsequently, in 1990, R. Whalley proposed a hybrid modelling technique using the distributed parameter method to model any long transmission line. This technique was then used by H Bartlett, R. Whalley, and S S I Rizvi to investigate the dynamic performance of a long and hollow shaft for marine transmission systems, showing that it can be adopted for such investigations (Bartlett, Whalley and Rizvi, 1998).

In the same year (1990), A. K. Schierwagen identified the mathematical problems arising in the distributed parameter Neuron Models (Schierwagen, 1990).

The system modelling was based on one dimensional cable model with consideration of the specific parameters of the membrane capacitance (C_m), membrane conductance (G_m) and intracellular (axial) resistivity (R_i). Refer Figure-2.8 (Schierwagen, 1990).

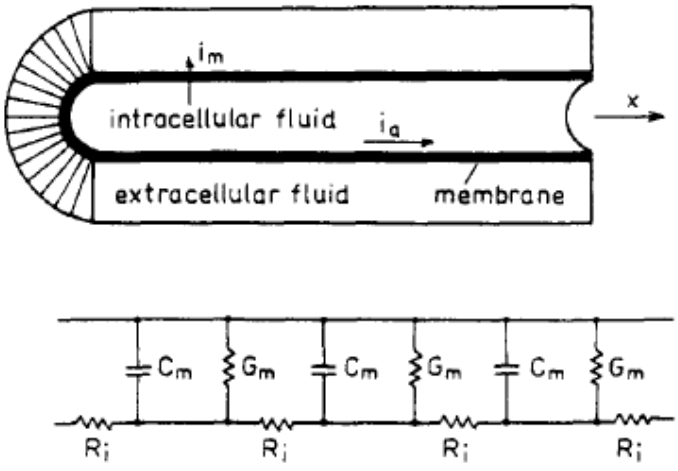

Figure-2.8: The one-dimensional cable model for an idealized nerve process (top) and its equivalent electrical circuit (bottom). The extracellular resistance has been neglected
(Schierwagen, 1990)

Considering the electrical circuit shown in Figure-2.8, x represents the distance in axial direction within a time t. The cable equations, in this regard, for the longitudinal (axial) current $I_a = I_a(x,t)$ and membrane voltage $V=V(x,t)$ within a cylindrical section having a length l and a diameter d can be presented as below (Schierwagen, 1990):

$$\frac{\partial V}{\partial x} = -R.I_a \text{ and } \frac{\partial I_a}{\partial x} = -I_m \qquad 2.8$$

Where the axial resistance, membrane capacitance and membrane conductance (all quantities are per unit length) are given respectively as follow:

$$R = \frac{4R_i}{\pi d^2}, \qquad 2.9$$

$$C = \pi.d.C_m \text{ and} \qquad 2.10$$

$$G = \pi.d.G_m \qquad 2.11$$

By applying Laplace transformation and considering the boundary conditions, which are two in this case since the cable of a finite length is extended from x=0 to x=l, the above equations can be further shaped to be represented in a transfer function form, which can be subsequently simulated to examine system performance (Schierwagen, 1990).

However, with respect of the branching structure, the modelling becomes more complex and complicated. This is due to the requirement for including boundary conditions at each and every branch point and terminal. This obviously, will lead to a very complicated expression for the respective solution.

To overcome this problem, models of different degrees of complexity were presented after development by Schierwagen (Schierwagen, 1990).

Further, there was another problem faced with respect of branching structures. It was the identification of the parameters. There was no solution to solve this problem except by adopting assumptions. Accordingly, the cable parameters R_i, C_m and G_m assumed constant over the neuron (Schierwagen, 1990).

The author of this research is of the opinion that Whalley's adopted distributed-lumped parameter modelled in 1988 may assist in overcoming these problems faced in modelling the distributed parameter Neuron Models, since it offers a simple mathematical model, which can be easily adopted considering even the four line parameters.

In 1995 G. Groppi, A. Belloli, E. Tronconi and P. Forzatti conducted a comparison between the lumped and distributed models in modelling the monolith catalytic combustors. They concluded generally, that lumped model is not advisable to be used to model segmented monolith catalytic combustors as it fails to predict the wall temperature profiles or the ignition of a homogeneous combustion. Distributed model is the appropriate modelling technique in such cases for modelling long monolith segments and to predict the temperatures of the gas exit (Groppi, Belloli, Tronconi and Forzatti, 1995).

Once again in 1998 H. Bartlett and R. Whalley presented a paper for modelling and analyzing the variable geometry; exhaust gas hybrid systems (Bartlett, Whalley, 1998). They offered a general modelling technique addressing the distributed-

lumped modelling technique to model the long pipes with two interconnected cross sections of different lengths using point wise impedance and restrictions. This is to enable them study the dynamic and the steady state response of the system (Bartlett, Whalley, 1998).

It is to be noted that the distributed-lumped modelling technique considered for modelling the pipeline based on its distributed nature on which, the lumped parameter method was inappropriate method for modelling the pipeline (Bartlett, Whalley, 1998).

In the same year (1998), R. GonzAlez-Garciaa, R. Rico Martinez and I. G. Kevrekidis stated that simplification approaches, specifically when ignoring some important features of the spatial response exhibited by the system for the purpose of simplifying the derivation of the mathematical model, may fail to capture fully, the observed dynamics of the system by experiment. Accordingly, they emphasize on increasing the needs for developing and identifying techniques for distributed parameter systems based on detailed spatiotemporal experimental data (Garciaa, Martinez and Kevrekidis, 1998).

This was what they focused on when presented their paper in which, they demonstrated a methodology to identify the distributed parameter system on the basis of an Artificial Neural Network (ANN). Then, it is coupled with a standard numerical analysis technique for spatial discretization. This is usually applied in the approximation method to solve the partial differential equations (Garciaa, Martinez and Kevrekidis, 1998).

However, the numerical solution of the partial differential equations is normally accomplished by using the FDTD and the method of lines in time to discretize the spatial derivatives. Further, the numerical integrator scheme is used as a template to construct the Artificial Neural Networks, in addition to the use of the spatially experimental measurements resolved earlier at some locations over the spatial domain to act as inputs and outputs. This process is built on earlier developed one by Rico-Martinez et al. in 1995, to identify the lumped parameter systems (Garciaa, Martinez and Kevrekidis, 1998).

In 2000, M. Aleyaasin, and M. Ebrahimi worked out modeling of a rotating shaft-disc system by using a series of interconnected, lumped and distributed elements developed by Whalley in 1988. The rotor system treated as distributed element and the rigid discs as a lumped element (Aleyaasin and Ebrahimi).

The modelling as stated above divided into two parts, distributed and lumped. There were right and left terminations for the distributed part, out of which each one had four parameters. These parameters were vertical slopes, displacement, shear forces and bending moments. On the other sides, there were also right and left terminations for the lumped part with the same four parameters mentioned previously (Aleyaasin and Ebrahimi).

Further, the researchers explored the time domain response for the modelled system from the frequency domain response data. For that, they used the inverse Fourier transform since the acquired results from the simulation did not include the noise (Aleyaasin and Ebrahimi).

In 2009 Javier A. Villegas, Stephen R. Duncan, Haigang G. Wang, Wuquiang Q. Yang, and Rambali S. Raghavan used the distributed parameter approach to model and control a batch fluidised bed dryer. It is known that the dynamics of this system are highly nonlinear, which leads to difficulties in predicting its behaviour. In this regard, Electric Capacitance Tomography - ECT was employed by the researchers in order to control and monitor the batch fluidised bed dryer's behaviour (Villegas, Duncan, Wang, Yang and Raghavan, 2009).

In the above study, the researchers applied a particle feedback variable to control online, the permittivity distribution in the system. Prior to this, a distributed system model was developed in combination with a lumped model. It was used to predict the changes occurring in the permittivity distribution within the bed when it is a function of the average particle moisture and the inlet air velocity. The purpose of this combination is to allow most of the exiting nonlinearities other than the system to be incorporated within the lumped model. This will have an impact on deriving a simple distributed parameter model, and thereafter, avoid the need in solving PDE's (Villegas, Duncan, Wang, Yang and Raghavan, 2009).

By verifying the derived mathematical model with the experimental results, the researchers succeeded in showing the ability of controlling the permittivity distribution by the mean of changing the inlet air velocity of the dryer (Villegas, Duncan, Wang, Yang and Raghavan, 2009).

Further, it is to highlight that the derivation of the distributed model, for the batch fluidised bed dryer, was based on the governing equations of the dynamic lumped model (Villegas, Duncan, Wang, Yang and Raghavan, 2009).

In 2010, R. Whalley and Alaa Abdul-Ameer presented a distributed-lumped model for heating, ventilation and air conditioning system. The inlet and extraction fans were modelled as lumped parameter elements for the purpose of easy adjustment of pressure changes at the inlet and outlet within a ventilated working area by the means of voltage variation across the fan motors. On the exit side, the distributed parameter approach was used to model the dimension of the ventilated volume. This has beneficial aspect in enabling changing the airflow dynamics as a prelude to preparing automatic control studies (Whalley and Abdul-Ameer, 2010).

With respect to the developed model, it maps the input pressure changes to the two outputs; volume input and airflow rates. Moreover, the fan dynamics apart of the system is modelled as lumped in the form of simple exponential time delay (Whalley and Abdul-Ameer, 2010).

Returning to the distributed parameter modelling technique presented by R. Whalley in 1988, the input pressure $p_1(s)$, the outputs; volume input $q_1(s)$ and airflow rates $q_2(s)$ are given as follow (Whalley and Abdul-Ameer, 2010):

$$\begin{bmatrix} p_1(s) \\ 0 \end{bmatrix} = \begin{bmatrix} \zeta w(s) & -\zeta (w^2(s)-1)^{\frac{1}{2}} \\ \zeta (w^2(s)-1)^{\frac{1}{2}} & -\zeta w(s) \end{bmatrix} \times \begin{bmatrix} q_1(s) \\ q_2(s) \end{bmatrix} \qquad 2.12$$

From which, the output flow rates $q_1(s)$ and $q_2(s)$ with respect to inversed system impedance and input pressure $p_1(s)$ can be given as below (Whalley and Abdul-Ameer, 2010):

$$\begin{bmatrix} q_1(s) \\ q_2(s) \end{bmatrix} = \frac{\begin{bmatrix} \zeta w(s) + f(p_2) \\ \zeta (w^2(s) - 1)^{\frac{1}{2}} \end{bmatrix}}{\zeta (w(s) f(p_2) + \zeta)} p_1(s) \qquad 2.13$$

Various system responses with respect to step changes applied on each input were represented and discussed while incorporating changes in fan, chilled water pump motors, ambient and heat transfer temperature to assess the changes on the output pressure, volume flow and air stream temperature at the inlet and outlet of the ventilated volume (Whalley and Abdul-Ameer, 2010).

In 2010 E. Barati and J.A. Esfahani stated that "*if a certain initial moisture and temperature is assumed in the food, it is possible to offer a new analytical solution*" or mathematical modelling of convective drying considering the temperature as lumped and spatialy distributed moisture in slab (Barati and Esfahani, 2010).

In this paper, E. Barati and J.A. Esfahani modeled the drying process of the water, heat transfers, and carrot slice by the means of energy balances and transient mass transfer equation (Barati and Esfahani, 2010).

While carrying out the mathematical modelling, some assumptions were made. First, the mass transfer is considered as one dimensional in the product by diffusion. Secondly, lumped technique is used to model the heat transfer within the food while neglecting the shrinkage during drying. In fact, this technique can be deployed

when the conditions correspond to a negligible temperature difference in the food. Thirdly, the food was considered as homogenous and finally, the physical properties of the food is assumed to be constant (Barati and Esfahani, 2010).

The main problem faced while modelling the system was the complexities of mass and heat transfer in the food while solving it analytically. It was introduced because of the strong coupling between mass and heat transfer during the process of evaporation. However, this was overcome by rearranging the boundary condition at the food surface (Barati and Esfahani, 2010).

Subsequently, in 2011 R. Whalley and Alaa Abdul-Ameer discussed the dynamic responses of cyclic ventilation systems using the same hybrid distributed-lumped parameter modelling technique described above (Whalley and Abdul-Ameer, 2011).

In 2011, R. Whalley, Alaa Abdul-Ameer and K.M. Ebrahimi represented the Hybrid model of a machine tool axis drives published in 2005 (Whalley, Abdul-Ameer and Ebrahimi, 2005) to illustrated the X-Y-Z axes response and resonance identification for a milling machine by using the distributed-lumped parameter modelling technique to derive the model. Figure-2.9 shows Milling machine X and Y traverse drive (Whalley, Abdul-Ameer and Ebrahimi, 2011).

Further, from accuracy point of view, system's spatial dispersion was included in the modeling process (Whalley, Abdul-Ameer and Ebrahimi, 2011).

The lead screw realization is treated as a pair of distributed lumped components, whereas, the motor drive, work piece and saddle, slides, ball-nut, and bearings are

described by lumped parameter models (Whalley, Abdul-Ameer and Ebrahimi, 2011).

Since the lead screw, as stated above, presented as a long shaft having (l) as a shaft length and (d) as a shaft diameter with an infinite series of infinitesimal components, a length of dx is used in order to describe the system as below (Whalley, Abdul-Ameer and Ebrahimi, 2011): -

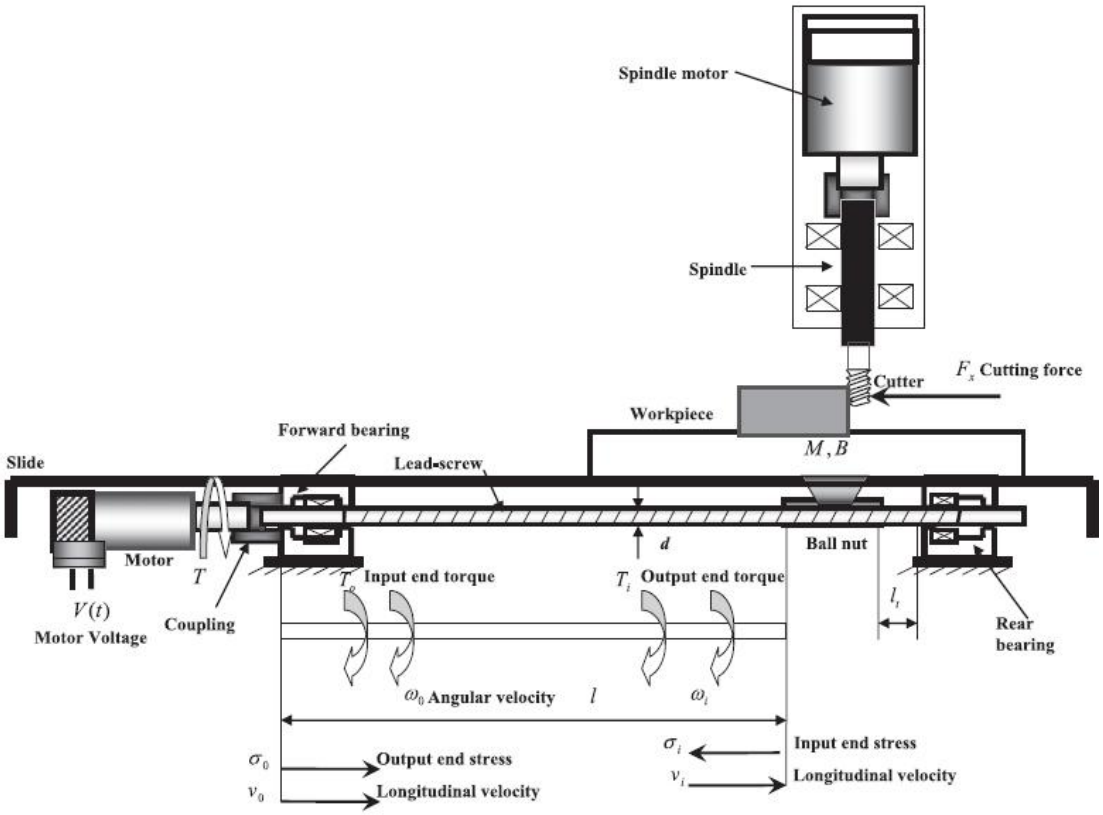

Figure-2.9: Milling machine X and Y traverse drive
(Whalley, Abdul-Ameer & Ebrahimi, 2011)

$$\begin{bmatrix} T_1(s) \\ 0 \end{bmatrix} = \begin{bmatrix} \zeta w(s) & -\zeta(w^2(s)-1)^{\frac{1}{2}} \\ \zeta(w^2(s)-1)^{\frac{1}{2}} & -\zeta w(s) \end{bmatrix} \times \begin{bmatrix} \omega_1(s) \\ \omega_2(s) \end{bmatrix} \qquad 2.14$$

$$\begin{bmatrix} \omega_1(s) \\ \omega_2(s) \end{bmatrix} = \frac{\begin{bmatrix} \zeta w(s) + R \\ \zeta (w^2(s) - 1)^{\frac{1}{2}} \end{bmatrix}}{\zeta (w(s) R + \zeta)} T_1(s) \qquad 2.15$$

Within the same year (2011), Alaa Abdul-Ameer proved that Whalley method (1988) can also be adopted on a hydraulic system. This was presented in his new technique developed for modelling fluid pipeline using the hybrid modelling technique proposed by Whalley (Abdul-Ameer, 2011).

Alaa Abdul-Ameer further, extended this approach to provide accurate transient responses anticipation for fluid pipeline system model, while including the frequency dependent fluid friction (Abdul-Ameer, 2011).

Similar to what stated earlier by R. GonzAlez-Garciaa, R. Rico Martinez and I. G. Kevrekidis in 1998, the neglect of the non uniform heat flux distribution while adopting the lumped parameter model technique to predict the transient behaviour of an evaporation system, which requires a dynamic model but this did not given the required results (Groppi, Belloli, Tronconi and Forzatti, 1995).

In this regard, the model for this system was developed to show more accuracy when two dimensional and non-uniform radiation heat flux distribution on the water wall considered. However, there was also a deficiency in having on line three dimensional combustion monitoring system in the furnace, as this type of model was rarely reported (Groppi, Belloli, Tronconi and Forzatti, 1995).

Shu Zheng, Zixue Luo, Xiangyu Zhang, and Huaichun Zhou worked out in 2011 and developed a distributed parameter model for the evaporation system based on three dimensional combustion monitoring in the furnace (Groppi, Belloli, Tronconi and Forzatti, 1995).

They further, put the imaginary wall surface forward in order to simplify the twin furnace problem (Groppi, Belloli, Tronconi and Forzatti, 1995).

Accordingly, a mathematical model was derived to predict the transient distribution of parameters (Groppi, Belloli, Tronconi and Forzatti, 1995).

It is to be highlighted that, the distributed parameter model for the evaporation system was based on dividing the system into three sub models named as tube wall model, flue gas model and water or steam model, connected with some coupling thermodynamic parameters (Groppi, Belloli, Tronconi and Forzatti, 1995).

The mathematical flue gas model is derived by using a rapidly covering algorithm based on the Monte Carlo technique (Groppi, Belloli, Tronconi and Forzatti, 1995), tube wall model by two dimensional steady state heat conduction model and water or steam model based on momentum, energy and mass conservation equations (Groppi, Belloli, Tronconi and Forzatti, 1995), which will ended with solving non linear equations (Groppi, Belloli, Tronconi and Forzatti, 1995).

As a summary, the above derived model proved that it can promote the transient response of the evaporation system by distributed parameter methods, as it has a

positive value with respect to safe and economic operation in a once through boiler (Groppi, Belloli, Tronconi and Forzatti, 1995).

To sum up all listed above, this research will emphasis on the hybrid modelling method using Distributed-Lumped Parameter Modelling Technique (DLPMT) developed by Whalley in 1988 as the appropriate method to model hybrid systems pertaining to long transmission lines while considering the four line parameters. The results will be compared with FEM and demonstrated in details.

Chapter-III

Research Methodology

3.1. Electric Power System Fundamentals

The electric power utilities are leading industries in the world (Glover and Sarma, 1994). The yearly growth rate of electric power generation, is continuously increasing owing to the extensively demand for electric power by consumers. The main fields, for example, where the electric power is widely used are in industries, businesses, houses, transportations, and offices (Al-Arainy, Qureshi and Malik, 2007).

Having such a challenging and a dynamic working environment, the design engineer is kept always ready to deal with these difficulties, especially if these problems occurs or linked to the future generation design of electric power generation systems (Glover and Sarma, 1994).

Basically, an electric power system can be defined as a network comprises interrelated machineries connected together and designed for the purpose of exchanging thermal and mechanical energies, continuously into electrical energy. Then, the generated electrical energy is delivered over long distances, taking into consideration acceptable tolerances to ensure safe use once it reaches its final destination. Upon usage by consumers, electrical energy is transformed once again

to non-electrical energies (Al-Arainy, Qureshi and Malik, 2007). This is in line with the conservation energy principle, which *simply states that during an interaction; energy can change from one form to another but that the total amount of energy remains constant. That is, energy cannot be created or destroyed* (Cengel and Boles, 1989).

Hence, the key role of the electric power system can be summarized as to generate, transmit, and distribute electrical energy in a safe, economical, efficient, environmentally compatible, reliable and communally satisfactory manner (Al-Arainy, Qureshi and Malik, 2007).

From the electric power system definition, it can be noticed that, one of the mandatory and essential element in the electrical network is the transmission lines, which are normally used to provide a community link between the remote ends of the eclectic power networks and its associated power equipment.

As a matter of fact, the transmission line can be represented by its four main distributed electrical parameters as stated below. Refer Figure-3.1 (Al-Arainy, Qureshi and Malik, 2005).

Series Resistance per unit length	R	Ohms/km
Series Inductance per unit length	L	Henry/km
Shunt Capacitance per unit length	C	Farad/km
Shunt Leakage conductance per unit length	G	Mhos/km

The series resistance is due to the line losses calculated from I^2R. On the other hand, the shunt conductance is due to the line losses calculated from V^2G and it occurs from the leakage currents passing between the conductors or between the ground and conductors. As a matter of fact, the shunt conductance of a transmission line is usually related to the insulator leakage and generally, considered as negligible due to its very small value. The third line parameter is the shunt capacitance (Glover and Sarma, 1994) and (Al-Arainy, Qureshi and Malik, 2007).

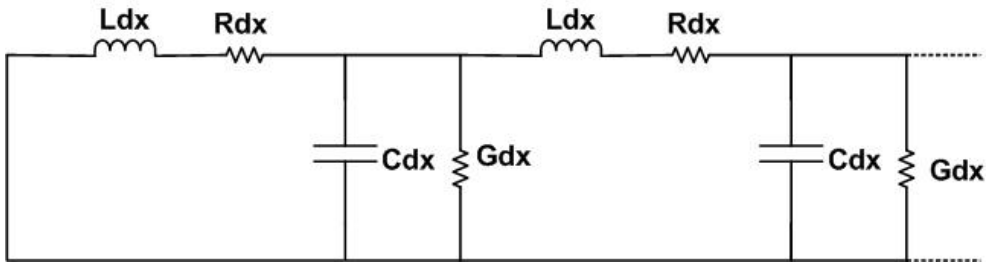

Figure-3.1: A long transmission line with its main distributed electrical parameters

At low frequencies the line components are considered as lumped such as inductors, resistors, and capacitors (Christopoulos, 2006).

It is to be noted that ideally, the transmission line has no losses. Thus, R and G are considered as zero. Accordingly, half the energy supplied by the source is stored in the magnetic field (inductance) and the second half is stored in the electric field (capacitance) (Christopoulos, 2006).

When the far end assumed as an open circuit, the current is obviously zero, and therefore, no energy is stored in the inductance. Recalling the conservation of energy principle, the total amount of energy remains constant, therefore, the second half of

the total stored energy in the inductance will be accommodated in the capacitance. Hence, the voltage doubles (Christopoulos, 2006).

However, practically, R and G are not equal to zero due to the existence of line losses and leakages. Considering these two parameters while modelling, leads to more complicated mathematical derivation, which will be further illustrated by the Author in the succeeding sections.

The most famous transmission lines used widely worldwide for transmitting electrical power supply are Over Head Transmission Lines - OHL, Underground Cable Transmission lines – UG/C and Gas Insulated Transmission Lines - GIL.

In fact, the complexity in designing and modelling the most suitable and convenient transmission lines for transmitting the electric powers, over extremely long distances with high effectiveness and efficiency was the focal research challenging the dissertation. In reality, this challenge has burdened on researchers to define, enhance and develop the Transmission Line Modelling techniques – TLM throughout the history starting in the early seventies as described in Chapter-II.

3.2. Project Overall Description

Dubai Electricity and Water Authority is currently executing, for the first time in Dubai, the installation of two transmission lines consist of 400kV underground cable circuits laid inside an open tunnel. These two circuits are required to connect two 400/132kV existing substations named as Nahda and Mushrif with a newly build 400/132kV substation known as Mamzar Beach (DEWA/EDF, 2009).

The first 400kV underground cable circuit transmission line is from Mushrif 400/132kV Substation to Mamzar Beach 400/132kV Substation. The approximate cable route length of this circuit is 11.5km. The second 400kV underground cable circuit transmission line is from Mamzar Beach 400/132kV Substation to Nahda 400/132kV Substation and the cable route length is 4km (DEWA/EDF, 2009). Refer Figure-3.2.

Figure-3.2: Block diagram shows substation's transmission line connections.

These two transmission lines are meant for transmitting full rated power under the cable rating in the worst climatic condition, taking into consideration the ventilation system, which can cope with the variable differences in power ratings and temperatures inside the tunnel (DEWA/EDF, 2009).

Below are the detailed technical descriptions of the project's main aspects.

3.2.1. 400kV Cables

The electrical system as stated above consists of two 400kV underground cable circuits installed inside a tunnel. Each one of these circuits is three single core cross-linked polyethylene (XLPE) cables and can supply 1500MVA, where, XLPE stands to cross linked polyethylene.

This type of electrical power cable is similar to all other types of electrical power cables in construction.

The main components of the cable are the conductor and the insulation. The conductor is used to carry the current and as it should be of low resistance to be able to do so. Copper is the preferred conductor. The insulation used is XLPE and it is used to isolate the conductive materials from each other and from their surroundings (Moore, 1997).

The other main components of the cable are screening, which is used to obtain a radial electrostatic field, a metal sheath, which is used to keep out moisture or to contain a pressurising medium, armouring, which is used to provide mechanical protection and corrosion protection for the metallic components, and a variety of additions extending, for example, to internal and external pipes to remove the heat generated in the cable (Moore, 1997).

Generally, as the voltage increases, the construction of the cable becomes more complex (Moore, 1997). Further, this cable is constructed to fulfil the requirement of the system, specifically, when operating with full load (DEWA/EDF, 2009).

Figure-3.3 shows the sectional view of the 400kV power cable and actual cable laid as shown in Appendix-A8, Picture-1.

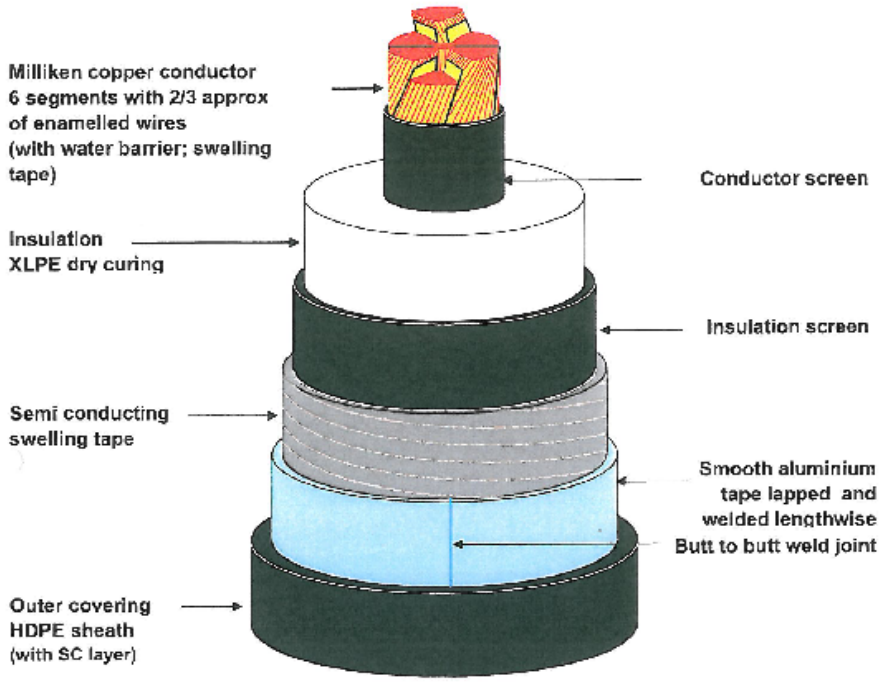

Figure-3.3: Sectional view of the 400kV power cable
(DEWA/Nexan, 2010)

3.2.2. Tunnels

The usage of tunnels for the purpose of installing underground transmission line power cables is usually due to accommodating multiple EHV cables. Further, from installation and operational point of view, it is easy to handle, install, test and maintain the cables. This is applicable even if deeply installed, as the cables will not affect other underground services (Matsumura, Fukuda, Fujiwara, Shiro, Watanabe, Sakaguchi, and Ooimo, 2006). Refer Appendix-A8, Picture-2.

In this project, the tunnel is constructed with strengthen concrete element which will be pre-cast or cast on situ having inlet and outlet air shafts to ensure the availability of natural / forced ventilation for the 400kV underground cables, laid inside this tunnel (DEWA/EDF, 2009).

3.2.3. Forced Cooling System

The main objective of having a ventilation system inside the tunnel under this project is to ensure maintaining the temperature of the cable conductor below 90°C, for which, the maximum air temperature within the tunnel should not exceed 62°C. Refer Appendix-A8, Picture-3.

The requirement of forced cooling system in this project is limited to natural air ventilation and forced air ventilation achieved by the means of fans.

Accordingly, the tunnel is divided into four main zones, where in each zone, two fans installed with one standby fan. Accordingly, the total numbers of fans installed inside the tunnel are 12, out of which 4 are as standby. These fans are powered by AC, 3 phase, and squirrel cage induction motors.

Besides, along with the ventilation shafts, there are exhaust shafts of a height of 4.5m above the ground level, and intake shafts of a height of 0.5 m above the ground level. Their installation numbers vary based on the route length of the cable. For instance, for Mushrif – Mamzer circuit, 13 exhaust shafts are installed and 10 intake shafts. Whereas for Nahda – Mamzer circuit, 4 exhaust shafts are installed and 6 intake shafts (DEWA/EDF, 2009).

Further, based on the design of the exhaust and intake shafts, the influence of wind on the ventilation system is considered to be negligible.

3.2.4. Terminal Load

The above project is connected to a terminal load consisting of four power transformers connected in parallel. Each power transformer is of 505MVA capacity, with a resistance of 0.979 ohm and an inductance of 0.345 Henry.

3.3. System Mathematical Modeling Methodology

The well known approach followed to solve any engineering problem is by formulating a mathematical model, which can be converted to the discrete time domain to evaluate the response performance, considering various aspects inline with the set of objectives required (Hui and Christopoulos, 1991).

As stated earlier, Finite Element method - FEM and the Transmission Line Modelling method - TLM intend to be deployed in this research, to examine and investigate the performance of the project described in Section-3.2 inline with the objectives in Chapter-I, Section-1.3.

As a matter of fact, the system in Section-3.2 is classified as a hybrid, since it comprises distributed and lumped elements. The distributed element represents the current and voltage passing throughout the length of the 400kV power cable. On the other side, the lumped elements represent the boundary conditions at the power

cable exit represented by the terminal load, and the system disturbances represented by fans installed inside the tunnel.

The modelling of this hybrid system will be based on the newly TLM for modelling long transmission lines developed by Whalley in 1988. The outcomes will be compared with the finite element method.

Accordingly, the mathematical derivation is divided into two parts. The first part is lumped, representing the fans and terminal loads and modelled by ordinary differential equations. The second part is the distributed, to represent the 400kV cables and modelled by partial differential equations (Close and Frederik, 1993).

It is to be noted that the distributed system will not have a finite number of points where state variables maybe defined. On the contrary, the lumped system can be described by a finite number of state variables (Close and Frederik, 1993).

Further, with TLM, the physical problem can be expressed with respect of an equivalent electronic network. Then, in the space time domain, a discrete model can be constructed considering the voltage pulse movement throughout the transmission lines as part of electric network (Rak, Gui, and Cogan, 1999).

In short, the fans and terminal load of the above referred hybrid system will be modelled as lumped. This is common for both FEM and TLM methods. With respect to the 400kV cables, these will be modelled as lumped while using the finite element method and as distributed while using TLM.

Further, it is important to add that, the 400kV cable long transmission line will be modelled considering the line with, and without losses.

3.3.1. Fan Mathematical Model

Apart of modelling, the fans are acting as a disturbance to the modelled hybrid system, which means adding a gain and a time delay. Further, the fans are normally, modelled as lumped element, and therefore, are presented by ordinary differential equations as below: -

$$T_1(s) = K_m I_f(s) \quad 3.1$$

$$I_f(s) = \frac{V_s(s)}{L_f s + R_f} \quad 3.2$$

$$T_1(s) = \frac{K_m V_s(s)}{L_f s + R_f} \quad 3.3$$

$$T_1(s) = \frac{K_m / R_f}{\tau s + 1} V_s(s) \quad 3.4$$

$1/(\tau s+1)$ is a time delay and K_m/R_f is a gain. This will act as a disturbance added to the overall system model while carrying out simulation.

It is to be highlighted that, the importance of paying attention to the disturbance while modelling is due to the over voltages and over currents on a transmission lines, which can develop from any input affecting the line. These disturbances can be from various sources such as induced or direct lightning strikes, sudden closing or opening of a line and faults or short circuits. Subsequently, these disturbances start to propagate travelling waves toward the end of an installed termination or

line. The terminations can be, for example, a load or a substation. Generally, the disturbances illustrated in the form of travelling waves are ultimately, either transmitted or reflected or distorted or attenuated throughout the time taken to propagate with the energies stored inside the propagated waves is fully absorbed (Al-Arainy, Qureshi and Malik, 2005).

3.3.2. Terminal Load Mathematical Model

The terminal load is same as the fan, acting as a lumped element and thus, is modelled also by ordinary differential equations as part of the mathematical model derivation.

The terminal load, which is connected to the hybrid system, consists of an inductive load represented in the form of resistive and inductive parts. In this regard, the terminal load impedance can be demonstrated as: -

$$V_L(s) = (L_L s + R_L) I_L(s) \qquad 3.5$$

3.3.3. 400kV Cable Mathematical Model - without Line Losses

Ideally, for simplicity, the line losses are ignored by most of the researchers while deriving the mathematical model of a transmission line. Thus, R and G of the transmission line parameters are considered as zero. In this case, the line behaves ideally as there is no attenuation in the wave magnitudes or any distortions in the waveforms of the forward, as well as the backward, travelling waves (Al-Arainy, Qureshi and Malik, 2005). Practically, this is not the case, as each transmission line is subjected to line losses.

Below are the mathematical models derivations considering ideal 400kV cable transmission line, by using Finite Element and TLM as modelling methods.

3.3.3.1. Finite Element Method

As it is known and detailed earlier, for modelling purpose while adopting FEM, the transmission line needs first to be divided into numbers of sections of equal length.

In this regard and with respect to above described hybrid system, the 400kV cable transmission line is selected to be divided into four sections each of 2.875km out of the total transmission line length, which is equal to 11.5km. Each section is treated as lumped in addition to the terminal load and fans. Figure-3.4, illustrate the transmission line divided into four finite element sections.

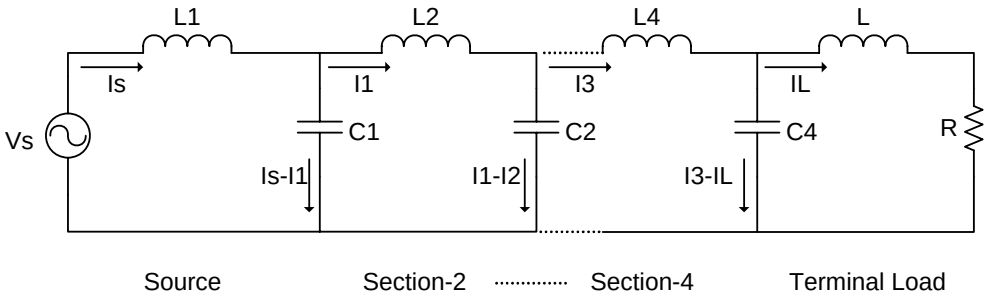

Figure-3.4: Transmission Line divided into four finite element sections considering its two line parameters

Always the lumped elements are linked with the ordinary differential equations, which will be, in this case, extracted from Figure-3.4 with respect to each segment by applying Kirchhoff voltage law.

Detailed ordinary differential equations and derivations using FEM are outlined below.

Considering no line losses (R and G = 0)

$$V_s = L_1 s I_s + \frac{1}{C_1 s}(I_s - I_1) \quad 3.6$$

$$0 = L_2 s I_1 + \frac{1}{C_2 s}(I_1 - I_2) + \frac{1}{C_1 s}(I_1 - I_s) \quad 3.7$$

$$0 = L_3 s I_2 + \frac{1}{C_3 s}(I_2 - I_3) + \frac{1}{C_2 s}(I_2 - I_1) \quad 3.8$$

$$0 = L_4 s I_3 + \frac{1}{C_4 s}(I_3 - I_L) + \frac{1}{C_3 s}(I_3 - I_2) \quad 3.9$$

$$0 = (L_L s + R_L) I_L + \frac{1}{C_4 s}(I_L - I_3) \quad 3.10$$

$$\begin{bmatrix} V_s \\ 0 \\ 0 \\ 0 \\ 0 \end{bmatrix} = \begin{bmatrix} L_1 s + \frac{1}{C_1 s} & -\frac{1}{C_1 s} & 0 \\ -\frac{1}{C_1 s} & L_2 s + \frac{1}{C_2 s} + \frac{1}{C_1 s} & -\frac{1}{C_2 s} \\ 0 & -\frac{1}{C_2 s} & L_3 s + \frac{1}{C_3 s} + \frac{1}{C_2 s} \\ 0 & 0 & -\frac{1}{C_3 s} \\ 0 & 0 & 0 \end{bmatrix} \text{----------}$$

$$\text{- - - - - - - - - - - - - - - -}\begin{bmatrix} 0 & 0 \\ 0 & 0 \\ -\frac{1}{C_3 s} & 0 \\ L_4 s + \frac{1}{C_4 s} + \frac{1}{C_3 s} & -\frac{1}{C_4 s} \\ -\frac{1}{C_4 s} & L_L s + R_L + \frac{1}{C_4 s} \end{bmatrix} \times \begin{bmatrix} I_s \\ I_1 \\ I_2 \\ I_3 \\ I_L \end{bmatrix} \qquad 3.11$$

From the above differential equations, it can be noticed that, there is a substantial increase in mathematical complexity while modelling using finite element form, as the number of segments increases. For example, in this regard, with four cable sections, the system model generated an impedance of 5 by 5 matrix having eleven eigenvalues. The size of the matrix can increase with the increase of the number of sections, with off course the increase in the mathematical complexity.

Maple software is used as an aiding tool to find out the inverse system impedance, as shown in Appendix – A3 and A4 in order to compute system's supplied and load currents.

3.3.3.2. Transmission Line Modelling Method

The 400kV cable is a long transmission line. Therefore, it is classified as a distributed element and presented in the mathematical model derivation by partial differential equations.

For mathematical modelling purpose, a length of dx of the 400kV cable transmission line in a positive x direction having a voltage V and current I is considered as shown in Figure-3.5 (Al-Arainy, Qureshi and Malik, 2005).

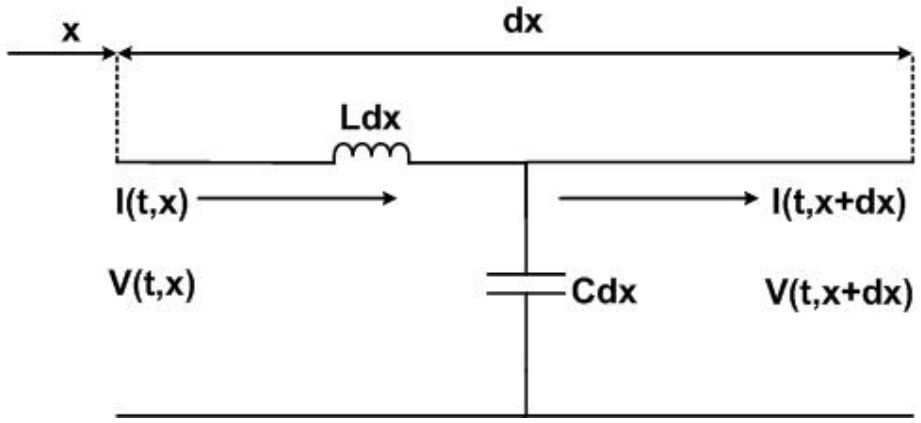

Figure-3.5: Distributed 400kV Cable transmission line model with line Inductance and Capacitance

In this regard, the voltage drop in the length dx, while ignoring line losses is given as follow in line with the hybrid modelling method proposed by Whalley (Bartlett, Whalley, and Rizvi, 1998): -

$$V(t,x) - V(t,x+dx) = L\frac{\partial I}{\partial t}(t,x).dx \qquad 3.12$$

$$V(t,x+dx) - V(t,x) = -L\frac{\partial I}{\partial t}(t,x).dx \qquad 3.13$$

This is the voltage drop through the line inductance per unit length.

$$I(t,x) - I(t,x+dx) = C\frac{\partial V}{\partial t}(t,x+dx).dx \qquad 3.14$$

$$I(t,x+dx) - I(t,x) = -C\frac{\partial V}{\partial t}(t,x+dx).dx \qquad 3.15$$

This is the shunt current through the line capacitance per unit length.

$$\frac{\partial V(t,x)}{\partial x} = -L\frac{\partial I}{\partial t}(t,x) \quad 3.16$$

$$\frac{\partial I(t,x)}{\partial x} = -C\frac{\partial V}{\partial t}(t,x+dx) \quad 3.17$$

Taking the Laplace transformation for equations (3.16) and (3.17) with respect of time, these equations can be expressed in s-domain as follow: -

$$\frac{dV(s,x)}{dx} = -LsI(s,x) \quad 3.18$$

$$\frac{dI(s,x)}{dx} = -CsV(s,x) \quad 3.19$$

Differentiate equations (3.18) and (3.19) with respect of x: -

$$\frac{d^2V}{dx^2} = -Ls\frac{dI}{dx} = -Ls^2I(s,x) \quad 3.20$$

$$\frac{d^2I}{dx^2} = -Cs\frac{dV}{dx} = -Cs^2V(s,x) \quad 3.21$$

Equations (3.20 and 3.21) are called the transmission line wave equations and below are the solution for these two equations.

If a propagation function is defined as: -

$$\Gamma(s) = s\sqrt{LC} \quad 3.22$$

Accordingly, the general solutions for V(s,x) and I(s,x) are: -

$$V(s,x) = A\cosh\Gamma(s)x + B\sinh\Gamma(s)x \quad 3.23$$

$$I(s,x) = D\sinh\Gamma(s)x + E\cosh\Gamma(s)x \quad 3.24$$

When x=0 in equations (3.23) and (3.24), V(s,0) = A and I(s,0) = E 3.25

Differentiate equations (3.23) and (3.24) to solve for B and D: -

$$\frac{dV}{dx}(s,x) = -LsI(s,x) = A\Gamma(s)\sinh\Gamma(s)x + B\Gamma(s)\cosh\Gamma(s)x \quad 3.26$$

$$\frac{dI}{dx}(s,x) = -CsV(s,x) = D\Gamma(s)\cosh\Gamma(s)x + E\Gamma(s)\sinh\Gamma(s)x \quad 3.27$$

Boundary conditions: When x=0 in equations (3.26) and (3.27),

$$-LsI(s,x) = B\Gamma(s) \text{ from which, } B = \frac{-Ls}{\Gamma(s)}I(s,0) = -\sqrt{\frac{L}{C}}I(s,0) \text{ and} \quad 3.28$$

$$D = \frac{-Cs}{\Gamma(s)}V(s,0) = -\frac{Cs}{s\sqrt{LC}}V(s,0) = -\sqrt{\frac{C}{L}}V(s,0) \quad 3.29$$

If the characteristic impedance is defined as: -

$$\zeta = \sqrt{\frac{L}{C}} \text{ then, } B = -\zeta I(s,0) \text{ and } D = -\zeta^{-1}V(s,0) \quad 3.30$$

Accordingly, equations (3.23) and (3.24) will be after substituting in A, B, D, and E:-

$$V(s,x) = \cosh\Gamma(s)xV(s,0) - \zeta\sinh\Gamma(s)xI(s,0) \quad 3.31$$

$$I(s,x) = -\zeta^{-1}\sinh\Gamma(s)xV(s,0) + \cosh\Gamma(s)xI(s,0) \quad 3.32$$

$$\begin{bmatrix} V(s,x) \\ I(s,x) \end{bmatrix} = \begin{bmatrix} \cosh\Gamma(s)x & -\zeta\sinh\Gamma(s)x \\ -\zeta^{-1}\sinh\Gamma(s)x & \cosh\Gamma(s)x \end{bmatrix} \begin{bmatrix} V(s,0) \\ I(s,0) \end{bmatrix} \quad 3.33$$

At a distance l along the cable, equation (3.33) will be: -

$$\begin{bmatrix} V(s,l) \\ I(s,l) \end{bmatrix} = \begin{bmatrix} \cosh\Gamma(s)l & -\zeta\sinh\Gamma(s)l \\ -\zeta^{-1}\sinh\Gamma(s)l & \cosh\Gamma(s)l \end{bmatrix} \begin{bmatrix} V(s,0) \\ I(s,0) \end{bmatrix} \quad 3.34$$

Re-arrange equation (3.34) as follow: -

$$V(s,x) - \cosh\Gamma(s)xV(s,0) = -\zeta\sinh\Gamma(s)xI(s,0) \quad 3.35$$

$$I(s,x) = -\zeta^{-1}\sinh\Gamma(s)xV(s,0) + \cosh\Gamma(s)xI(s,0) \quad 3.36$$

$$\zeta^{-1}\sinh\Gamma(s)xV(s,0) = -I(s,x) + \cosh\Gamma(s)xI(s,0) \quad 3.37$$

$$\begin{bmatrix} 1 & -\cosh\Gamma(s)x \\ 0 & \zeta^{-1}\sinh\Gamma(s)x \end{bmatrix}\begin{bmatrix} V(s,x) \\ V(s,0) \end{bmatrix} = \begin{bmatrix} 0 & -\zeta\sinh\Gamma(s)x \\ -1 & \cosh\Gamma(s)x \end{bmatrix}\begin{bmatrix} I(s,x) \\ I(s,0) \end{bmatrix} \quad 3.38$$

$$\begin{bmatrix} V(s,x) \\ V(s,0) \end{bmatrix} = \begin{bmatrix} 1 & -\cosh\Gamma(s)x \\ 0 & \zeta^{-1}\sinh\Gamma(s)x \end{bmatrix}^{-1}\begin{bmatrix} 0 & -\zeta\sinh\Gamma(s)x \\ -1 & \cosh\Gamma(s)x \end{bmatrix}\begin{bmatrix} I(s,x) \\ I(s,0) \end{bmatrix} \quad 3.39$$

$$\begin{bmatrix} V(s,x) \\ V(s,0) \end{bmatrix} = \frac{\begin{bmatrix} \zeta^{-1}\sinh\Gamma(s)x & \cosh\Gamma(s)x \\ 0 & 1 \end{bmatrix}}{\zeta^{-1}\sinh\Gamma(s)x}\begin{bmatrix} 0 & -\zeta\sinh\Gamma(s)x \\ -1 & \cosh\Gamma(s)x \end{bmatrix}\begin{bmatrix} I(s,x) \\ I(s,0) \end{bmatrix} \quad 3.40$$

$$\begin{bmatrix} V(s,x) \\ V(s,0) \end{bmatrix} = \frac{\begin{bmatrix} -\cosh\Gamma(s)x & -\sinh^2\Gamma(s)x+\cosh^2\Gamma(s)x \\ -1 & \cosh\Gamma(s)x \end{bmatrix}}{\zeta^{-1}\sinh\Gamma(s)x}\begin{bmatrix} I(s,x) \\ I(s,0) \end{bmatrix} \quad 3.41$$

As: $\cosh^2\Gamma(s)x-\sinh^2\Gamma(s)x=1$ 3.42

$$\frac{\cosh\Gamma(s)x}{\sinh\Gamma(s)x}=ctnh\Gamma(s)x\,,\frac{1}{\sinh\Gamma(s)x}=\operatorname{csc}h\Gamma(s)x\,,\frac{1}{\cosh\Gamma(s)x}=\sec h\Gamma(s)x \quad 3.43$$

Then,

$$\begin{bmatrix} V(s,x) \\ V(s,0) \end{bmatrix} = \begin{bmatrix} -\zeta ctnh\Gamma(s)x & \zeta\operatorname{csc}h\Gamma(s)x \\ -\zeta\operatorname{csc}h\Gamma(s)x & \zeta ctnh\Gamma(s)x \end{bmatrix}\begin{bmatrix} I(s,x) \\ I(s,0) \end{bmatrix} \quad 3.44$$

Let: $V(s,0)=V_s(s),V(s,l)=V_L(s)$ and $I(s,0)=I_s(s),I(s,l)=I_L(s)$ 3.45

$$-ctnh\Gamma(s)l=(e^{2\Gamma(s)l}+1)/(e^{2\Gamma(s)l}-1)=w(s) \quad 3.46$$

$$-\operatorname{csc}h\Gamma(s)l=(ctnh^2\Gamma(s)l-1)^{1/2}=(w\ (s)-1)^{1/2} \quad 3.47$$

Hence, below is the equivalent to equation (3.44)

$$\begin{bmatrix} V_s(s) \\ V_L(s) \end{bmatrix} = \begin{bmatrix} \zeta w(s) & -\zeta(w^2(s)-1)^{\frac{1}{2}} \\ \zeta(w^2(s)-1)^{\frac{1}{2}} & -\zeta w(s) \end{bmatrix}\begin{bmatrix} I_s(s) \\ I_L(s) \end{bmatrix} \quad 3.48$$

This is the 400kV cable transmission line model using the Distributed Parameter

System modelling technique.

In the numerical solution, it is important to specify the finite spatial length (l), finite time interval (Δt) and the spatial (Δx). The importance behind that is that without the finite spatial length (l), there will be a requirement of unlimited number of memory storage locations. It is necessary to ensure that at the highest frequency of interest (l) is always less than the wave length (Christopoulos, 2006).

In the same manner, without the finite time interval (Δt), longer running time is needed. Further, (Δt) can be a small set value but it cannot be zero (Christopoulos, 2006).

3.3.3.3. Distributed-Lumped Mathematical Model

From equations (3.5 and 3.48)

$$\begin{bmatrix} V_s(s) \\ V_L(s)+L_L s+R_L \end{bmatrix} = \begin{bmatrix} \zeta w(s) & -\zeta(w^2(s)-1)^{\frac{1}{2}} \\ \zeta(w^2(s)-1)^{\frac{1}{2}} & -\zeta w(s) \end{bmatrix} \begin{bmatrix} I_s(s) \\ I_L(s) \end{bmatrix} \quad 3.49$$

By considering $V_L(s)=0$ as the only source supplying this system is $V_s(s)$ equation (3.49) is re-written as below: -

$$\begin{bmatrix} V_s(s) \\ L_L s+R_L \end{bmatrix} = \begin{bmatrix} \zeta w(s) & -\zeta(w^2(s)-1)^{\frac{1}{2}} \\ \zeta(w^2(s)-1)^{\frac{1}{2}} & -\zeta w(s) \end{bmatrix} \begin{bmatrix} I_s(s) \\ I_L(s) \end{bmatrix} \quad 3.50$$

$$\begin{bmatrix} V_s(s) \\ 0 \end{bmatrix} = \begin{bmatrix} \zeta w(s) & -\zeta(w^2(s)-1)^{\frac{1}{2}} \\ \zeta(w^2(s)-1)^{\frac{1}{2}} & -\zeta w(s)-(L_L s+R_L) \end{bmatrix} \begin{bmatrix} I_s(s) \\ I_L(s) \end{bmatrix} \quad 3.51$$

$$\begin{bmatrix} I_s(s) \\ I_L(s) \end{bmatrix} = [Z]^{-1} \begin{bmatrix} V_s(s) \\ 0 \end{bmatrix} = [Z]^{-1} [V_s(s)] \tag{3.52}$$

$$\text{Where } [Z]^{-1} = \frac{\begin{bmatrix} -\zeta w(s) - (L_L s + R_L) \\ -\zeta (w^2(s) - 1)^{\frac{1}{2}} \end{bmatrix}}{-\zeta w(s)(L_L s + R_L) + \zeta)} = \frac{\begin{bmatrix} \zeta w(s) + (L_L s + R_L) \\ \zeta (w^2(s) - 1)^{\frac{1}{2}} \end{bmatrix}}{\zeta w(s)(L_L s + R_L) + \zeta^2} \tag{3.53}$$

Substitute equations (3.53) in (3.52)

$$\begin{bmatrix} I_s(s) \\ I_L(s) \end{bmatrix} = \frac{\begin{bmatrix} \zeta w(s) + (L_L s + R_L) \\ \zeta (w^2(s) - 1)^{\frac{1}{2}} \end{bmatrix}}{\zeta w(s)(L_L s + R_L) + \zeta^2} V_s(s) \tag{3.54}$$

$$\begin{bmatrix} I_s(s) \\ I_L(s) \end{bmatrix} = \begin{bmatrix} \zeta w(s) + (L_L s + R_L) \\ \zeta (w^2(s) - 1)^{\frac{1}{2}} \end{bmatrix} \frac{V_s(s)}{\Delta(s)} \tag{3.55}$$

$$\text{Where } \Delta(s) = \zeta w(s)(L_L s + R_L) + \zeta^2 \tag{3.56}$$

Considering equation (3.4) as disturbance / delay added to the system, equation (3.55) can be illustrated as below:

$$\begin{bmatrix} I_s(s) \\ I_L(s) \end{bmatrix} = \begin{bmatrix} \zeta w(s) + (L_L s + R_L) \\ \zeta (w^2(s) - 1)^{\frac{1}{2}} \end{bmatrix} \frac{V_s(s)}{\Delta(s)} \frac{K_m / R_f}{\tau s + 1} \tag{3.57}$$

3.3.3.4. Subassembly Simulation for w(s)

$$w(s) = \frac{e^{2l\Gamma(s)} + 1}{e^{2l\Gamma(s)} - 1} \tag{3.58}$$

$$\Gamma(s) = s\sqrt{LC} \tag{3.59}$$

In order to be able to design w(s) in Simulink, we have to put it in delay form as

follow: -

$$w(s)=\frac{1+e^{-2l\Gamma(s)}}{1-e^{-2l\Gamma(s)}}=\frac{1+e^{-2ls\sqrt{LC}}}{1-e^{-2ls\sqrt{LC}}}=\frac{1+e^{-Ts}}{1-e^{-Ts}} \text{ where } T=2l\sqrt{LC} \quad 3.60$$

3.3.3.5. Subassembly Simulation for $\zeta(w^2(s)-1)^{1/2}$

By substituting equation (3.60) in the expression $\zeta(w^2(s)-1)^{1/2}$, we get the following: -

$$(w^2(s)-1)^{1/2}=\frac{2e^{-l\Gamma(s)}}{1-e^{-2l\Gamma(s)}}=\frac{2e^{-ls\sqrt{LC}}}{1-e^{-2ls\sqrt{LC}}}=\frac{2e^{-0.5Ts}}{1-e^{-Ts}} \text{ where } T=2l\sqrt{LC} \quad 3.61$$

3.3.4. 400kV Cable Mathematical Model - with Line Losses

The ideal transmission line has no line losses. However, the transmission line in practice has losses R and G where these parameters are not equal to zero. In this case, the line will have attenuation in the wave magnitudes or distortions in the waveforms of the forward as well as the backward travelling waves (Al-Arainy, Qureshi and Malik, 2005).

The losses in the transmission line can be minimized by increasing the size of the conductor and by using bundled conductors (Mohan, 2012). However, increasing the size of the conductor is not practical as it will affect the overall design of the transmission line to accommodate this large size of conductor. Handling the transmission line during manufacturing and installation are other problems that can be faced, in addition to the increase in the cost.

To avoid such increase in the cost and related design issues, the resistance per unit length (R) of the transmission line is usually kept small as much as possible. On the other side, the shunt conductance (G) is considered as negligible due to its small value. This is in fact, a reason for neglecting (G) by most researchers while carrying out transmission line modelling. Also, it is to avoid complexity in mathematical derivation (Mohan, 2012).

Recalling from Chapter-I, one of the objectives of this research is to consider all the four transmission line parameters in the modelling of long transmission line. This is in order to illustrate the more accurate modelling method to be adopted in such cases and to achieve satisfactory results.

Below are the mathematical models derivations considering 400kV cable transmission line losses, by using Finite Element and TLM as modelling methods.

3.3.4.1. Finite Element Method

As detailed earlier, for modelling purpose while adopting FEM, the transmission line or any system needs to be divided into a number of sections, of equal length.
In this regard and with respect to above described hybrid system, the 400kV cable transmission line is selected to be divided into four sections each of 2.875km out of the total transmission line length, which is equal to 11.5km. Each section is treated as lumped in addition to the terminal load and fans. Figure-3.6, illustrate the transmission line divided into four finite element sections with its two line parameters.

The lumped element models are always linked with the use ordinary differential equations, which will be in this case extracted from Figure-3.6 with respect to each segment by applying Kirchhoff voltage law.

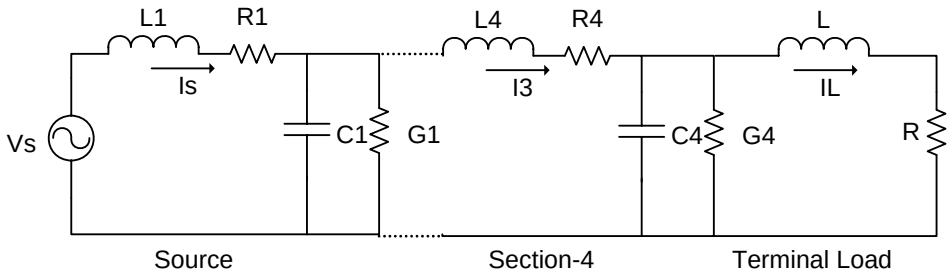

Figure-3.6: Transmission Line divided into four finite element sections considering its four line parameters.

Detailed ordinary differential equations and derivations using FEM are outlined below.

Considering no line losses (R and G ≠ 0)

$$V_s = L_1 s + R_1) I_s + \frac{G_1}{C_1 s G_1 + 1}(I_s + I_1) \qquad 3.62$$

$$0 = \frac{G_1}{C_1 s G_1 + 1}(I_1 - I_s) + (L_2 s + R_2) I_1 + \frac{G_2}{C_2 s G_2 + 1}(I_1 - I_2) \qquad 3.63$$

$$0 = \frac{G_2}{C_2 s G_2 + 1}(I_2 - I_1) + (L_3 s + R_3) I_2 + \frac{G_3}{C_3 s G_3 + 1}(I_2 - I_3) \qquad 3.64$$

$$0 = \frac{G_3}{C_3 s G_3 + 1}(I_3 - I_2) + (L_4 s + R_4) I_3 + \frac{G_4}{C_4 s G_4 + 1}(I_3 - I_L) \qquad 3.65$$

$$0 = \frac{G_4}{C_4 s G_4 + 1}(I_L - I_3) + (L_L s + R_L) I_L \qquad 3.66$$

$$\begin{bmatrix} V_s \\ 0 \\ 0 \\ 0 \\ 0 \end{bmatrix} = \begin{bmatrix} L_1 s + R_1 + \frac{G_1}{C_1 s G_1 + 1} & -\frac{G_1}{C_1 s G_1 + 1} & 0 \\ -\frac{G_1}{C_1 s G_1 + 1} & \frac{G_1}{C_1 s G_1 + 1} + L_2 s + R_2 + \frac{G_2}{C_2 s G_2 + 1} & \frac{G_2}{C_2 s G_2 + 1} \\ 0 & -\frac{G_2}{C_2 s G_2 + 1} & \frac{G_2}{C_2 s G_2 + 1} + L_3 s + R_3 + \frac{G_3}{C_3 s G_3 + 1} \\ 0 & 0 & -\frac{G_3}{C_3 s G_3 + 1} \\ 0 & 0 & 0 \end{bmatrix} \text{ - - - -}$$

$$\text{- - - - - - - - -} \begin{bmatrix} 0 & 0 \\ 0 & 0 \\ -\frac{G_3}{C_3 s G_3 + 1} & 0 \\ \frac{G_3}{C_3 s G_3 + 1} + L_4 s + R_4 + \frac{G_4}{C_4 s G_4 + 1} & 0 \\ -\frac{G_4}{C_4 s G_4 + 1} & L_L s + R_L + \frac{G_4}{C_4 s G_4 + 1} \end{bmatrix} \times \begin{bmatrix} I_s \\ I_1 \\ I_2 \\ I_3 \\ I_L \end{bmatrix} \quad 3.67$$

From the above extracted system differential equations, it can be noticed that, there is a substantial increase in mathematical complexity while modelling using the Finite Element form as the number of segments increases. For example, with four cable sections, the system model generated an impedance of 5 by 5 matrix having eleven eigenvalues. The size of the matrix can increase with the increase of the number of sections, with off course an increase in the mathematical complexity.

Maple software is used as a tool to find out the inverse of system impedance matrix as shown in Appendix – A5 and A6 in order to compute system's supplied and load currents.

3.3.4.2. Transmission Line Modelling Method

The 400kV cable is a long transmission line. Therefore, it is classified as a distributed element and presented in the mathematical model derivation by partial differential equations.

For mathematical modelling purpose, a length of dx of the 400kV cable transmission line in a positive x direction having a voltage V and current I is considered as shown in Figure-3.7 (Al-Arainy, Qureshi and Malik, 2005).

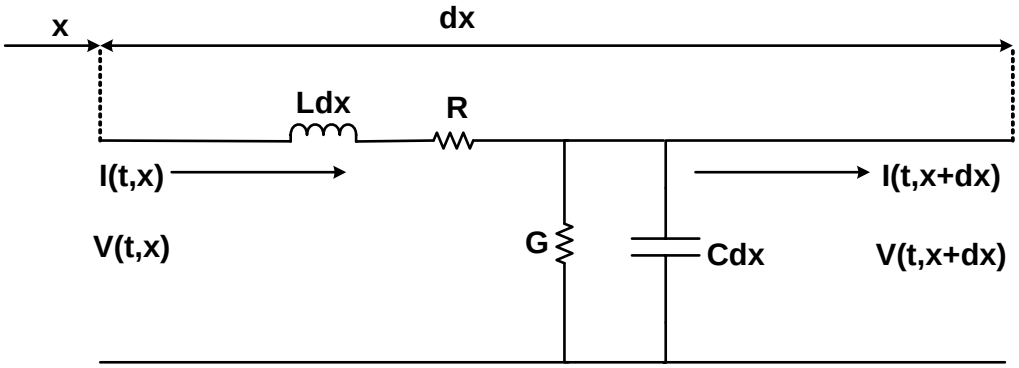

Figure-3.7: Distributed 400kV Cable transmission line model with line Inductance, Series Resistance, Capacitance and Shunt Resistance

In this regard, the voltage drop in the length dx, while considering line losses is given as follow in line with the hybrid modelling method proposed by Whalley (Bartlett, Whalley, and Rizvi, 1998): -

$$V(t,x) - V(t,x+dx) = L\frac{\partial I}{\partial t}(t,x).dx + RI(t,x) \qquad 3.68$$

$$V(t,x+dx) - V(t,x) = -L\frac{\partial I}{\partial t}(t,x).dx - RI(t,x) \qquad 3.69$$

This is the voltage drop through the line inductance and resistance per unit length.

$$I(t,x) - I(t,x+dx) = C\frac{\partial V}{\partial t}(t,x+dx).dx + GV(t,x+dx) \quad 3.70$$

$$I(t,x+dx) - I(t,x) = -C\frac{\partial V}{\partial t}(t,x+dx).dx - GV(t,x+dx) \quad 3.71$$

This is the shunt current through the line capacitance and shunt conductance per unit length.

$$\frac{\partial V(t,x)}{\partial x} = -L\frac{\partial I}{\partial t}(t,x) - RI(t,x) \quad 3.72$$

$$\frac{\partial I(t,x)}{\partial x} = -C\frac{\partial V}{\partial t}(t,x+dx) - GV(t,x+dx) \quad 3.73$$

Taking the Laplace transformation for equations (3.72) and (3.73) with respect of time, these equations can be expressed in the frequency domain as follow: -

$$\frac{dV(s,x)}{dx} = -(Ls+R)I \quad 3.74$$

$$\frac{dI(s,x)}{dx} = -(Cs+G)V \quad 3.75$$

Differentiate equations (3.74) and (3.75) with respect of x: -

$$\frac{d^2V}{dx^2} = -(Ls+R)\frac{dI}{dx} \quad 3.76$$

$$\frac{d^2I}{dx^2} = -(Cs+G)\frac{dV}{dx} \quad 3.77$$

Equations (3.76 and 3.77) are called the transmission line wave equations and below are the solution for these equations.

If a propagation function is defined as: -

$$\Gamma(s) = \sqrt{(Ls+R)(Cs+G)} \quad 3.78$$

Accordingly, the general solutions for V(s,x) and I(s,x) are: -

$$V(s,x) = A\cosh\Gamma(s)x + B\sinh\Gamma(s)x \quad 3.79$$

$$I(s,x) = D\sinh\Gamma(s)x + E\cosh\Gamma(s)x \quad 3.80$$

When x=0 in equations (3.79) and (3.88), V(s,0) = A and I(s,0) = E 3.81

Differentiate equations (3.79) and (3.88) to solve for B and D: -

$$\frac{dV}{dx}(s,x) = -(Ls+R)I(s,x) = A\Gamma(s)\sinh\Gamma(s)x + B\Gamma(s)\cosh\Gamma(s)x \quad 3.82$$

$$\frac{dI}{dx}(s,x) = -(Cs+G)V(s,x) = D\Gamma(s)\cosh\Gamma(s)x + E\Gamma(s)\sinh\Gamma(s)x \quad 3.83$$

Boundary conditions: When x=0 in equations (3.82) and (3.83),

$-(Ls+R)I(s,x) = B\Gamma(s)$ from which, $B = \frac{-(Ls+R)}{\Gamma(s)}I(s,0) = -\sqrt{\frac{Ls+R}{Cs+G}}I(s,0)$ and 3.84

$$D = \frac{-(Cs+G)}{\Gamma(s)}V(s,0) = -\frac{Cs+G}{s\sqrt{(Ls+R)(Cs+G)}}V(s,0) = -\sqrt{\frac{Cs+G}{Ls+R}}V(s,0) \quad 3.85$$

If the characteristic impedance is defined as: -

$\zeta = \sqrt{\frac{Ls+R}{Cs+G}}$ then, $B = -\zeta I(s,0)$ and $D = -\zeta^{-1}V(s,0)$ 3.86

Accordingly, equations (3.79) and (3.80) will be after substituting in A, B, D, and E: -

$$V(s,x) = \cosh\Gamma(s)xV(s,0) - \zeta\sinh\Gamma(s)xI(s,0) \quad 3.87$$

$$I(s,x) = -\zeta^{-1}\sinh\Gamma(s)xV(s,0) + \cosh\Gamma(s)xI(s,0) \quad 3.88$$

$$\begin{bmatrix} V(s,x) \\ I(s,x) \end{bmatrix} = \begin{bmatrix} \cosh\Gamma(s)x & -\zeta\sinh\Gamma(s)x \\ -\zeta^{-1}\sinh\Gamma(s)x & \cosh\Gamma(s)x \end{bmatrix} \begin{bmatrix} V(s,0) \\ I(s,0) \end{bmatrix} \quad 3.89$$

At a distance l along the cable, equation (3.89) will be: -

$$\begin{bmatrix} V(s,l) \\ I(s,l) \end{bmatrix} = \begin{bmatrix} \cosh\Gamma(s)l & -\zeta\sinh\Gamma(s)l \\ -\zeta^{-1}\sinh\Gamma(s)l & \cosh\Gamma(s)l \end{bmatrix} \begin{bmatrix} V(s,0) \\ I(s,0) \end{bmatrix} \quad 3.90$$

Re-arrange equation (3.90) as follow: -

$$V(s,x) - \cosh\Gamma(s)xV(s,0) = -\zeta\sinh\Gamma(s)xI(s,0) \quad 3.91$$

$$I(s,x) = -\zeta^{-1}\sinh\Gamma(s)xV(s,0) + \cosh\Gamma(s)xI(s,0) \quad 3.92$$

$$\zeta^{-1}\sinh\Gamma(s)xV(s,0) = -I(s,x) + \cosh\Gamma(s)xI(s,0) \quad 3.93$$

$$\begin{bmatrix} 1 & -\cosh\Gamma(s)x \\ 0 & \zeta^{-1}\sinh\Gamma(s)x \end{bmatrix}\begin{bmatrix} V(s,x) \\ V(s,0) \end{bmatrix} = \begin{bmatrix} 0 & -\zeta\sinh\Gamma(s)x \\ -1 & \cosh\Gamma(s)x \end{bmatrix}\begin{bmatrix} I(s,x) \\ I(s,0) \end{bmatrix} \quad 3.94$$

$$\begin{bmatrix} V(s,x) \\ V(s,0) \end{bmatrix} = \begin{bmatrix} 1 & -\cosh\Gamma(s)x \\ 0 & \zeta^{-1}\sinh\Gamma(s)x \end{bmatrix}^{-1}\begin{bmatrix} 0 & -\zeta\sinh\Gamma(s)x \\ -1 & \cosh\Gamma(s)x \end{bmatrix}\begin{bmatrix} I(s,x) \\ I(s,0) \end{bmatrix} \quad 3.95$$

$$\begin{bmatrix} V(s,x) \\ V(s,0) \end{bmatrix} = \frac{\begin{bmatrix} \zeta^{-1}\sinh\Gamma(s)x & \cosh\Gamma(s)x \\ 0 & 1 \end{bmatrix}}{\zeta^{-1}\sinh\Gamma(s)x}\begin{bmatrix} 0 & -\zeta\sinh\Gamma(s)x \\ -1 & \cosh\Gamma(s)x \end{bmatrix}\begin{bmatrix} I(s,x) \\ I(s,0) \end{bmatrix} \quad 3.96$$

$$\begin{bmatrix} V(s,x) \\ V(s,0) \end{bmatrix} = \frac{\begin{bmatrix} -\cosh\Gamma(s)x & -\sinh^2\Gamma(s)x + \cosh^2\Gamma(s)x \\ -1 & \cosh\Gamma(s)x \end{bmatrix}}{\zeta^{-1}\sinh\Gamma(s)x}\begin{bmatrix} I(s,x) \\ I(s,0) \end{bmatrix} \quad 3.97$$

As:

$$\cosh^2\Gamma(s)x - \sinh^2\Gamma(s)x = 1 \quad 3.98$$

$$\frac{\cosh\Gamma(s)x}{\sinh\Gamma(s)x} = ctnh\Gamma(s)x\,,\frac{1}{\sinh\Gamma(s)x} = \operatorname{csc}h\Gamma(s)x\,,\frac{1}{\cosh\Gamma(s)x} = \sec h\Gamma(s)x \quad 3.99$$

Then,

$$\begin{bmatrix} V(s,x) \\ V(s,0) \end{bmatrix} = \begin{bmatrix} -\zeta ctnh\Gamma(s)x & \zeta\operatorname{csc}h\Gamma(s)x \\ -\zeta\operatorname{csc}h\Gamma(s)x & \zeta ctnh\Gamma(s)x \end{bmatrix}\begin{bmatrix} I(s,x) \\ I(s,0) \end{bmatrix} \quad 3.100$$

Let: $V(s,0) = V_s(s), V(s,l) = V_L(s)$ and $I(s,0) = I_s(s), I(s,l) = I_L(s)$ 3.101

$$-ctnh\Gamma(s)l = (e^{2\Gamma(s)l} + 1)/(e^{2\Gamma(s)l} - 1) = w(s) \quad 3.102$$

$$-\operatorname{csc}h\Gamma(s)l = (ctnh^2\Gamma(s)l - 1)^{1/2} = (w\ (s) - 1)^{1/2} \quad 3.103$$

Hence, below is the equivalent to equation (3.100)

$$\begin{bmatrix} V_s(s) \\ V_L(s) \end{bmatrix} = \begin{bmatrix} \zeta w(s) & -\zeta(w^2(s)-1)^{\frac{1}{2}} \\ \zeta(w^2(s)-1)^{\frac{1}{2}} & -\zeta w(s) \end{bmatrix} \begin{bmatrix} I_s(s) \\ I_L(s) \end{bmatrix} \quad 3.104$$

This is the transmission line model using Distributed Parameter System modelling technique.

It is to be noted that in the numerical solution, it is important to specify the finite spatial length (l), finite time interval (Δt) and the spatial (Δx). The importance behind that is that without the finite spatial length (l), there will be a requirement of unlimited number of memory storage locations. As tagged information, it is necessary to ensure that at the highest frequency of interest; (l) is always less than the wave length (Christopoulos, 2006).

In the same manner, without the finite time interval (Δt), longer running time is needed. Further, (Δt) can be a small set value but it cannot be zero (Christopoulos, 2006).

3.3.4.3. Distributed-Lumped Mathematical Model

From equations (3.5 and 3.104)

$$\begin{bmatrix} V_s(s) \\ V_L(s)+L_L s+R_L \end{bmatrix} = \begin{bmatrix} \zeta w(s) & -\zeta(w^2(s)-1)^{\frac{1}{2}} \\ \zeta(w^2(s)-1)^{\frac{1}{2}} & -\zeta w(s) \end{bmatrix} \begin{bmatrix} I_s(s) \\ I_L(s) \end{bmatrix} \quad 3.105$$

By considering $V_L(s)=0$ as the only source supplying this system is $V_s(s)$ equation (3.105) is re-writing as below: -

$$\begin{bmatrix} V_s(s) \\ L_L s + R_L \end{bmatrix} = \begin{bmatrix} \zeta w(s) & -\zeta (w^2(s)-1)^{\frac{1}{2}} \\ \zeta (w^2(s)-1)^{\frac{1}{2}} & -\zeta w(s) \end{bmatrix} \begin{bmatrix} I_s(s) \\ I_L(s) \end{bmatrix} \quad 3.106$$

$$\begin{bmatrix} V_s(s) \\ 0 \end{bmatrix} = \begin{bmatrix} \zeta w(s) & -\zeta (w^2(s)-1)^{\frac{1}{2}} \\ \zeta (w^2(s)-1)^{\frac{1}{2}} & -\zeta w(s) - (L_L s + R_L) \end{bmatrix} \begin{bmatrix} I_s(s) \\ I_L(s) \end{bmatrix} \quad 3.107$$

$$\begin{bmatrix} I_s(s) \\ I_L(s) \end{bmatrix} = [Z]^{-1} \begin{bmatrix} V_s(s) \\ 0 \end{bmatrix} = [Z]^{-1} [V_s(s)] \quad 3.108$$

$$\text{Where } [Z]^{-1} = \frac{\begin{bmatrix} -\zeta w(s) - (L_L s + R_L) \\ -\zeta (w^2(s)-1)^{\frac{1}{2}} \end{bmatrix}}{-\zeta w(s)(L_L s + R_L) + \zeta)} = \frac{\begin{bmatrix} \zeta w(s) + (L_L s + R_L) \\ \zeta (w^2(s)-1)^{\frac{1}{2}} \end{bmatrix}}{\zeta w(s)(L_L s + R_L) + \zeta^2} \quad 3.109$$

Substitute equations (3.109) in (3.108)

$$\begin{bmatrix} I_s(s) \\ I_L(s) \end{bmatrix} = \frac{\begin{bmatrix} \zeta w(s) + (L_L s + R_L) \\ \zeta (w^2(s)-1)^{\frac{1}{2}} \end{bmatrix}}{\zeta w(s)(L_L s + R_L) + \zeta^2} V_s(s) \quad 3.110$$

$$\begin{bmatrix} I_s(s) \\ I_L(s) \end{bmatrix} = \begin{bmatrix} \zeta w(s) + (L_L s + R_L) \\ \zeta (w^2(s)-1)^{\frac{1}{2}} \end{bmatrix} \frac{V_s(s)}{\Delta(s)} \quad 3.111$$

$$\text{Where } \Delta(s) = \zeta w(s)(L_L s + R_L) + \zeta^2 \quad 3.112$$

Considering equation (3.4) as disturbance / delay added to the system, equation (3.111) can be illustrated as below:

$$\begin{bmatrix} I_s(s) \\ I_L(s) \end{bmatrix} = \begin{bmatrix} \zeta w(s) + (L_L s + R_L) \\ \zeta (w^2(s)-1)^{\frac{1}{2}} \end{bmatrix} \frac{V_s(s)}{\Delta(s)} \frac{K_m / R_f}{\tau s + 1} \quad 3.113$$

3.3.4.4. Subassembly Simulation for w(s)

$$w(s) = \frac{e^{2l\Gamma(s)} + 1}{e^{2l\Gamma(s)} - 1} \quad 3.114$$

In order to be able to design w(s) in Simulink, we have to put it in delay form as follow: -

$$\Gamma(s) = \sqrt{(Ls+R)(Cs+G)} = \sqrt{RG(\frac{Ls}{R}+1)(\frac{Cs}{G}+1)} = \sqrt{RG}\sqrt{(\frac{Ls}{R}+1)(\frac{Cs}{G}+1)} \quad 3.115$$

$$\zeta(s) = \sqrt{\frac{Ls+R}{Cs+G}} = \sqrt{\frac{R(\frac{Ls}{R}+1)}{G(\frac{Cs}{G}+1)}} = \sqrt{\frac{R}{G}}\sqrt{\frac{(\frac{Ls}{R}+1)}{(\frac{Cs}{G}+1)}} \quad 3.116$$

$$\zeta(s) = \sqrt{\frac{R}{G}}\sqrt{\frac{(Ts+1)^2}{(\tau s+1)^2}} = \bar{\alpha}\frac{(Ts+1)}{(\tau s+1)} \quad 3.117$$

$$\frac{1}{G} > R \text{ and } L >> C \quad 3.118$$

$$(\frac{Cs}{G}+1)\frac{(Ts+1)}{(\tau s+1)} \cong \frac{Ls}{R}+1 \quad 3.119$$

Substitute equation (3.119) in (3.115)

$$\Gamma(s) = \sqrt{RG}\sqrt{\frac{(Ts+1)^2}{(\tau s+1)^2}(\frac{Cs}{G}+1)^2} \quad 3.120$$

$$\Gamma(s) = \sqrt{RG}\frac{(Ts+1)}{(\tau s+1)}(\frac{Cs}{G}+1) \quad 3.121$$

Let $\alpha = \sqrt{RG}$ and $\chi = \frac{(Ts+1)}{(\tau s+1)}(\frac{Cs}{G}+1)$ 3.122

Accordingly,

$$\Gamma(s)=\alpha\chi(s) \qquad 3.123$$

Substitute equation (3.122) in (3.114)

$$w(s)=\frac{e^{2l\alpha\chi(s)}+1}{e^{2l\alpha\chi(s)}-1}=\frac{1+e^{-2l\alpha\chi(s)}}{1-e^{-2l\alpha\chi(s)}} \qquad 3.124$$

Where $\chi(s)$ can be put as a linear equation: -

$$\chi(s)=as+b \qquad 3.125$$

$$a=\left[\frac{C}{G}+T-\tau\right] \text{ and b=1} \qquad 3.126$$

Substitute equation (3.126) in (3.124)

$$w(s)=\frac{1+e^{-2l\alpha(as+b)}}{1-e^{-2l\alpha(as+b)}}=\frac{1+e^{-2l\alpha b}e^{-2l\alpha as}}{1-e^{-2l\alpha b}e^{-2l\alpha as}} \qquad 3.127$$

where:

$e^{-2l\alpha b}$ is the attenuation and $e^{-2l\alpha a}$ is the finite time delay 3.128

3.3.4.5. Subassembly Simulation for $\zeta(w^2(s)-1)^{1/2}$

By substituting equation (3.127) in the expression $\zeta(w^2(s)-1)^{1/2}$, we get the following: -

$$(w^2(s)-1)^{1/2}=\frac{2e^{-l\alpha\chi(s)}}{1-e^{-2l\alpha\chi(s)}}=\frac{2e^{-l\alpha(as+b)}}{1-e^{-2l\alpha(as+b)}}=\frac{2e^{-l\alpha as}e^{-l\alpha b}}{1-e^{-2l\alpha as}e^{-2l\alpha b}} \qquad 3.129$$

Chapter-IV

Simulation Results and Discussions

4.1. Introduction

By definition, steady state responses are defined as the responses that persist for a long time following any input signal (Drof and Bishop, 2009). The initiated input signals can be a DC signal such as step unit or an AC signal such as sine-wave.

The dynamic or transient response is the system response, which starts from initial to the final system states (Ogata, 2010).

Both these two responses are required after subjecting the system to initiating signals, in order to analyze the design and the performance of the modelled hybrid system.

The computer simulation for example, pertaining to the EM field in case of applying the Transmission Line Modelling Method is accomplished by filling the propagation space with transmission line networks (Christopoulos, Mallik, Naylor and Johns, 1988).

In this regard, the next coming sections will illustrate in details the simulation part of the modelled hybrid system when FEM and TLM methods are applied in line with details given in Chapter-III.

Detailed discussions will be offered, highlighting the advantages of each method inline with earlier discussion in previous chapters.

The simulation is based on MATLAB, The Language of Technical Computing software, in which Version 7.8.0.347 (R2009a), 64-bit (win64), February 12, 2009, and license Number is 161051 are considered.

Maple-6, 2001 is supportive software used in this research to compute the inverse of the system impedance matrix due to complexity arises from the large size matrices introduced as an outcome from the mathematical derivation. Refer to Appendix-A3 to A6 for the detailed commands used and calculations obtained.

Finally, the memory of the digital computer used apart of FEM simulation is 4GB DDR3.

4.2. Finite Element Method Models

Figures - 4.1 to 4.8 show the simulated model, using MATLAB with built in Simulink, to investigate the response of the derived mathematical model in Chapter-III, Sections - 3.3.1 and 3.3.3.1. The investigation covers various system responses when the simulated model is subjected to DC and AC voltages and with and without inclusion of the fan's lumped model.

The substituted values considered in the simulated model are as indicated in Appendix-A1.

4.2.1. Simulation of Overall Hybrid System Model without Losses

Figure - 4.1 shows the block diagram of the mathematical system model derived in Chapter-III, Section- 3.3.3.1, without including the fan's lumped model. The simulation was carried out by using MATLAB with built in Simulink software. The modelled system is described and simulated in the form of a transfer function having a supply current derived from one remote end as an input, and a terminal load current received by the other remote end, as an output. This is a part of an electrical transmission power network, where in this case a static load in the form of four power transformers connected in parallel, each of 505MVA capacity, with a resistance of 0.979 ohm and an inductance of 0.345 Henry are employed.

The transfer function of the system, when the 400kV cable transmission line is divided into four segments to derive the mathematical model, is of ninth order with respect of the numerator and of the tenth order with respect of the denominator.

Appendix – A3 and A4 gives further detailed symbolic commands used and numerical calculations obtained in finding the inverse impedance of the system model and subsequently, system transfer function from which, the supply and terminal load currents will be obtained.

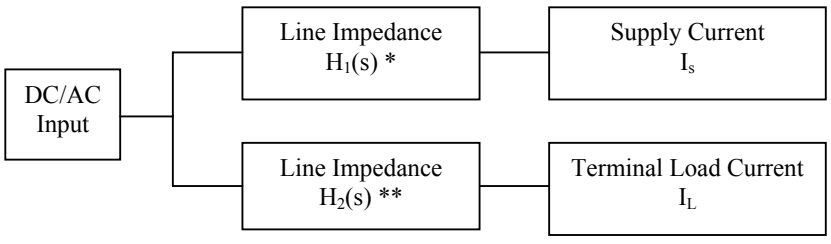

Figure-4.1: Block diagram of FEM for 400kV cables transmission line subjected to step/sine wave input (excluding Fan's effect and line losses)

$$* H_1(s) = \frac{Num_1}{Den_1} \quad (4.1)$$

Where from Appindex-3A and 3B:

Num1 (Symbolically)

$= L^3C^4L_Ls^8 + L^3C^4R_Ls^7 + (6L^2C^3L_L+L^3C^3)s^6 + 6L^2C^3R_Ls^5 + (10LC^2L_L + 5L^2C^2)s^4 + 10LC^2R_Ls^3 + 10CL_Ls^2 + 4CR_Ls + 1$ (4.2)

Num1 (Numerically)

$= 0.2228570183e^{-10}s^8 + 0.6327464401e^{-10}s^7 + 0.8905546355s^6 + 2.525396217s^5 + 0.9897483575s^4 + 0.2799798909e^{11}s^3 + 0.2652885032e^{20}s^2 + 0.7449641878e^{20}s + 0.3223680470e^{27}$ (4.3)

Den1 (Symbolically)

$= L^4C^4L_Ls^9 + L^4C^4R_Ls^8 + (L^4C^3+7L^3C^3L_L)s^7 + 7L^3C^3R_Ls^6 + (6L^3C^2+15L^2C^2L_L)s^5 + 15L^2C^2R_Ls^4 + (10L^2C+10LCL_L)s^3 + 10LCR_Ls^2 + (4L+L_L)s + R_L$ (4.4)

Den1 (Numerically)

$= 0.1419599207e^{-13}s^9 + 0.4030594823e^{-13}s^8 + 0.6617142428e^{-3}s^7 + 0.1876790288e^{-2}s^6 + 9450084.334s^5 + 26752078.58s^4 + 0.4209284193e^{17}s^3 + 0.1186355470e^{18}s^2 + 0.2861596669e^{26}s + 0.7891569770e26$ (4.5)

$$** H_2(s) = \frac{Num_2}{Den_2} \quad (4.6)$$

Where:

$Num_2 = 0.3223680471e^{27}$ (4.7)

Den_2 (Symbolically)=

$$L^4C^4L_LS^9 + L^4C^4R_LS^8 + (L^4C^3+7L^3C^3L_L)s^7 + 7L^3C^3R_LS^6 + (6L^3C^2+15L^2C^2L_L)s^5 + 15L^2C^2R_Ls^4 + (10L^2C+10LCL_L)s^3 + 10LCR_Ls^2 + (4L+L_L)s + R_L \quad (4.8)$$

Den_2 (Numerically)

$$= 0.1419599207e^{-13}s^9 + 0.4030594823e^{-13}s^8 + 0.6617142428e^{-3}s^7 + 0.1876790288e^{-2}s^6 + 9450084.334s^5 + 26752078.58s^4 + 0.4209284193e^{17}s^3 + 0.1186355470e^{18}s^2 + 0.2861596669e^{26}s + 0.7891569770e26 \quad (4.9)$$

Figure - 4.2 shows the block diagram of the mathematical system model derived in Chapter-III, Section- 3.3.1 and 3.3.3.1, with the inclusion of the fan's lumped model to the 400kV cable transmission line model. The simulation is carried out as shown in Figure - 4.1. However, it is to be noted that the 400kV cable transmission line transfer function order or computation is affected due to the inclusion of the fan model. In this regard, the system's transfer function remains in the same order as described earlier.

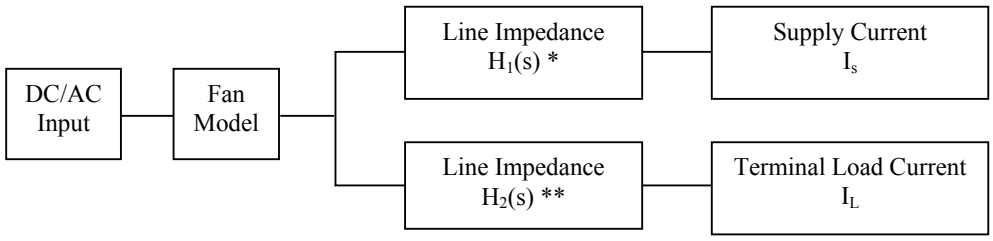

Figure-4.2: Block diagram of FEM for 400kV cables transmission line subjected to step/sine wave input (including Fan's effect and excluding line losses)

4.2.1.1. DC Input

Figure - 4.3 shows the 400kV cable transmission line's response when subjected to a step or a unity DC voltage signal, while ignoring the effect of the disturbance. It can be seen in the resulted response that both the supply and the terminal load currents reach the steady state phase simultaneously within 3.708 seconds. The supply current settles at 4.295A in the steady state, while the terminal load current settles at 4.085A. Further, the system has oscillations throughout the input response due to the effect of the inductive load of the cable and due the other additional eigenvalues generated by FEM, causing disturbances in system response coming from noises added.

Figure - 4.4 shows the overall system response, when the fan model is added to the 400kV cable transmission line model and subjected to a step or a unity DC voltage signal. It can be seen in the resulted response that both the supply and the terminal load currents reach the steady state phase simultaneously within 2.8 seconds. The supply current settles at 4.96A in the steady state, while the terminal load current settles at 4.95A, with minor oscillations throughout the input response.

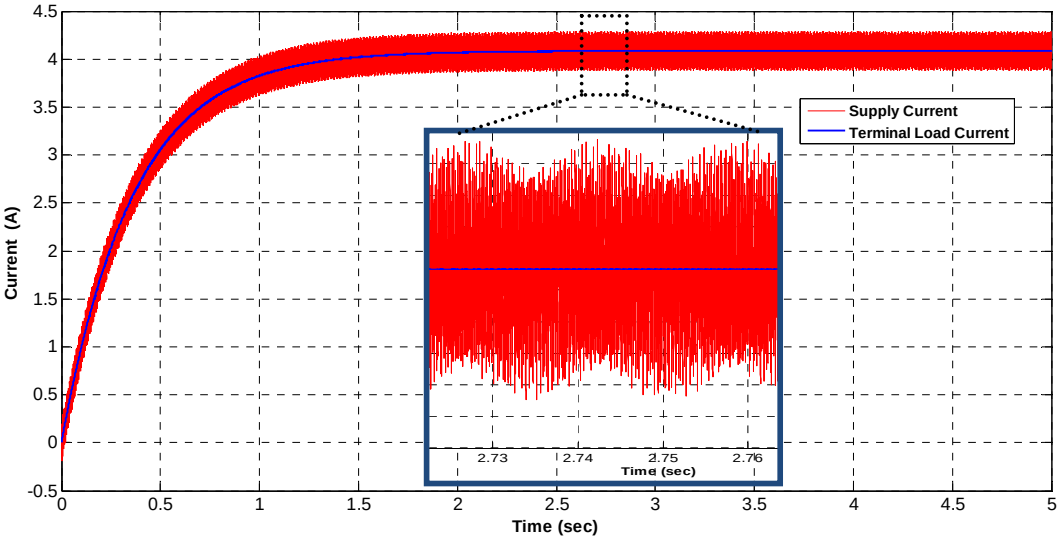

Figure-4.3: FEM: 400kV Cables transmission line response to step input - DC voltage (Excluding Fan's effect and line losses)

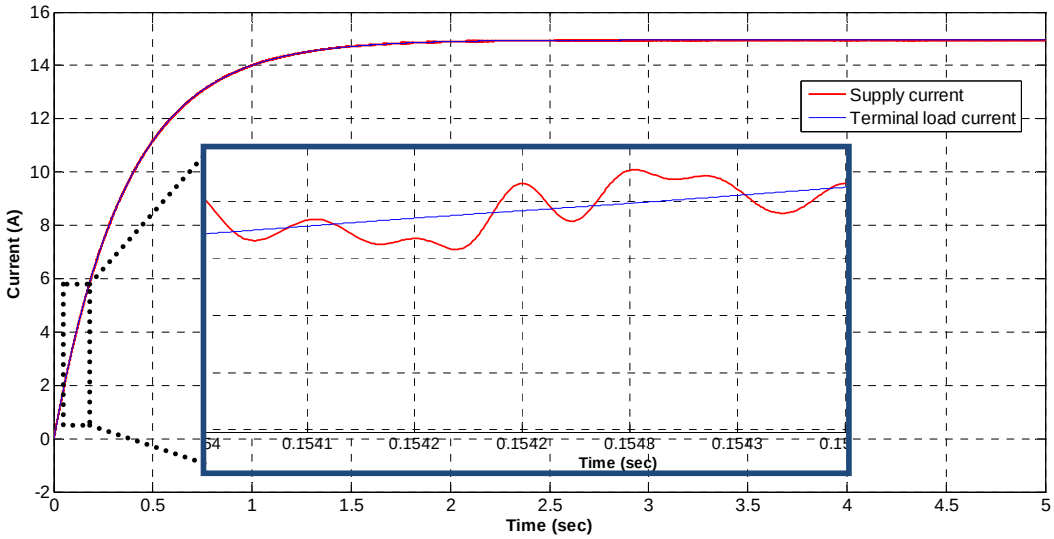

Figure-4.4: FEM: 400kV Cables transmission line response to step input - DC voltage (including Fan's effect and excluding line losses)

4.2.1.2. AC Input

Figure - 4.5 shows the 400kV cable transmission line's response when subjected to a sine wave or AC voltage signal of amplitude set as 400kV, while ignoring the

effect of the disturbances. As it is known, the system takes 0.02 seconds to complete one cycle based on the set frequency, which is in this case 50 Hz. Within a time of 5 seconds, 250 cycles propagate representing the performance of both; the supply and the terminal load currents with reference to the applied 400kV AC voltage acting as the system input.

The maximum value or the amplitude reached by supply current as a response to the applied 400kV AC voltage is 28.44kA in 5 seconds, whereas, the minimum value achieved is -14.54kA in zero seconds. In a similar way, the maximum value or the amplitude reached by terminal load current, as a response to the applied 400kV AC voltage is 28.3kA in 5 seconds, whereas, the minimum value is -14.35kA in zero seconds. Further, it is to be noted that, the supply current oscillate throughout supply current response, due to the reasons indicated earlier.

Figure - 4.6 shows the overall system response, when the fan model is included in the 400kV cable transmission line model and subjected to a sine wave or AC voltage signal of amplitude set as 400kV.

The maximum value or the amplitude reached by the supply current in response to 400kV AC voltage input is 100.2kA in 5 seconds, whereas, the minimum value is -49.1kA in zero seconds. Similarly, the maximum value or the amplitude reached by terminal load current in response to 400kV AC voltage is 100.6kA in 5 seconds, whereas, the minimum value is -49.48kA at zero second. Further, it is noticed that the supply current oscillation is negligible upon the inclusion of the time delay model.

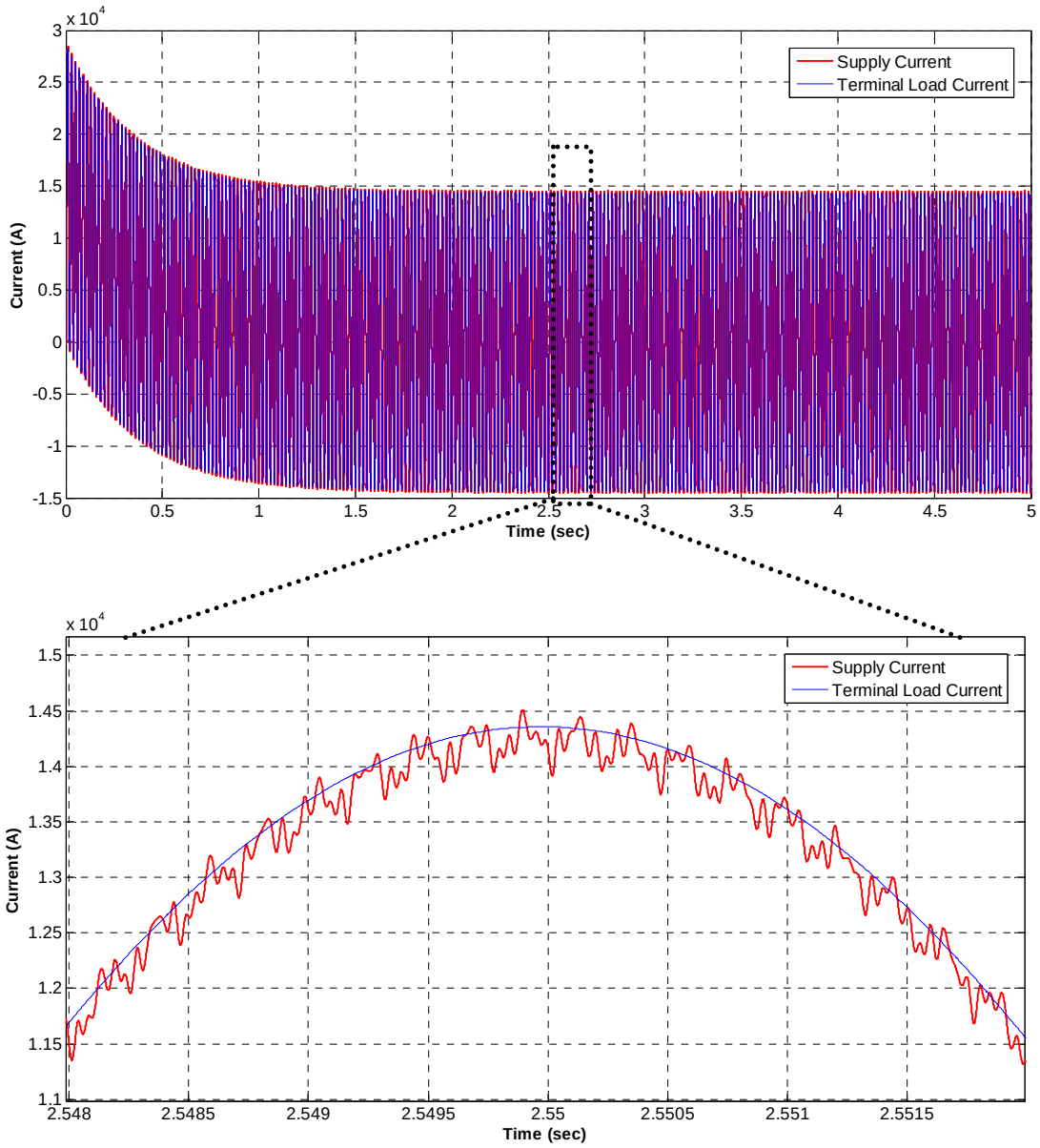

Figure-4.5: FEM: 400kV Cables transmission line response to sine wave input - AC voltage (excluding Fan's effect and line losses)

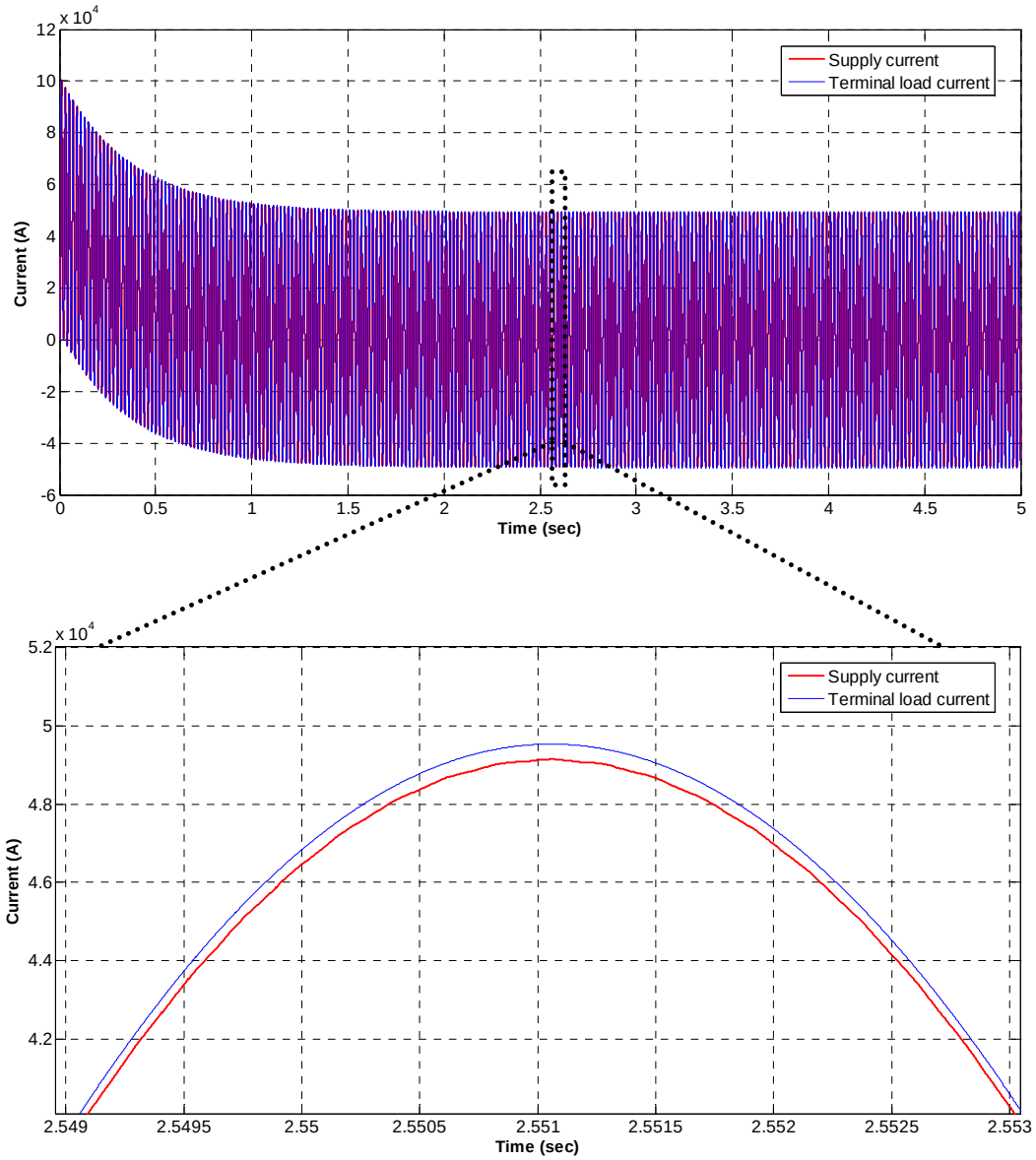

Figure-4.6: FEM: 400kV Cables transmission line response to sine wave input - AC voltage (including Fan's effect and excluding line losses)

4.2.2. Simulation of Overall Hybrid System Model with Losses

The simulation models illustrated in Figures - 4.7 and 4.8 are same as the simulation models shown in Figures - 4.1 and 4.2 except that these two models are for the 400kV Cable transmission line with its four line parameters as the derived mathematical model in Chapter-III, Section- 3.3.4.1.

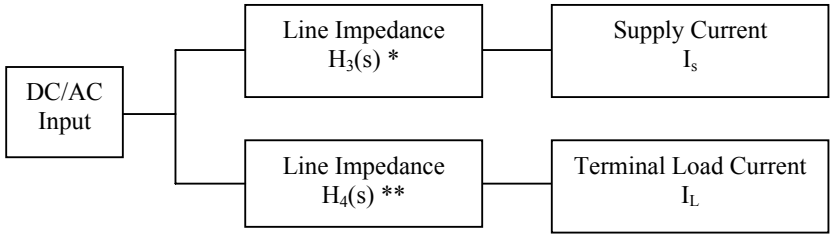

Figure-4.7: Block diagram of FEM for 400kV cables transmission line subjected to step/sine wave input (excluding Fan's effect and including line losses)

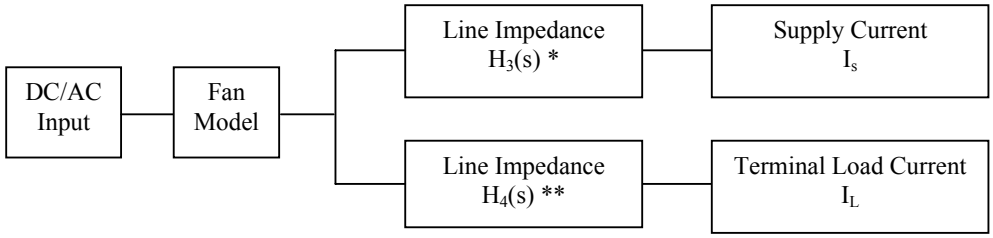

Figure-4.8: Block diagram of FEM for 400kV cables transmission line subjected to step/sine wave input (including Fan's effect and line losses)

$$* H_3(s) = \frac{Num_3}{Den_3} \qquad 4.10$$

Where from Appindex-4A and 4B:

Num3 (Numerically)=

$$0.3027452857e^{-74}s^9 + 0.8983326383e^{-61}s^8 + 0.1066244882e^{-47}s^7 + 0.6327712593e^{-35}s^6 + 0.1877614951e^{-22}s^5 + 0.2228570183e^{-10}s^4 + 0.1084648625e^{-8}s^3 + 0.1850343617e^{-7}s^2 + 0.1237603439e\text{-}6s + 0.2256017150e^{-6} \quad (4.11)$$

Den3 (Numerically)=

$$0.1928487470e^{-77}s^{10} + 0.5722378906e^{-64}s^9 + 0.6791979902e^{-51}s^8 + 0.4030752922e^{-38}s^7 + 0.1196040724e^{-25}s^6 + 0.1419599207e^{-13}s^5 + 0.9077769649e^{-12}s^4 + 0.2234109438e^{-10}s^3 + 0.2588869839e^{-9}s^2 + 0.1347984798e^{-8}s + 0.2195265755e^{-8} \quad (4.12)$$

$$** H_4(s) = \frac{Num_4}{Den_4} \quad (4.13)$$

Where:

Num4 (Numerically)=

$$0.4379283510e^{-37}s + 0.2598919616e^{-24} \quad (4.14)$$

Den4 as equation (4.12) (4.15)

$$\text{Fan Model} = \frac{3.66}{1.129e^{-3}s + 1} \quad (4.16)$$

Upon simulating the above model in MATLAB, the fundamental sampling time was set as (e^{-13}) seconds to simulate the system and to obtain its results. Nevertheless, despite the long run time taken by MATLAB software the system

response, FEM shows numerical instability and therefore, the desired output was not achievable.

4.3. Transmission Line Modelling Method

Figures – 4.9 to 4.21 show the simulated model using MATLAB and Simulink to model the derived mathematical model in Chapter-III, Sections – 3.3.1 and 3.3.3.2 along with various system responses when the model is subjected to DC and AC voltages, with and without the inclusion of disturbances.

The substituted values considered in the model are as indicated in Appendix-A1.

4.3.1. Simulation of Overall Hybrid System Model without Losses

Figures - 4.9 and 4.10 show the block diagrams of the simulated model when using MATLAB with built in Simulink software to model the derived mathematical model in Chapter-III, Sections - 3.3.1 and 3.3.3.2 without and with, the fan's lumped model, respectively.

The modelled system is described and simulated in the form of series block diagrams having a supply current derived from one remote end as an input, and a terminal load current received by the other remote end, as an output. This is a part of an electric transmission power network, where in this case a static load in the form of four power transformers connected in parallel, each of 505MVA capacity, with a resistance of 0.979 ohm and an inductance of 0.345 Henry from the terminal load.

In general, the series model topology normally, replicates the actual system arrangement. However, the derived functions involved in the simulation should be in the form of transfer functions. See Appendix-A7.

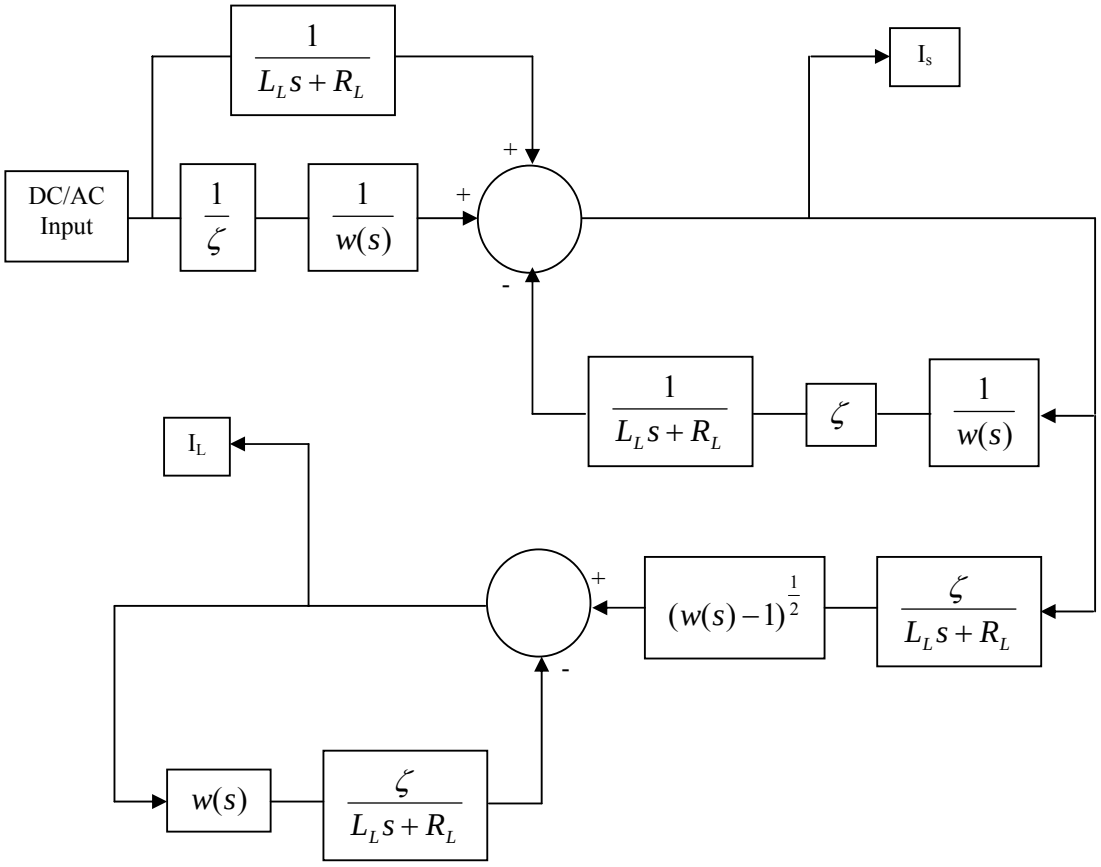

Figure-4.9: Block diagram of TLM for 400kV cables transmission line subjected to step/sine wave input (excluding Fan's effect and line losses)

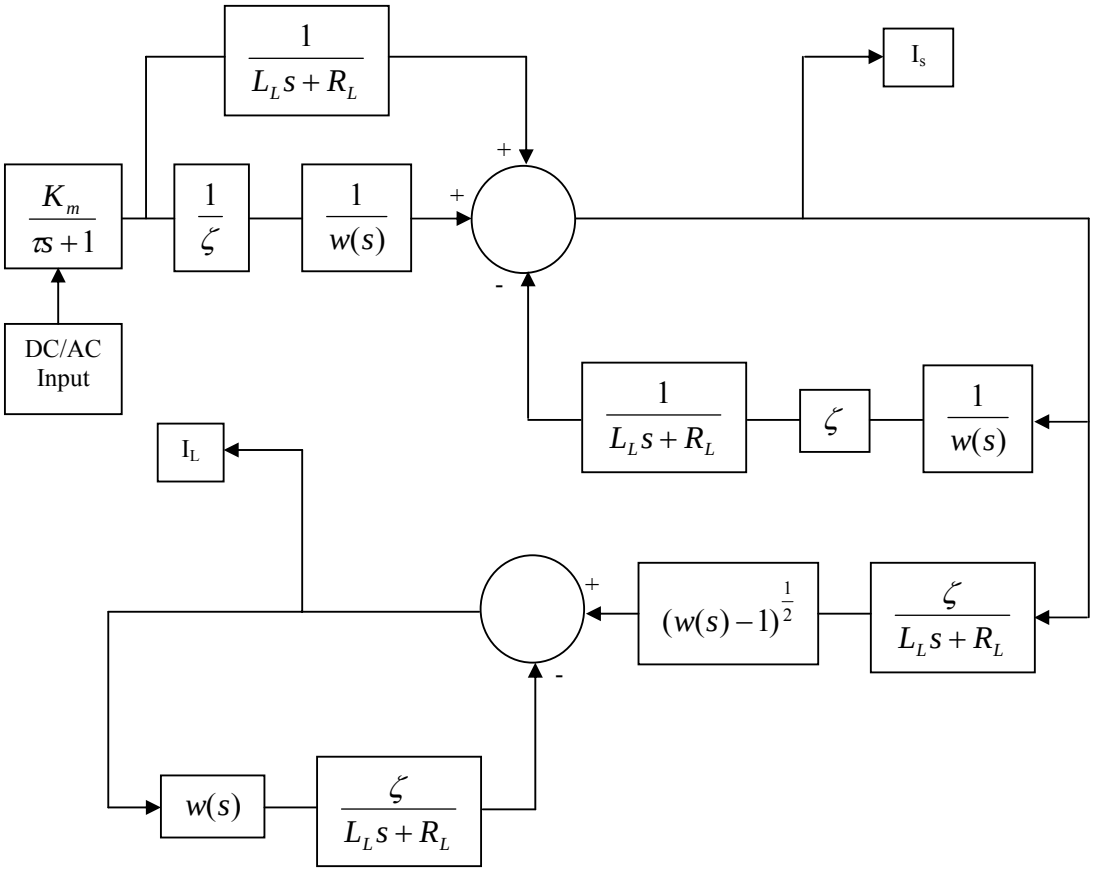

Figure-4.10: Block diagram of TLM for 400kV cables transmission line subjected to step/sine wave input (including Fan's effect and excluding line losses)

/

4.3.1.1. DC Input

Figure - 4.11 shows the 400kV cable transmission line's response when subjected to a step or a unity DC voltage signal, while ignoring the effect of the disturbance. It can be seen from the resulting response that both the supply and the terminal load currents reach the steady state phase simultaneously within 3.468 and 3.469 seconds respectively, as both currents settle at 4.085A, in steady state.

Further, the system is over damped as $\zeta > 1$, with minor oscillations on the supply current response.

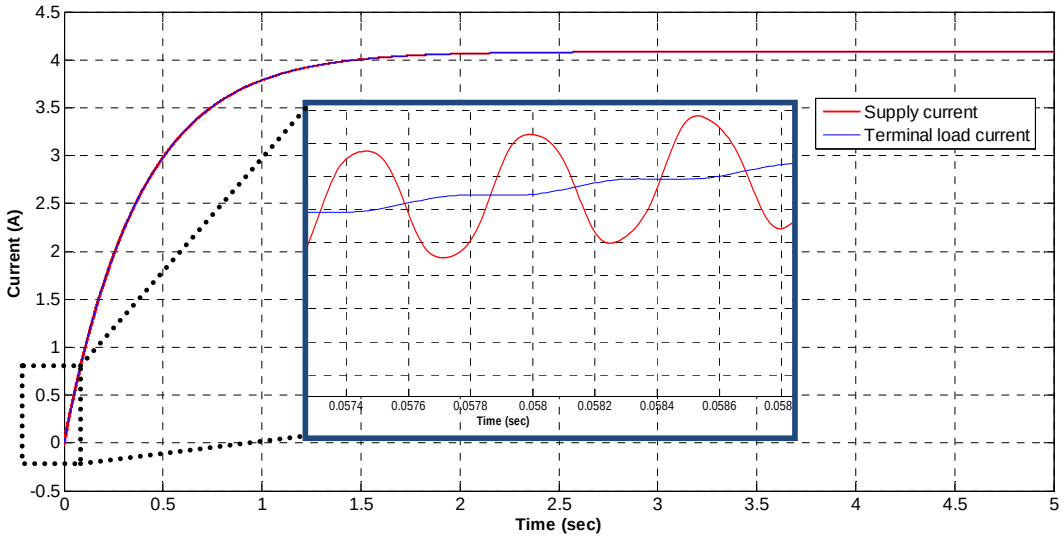

Figure-4.11: TLM: 400kV Cables transmission line response to step input - DC voltage (Excluding Fan's effect and line losses)

Figure - 4.12 show the 400kV cable transmission line's responses when subjected to a step or a unity DC voltage signal, while including the effect of the disturbance. It can be seen in the resulted response that both the supply and the terminal load currents reach the steady state phase simultaneously in about 2.991 seconds. The

desired output shows almost alignment between the value of the supply current and the terminal load current, where both currents settle at 14.95A, in steady state.

Further, the system is over damped as $\zeta > 1$, with very minor oscillations on the supply current response.

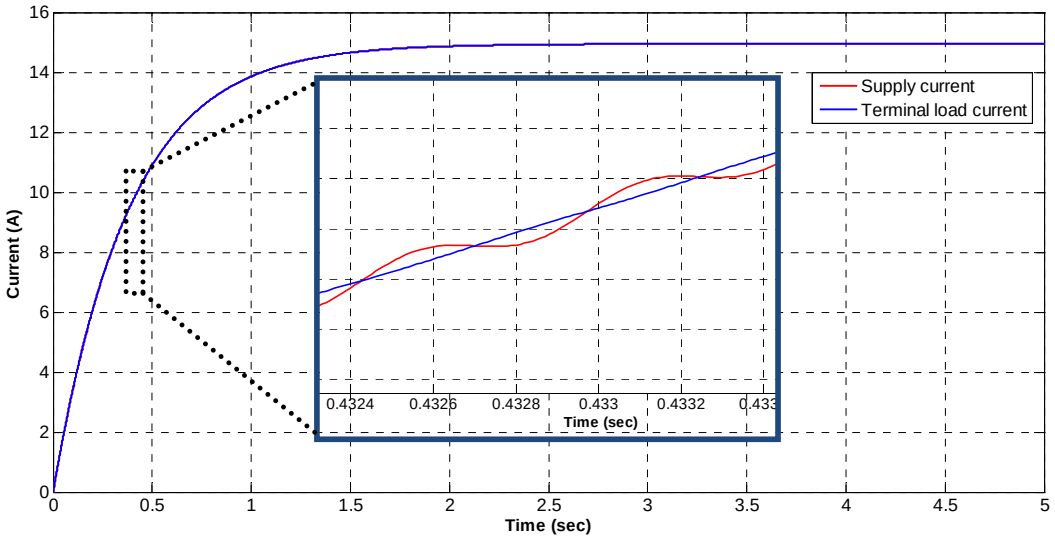

Figure-4.12: TLM: 400kV Cables transmission line response to step input - DC voltage (including Fan's effect and excluding line losses)

4.3.1.2. AC Input

Figure - 4.13 shows the 400kV cable transmission line's response when subjected to a sine wave or AC voltage signal of 400kV amplitude, while ignoring the effect of the disturbances. As it is known, the system is taking 0.02 seconds to complete one cycle based on the set frequency, which is in this case 50 Hz. Within a time of 5 seconds, 250 cycles propagate representing the performance of both; the supply and the terminal load currents with reference to the applied 400kV AC voltage acting as the system input.

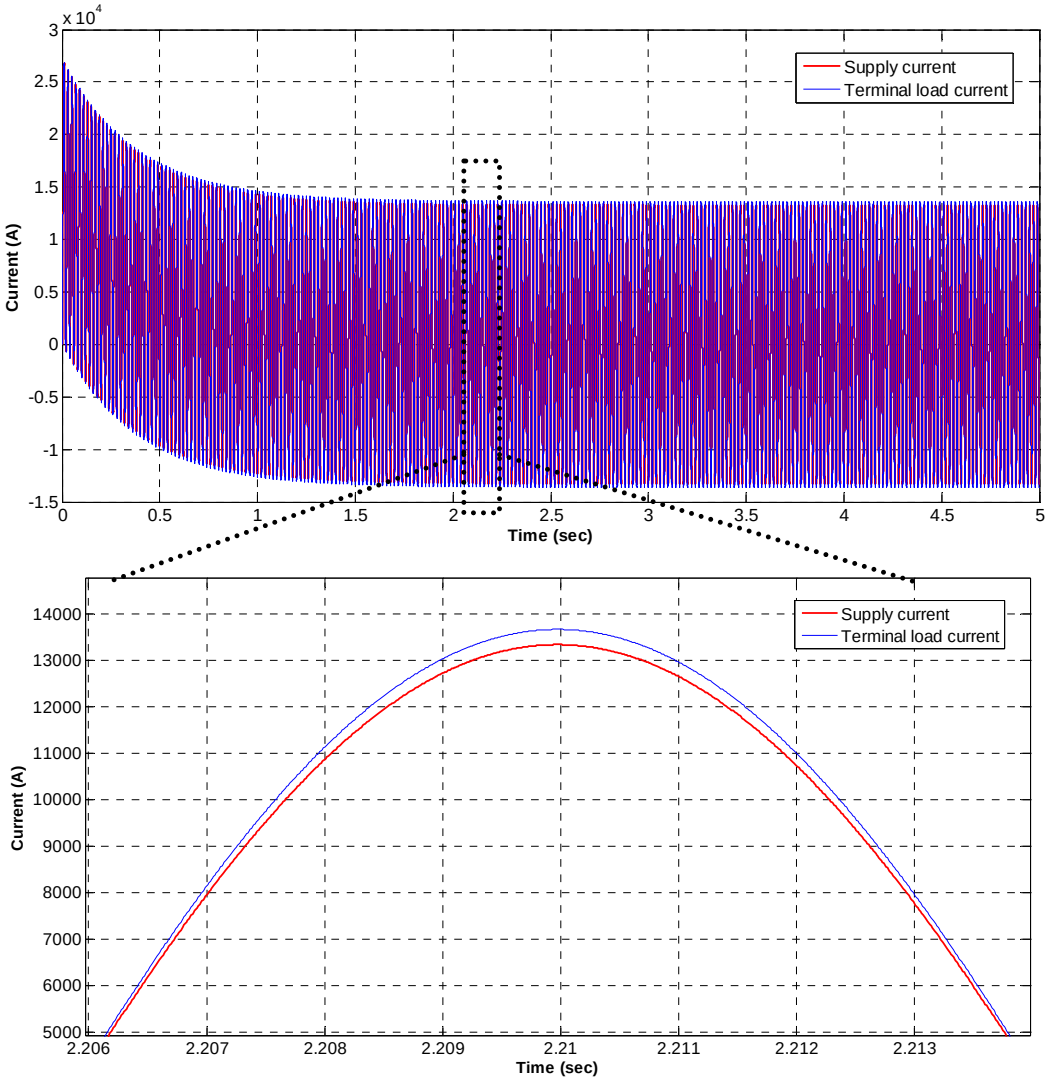

Figure-4.13: TLM: 400kV Cables transmission line response to sine wave input - AC voltage (excluding Fan's effect and line losses)

The maximum value or the amplitude reached by the supply current as a response to the applied 400kV AC voltage is 26.77kA in 5 seconds, whereas, the minimum value achieved is -13.3kA in zero seconds. In similar way, the maximum value or the amplitude reached by terminal load current, as a response to the applied 400kV AC voltage is 26.89kA in 5 seconds, whereas, the minimum value is -13.65kA in

zero seconds. Further, it is to be noted that the supply current is oscillating throughout system response.

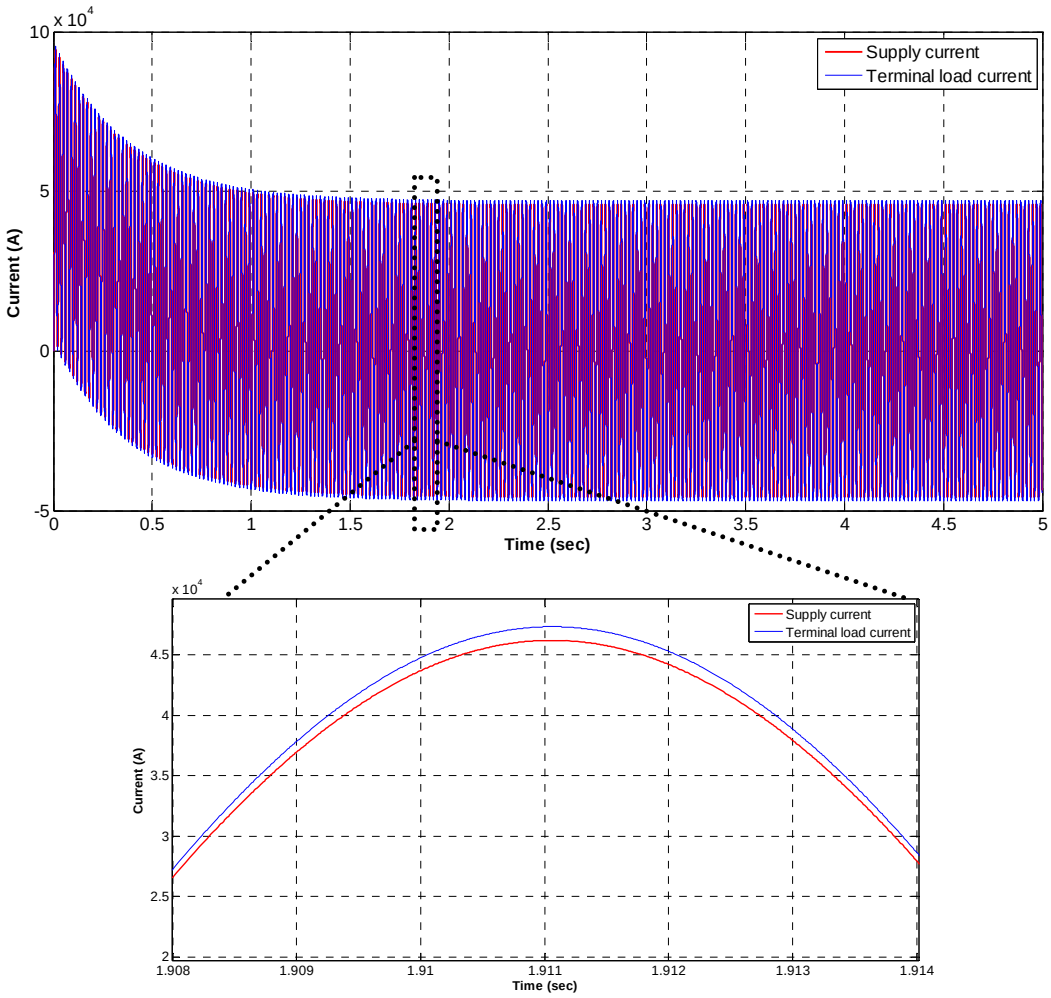

Figure-4.14: TLM: 400kV Cables transmission line response to sine wave input - AC voltage (including Fan's effect and excluding line losses)

Figure - 4.14 shows the overall system response, when the fan model is included the 400kV cable transmission line model and subjected to a sine wave or AC voltage signal of amplitude 400kV.

The maximum value or the amplitude reached by supply current as a response to 400kV AC voltage is 94.37kA in 5 seconds, whereas, the minimum value is -

45.86kA in zero seconds. Similarly, the maximum value or the amplitude reached by terminal load current in response to 400kV AC voltage is 95.53kA in 5 seconds, whereas, the minimum value is -46.99kA in zero seconds. Further, it is noticed that the supply current oscillation is negligible with the inclusion of the time delay model.

4.3.2. Simulation of Overall Hybrid System Model with Losses

Figures - 4.15 and 4.16 show the block diagrams of the simulated model when using MATLAB with built in Simulink software to model the derived mathematical model in Chapter-III, Sections - 3.3.1 and 3.3.4.2 without and with the fan's lumped model, respectively.

The modelled system is described and simulated in the form of series blocks having a supply current derived from one remote end as an input, and a terminal load current received by the other remote end, as an output. This is a part of an electric transmission power network, which in this case feeds a static load in the form of four power transformers connected in parallel, each of 505MVA capacity, with a resistance of 0.979 ohm and an inductance of 0.345 Henry from the terminal load.

In general, the series model topology normally, replicates the actual system arrangement that's enables the simulation, in MATLAB software. However, the derived functions involved in the simulation should be in the form of transfer functions.

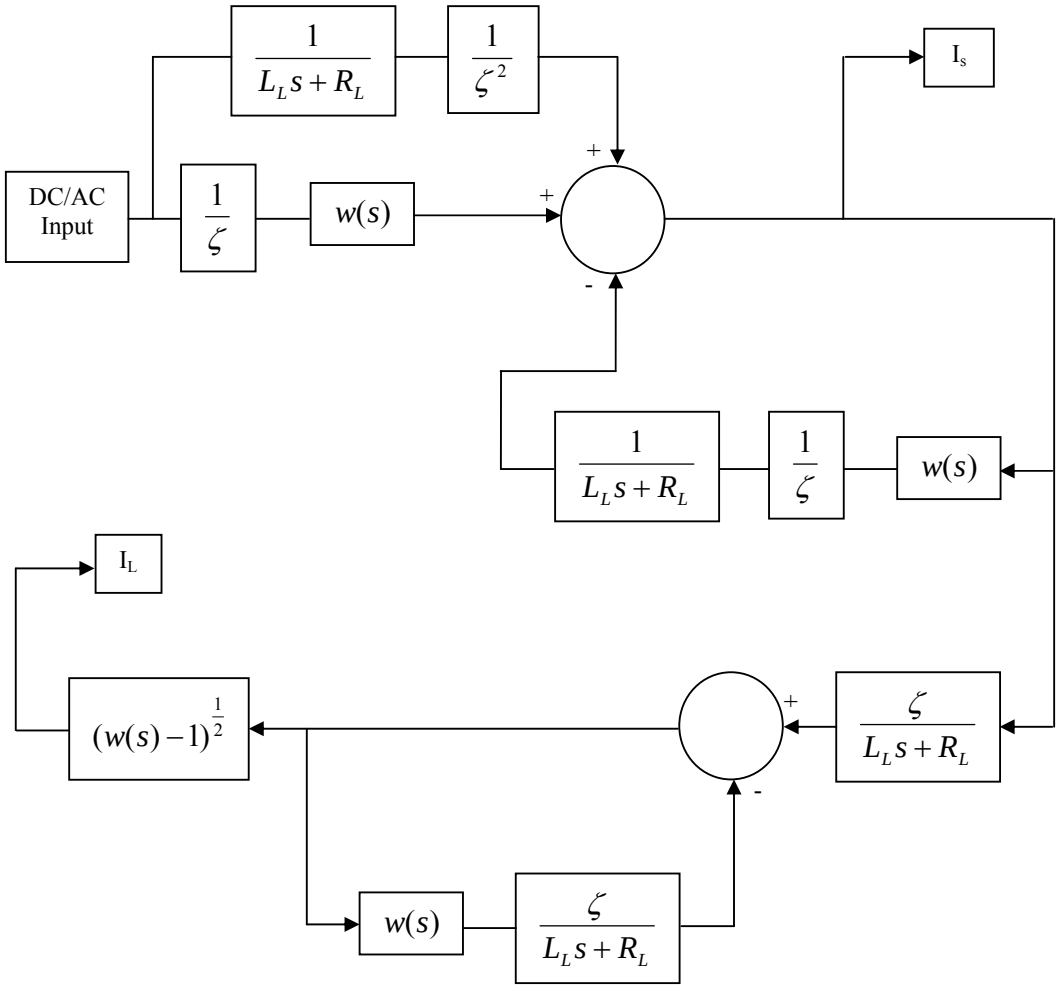

Figure-4.15: Block diagram of TLM for 400kV cables transmission line subjected to step/sine wave input (excluding Fan's effect and including line losses)

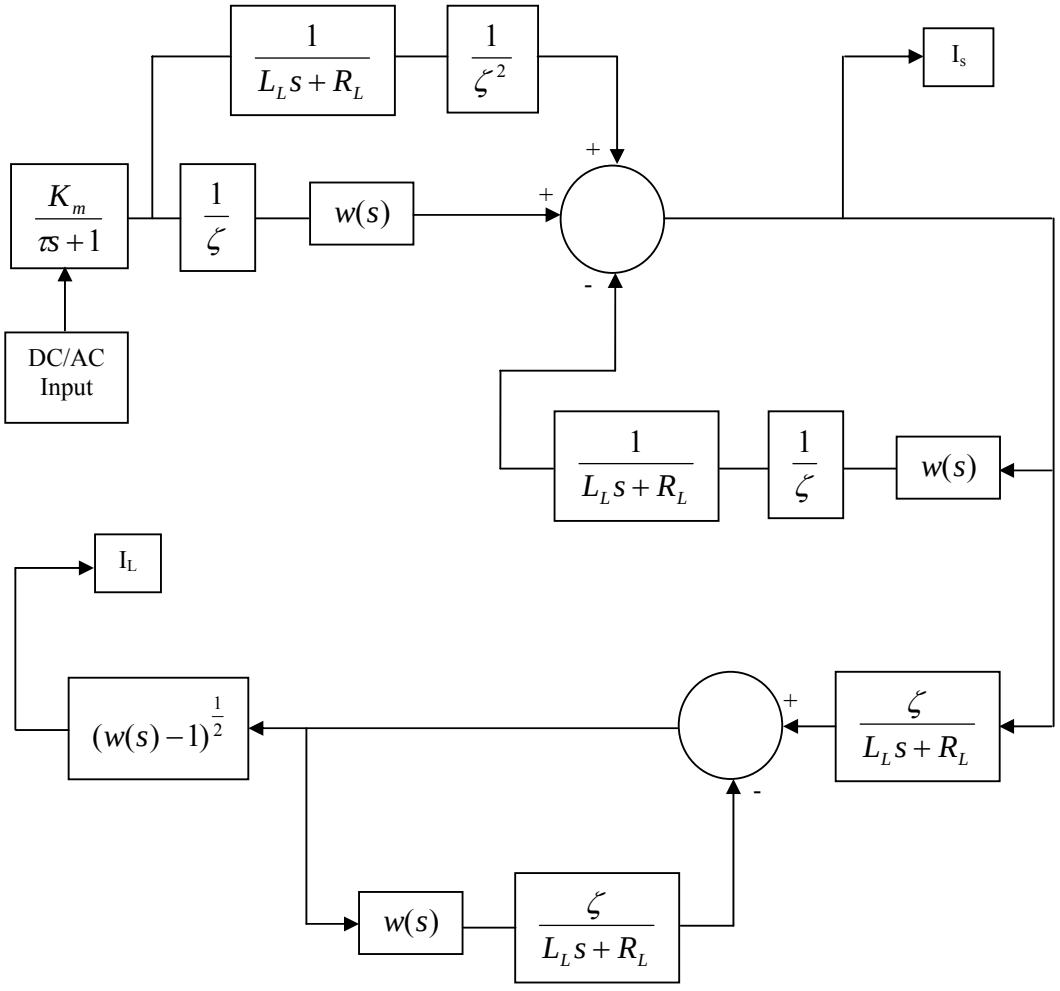

Figure-4.16: Block diagram of TLM for 400kV cables transmission line subjected to step/sine wave input (including Fan's effect and line losses)

4.3.2.1. Bode Diagram

When R and G are included in the model in the mathematical derivation introduced earlier in Chapter-III, Section - 3.3.4.2, the damping ratio $\zeta(s)$ and the wave propagation $\Gamma(s)$ becomes function of time. This is because the characteristic impedance becomes complex when R and G are not equal to zero.

In order to be able to simulate 400kV cable transmission line model by TLM, an equivalent transfer function, as highlighted in equations 3.117 and 3.121, requires approximating to be able to proceed further. In this regard, the function is extracted from the frequency domain by using the Bode diagram as shown in Figure – 4.17. The bases of assumption here to derive the equivalent transfer function ensuring that both; the high frequency and the low frequency of the approximated transfer function match the original transfer function having minimum of one intersection point. The original transfer function is of the first order. Hence, to get one intersection point, the approximated transfer function should have -40dB slope.

In fact, the purpose of selecting -40dB as the slope of the approximated transfer function with one intersection point is linked with the original transfer function of the modelled system. As per equations 3.78 and 3.86, the wave propagation $\Gamma(s)$ and damping ratio $\zeta(s)$ are function of time and under square root. An approximated second order function is required in this case to eliminate the square root and subsequently, simulate the derived model. Further, the original transfer function is propagating within a short frequency band. Hence, the approximated transfer function with one intersection point will serve the requirement. The wider

the frequency band is, the more intersection points are needed to be considered with an appropriate selection of slope.

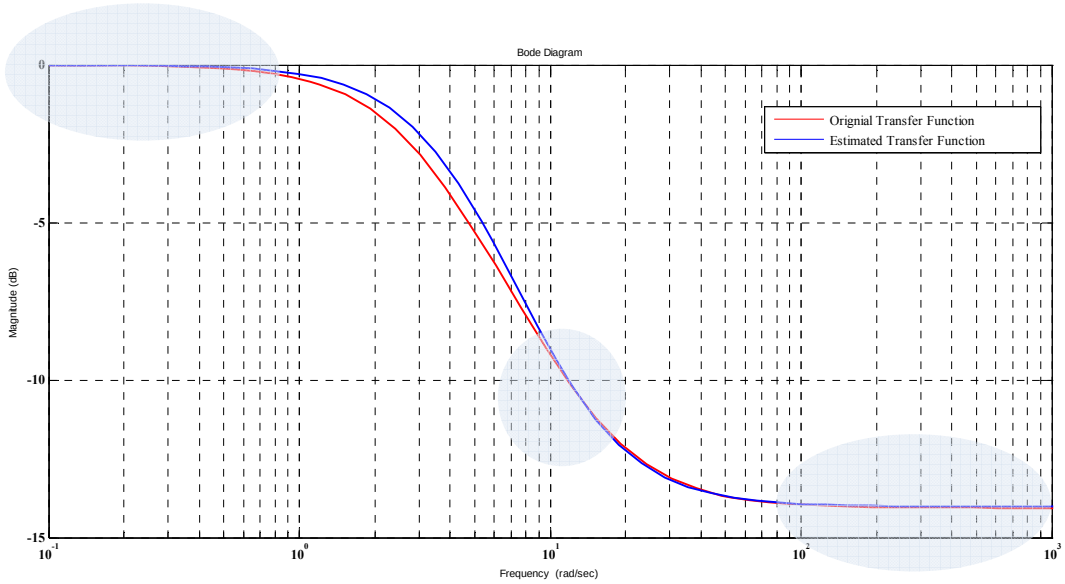

Figure-4.17: Bode diagram showing the original and approximated transfer functions

4.3.2.2. DC Input

Figure - 4.18 shows the 400kV cable transmission line's response when subjected to a step or a unity DC voltage signal, while ignoring the effect of the disturbance. It can be seen in the resulted response that both the supply and the terminal load currents reach the steady state phase simultaneously within 2.861 and 3.246 seconds respectively, at which, both currents settle at 0.01129A and 0.007535A in the steady state. The maximum overshoot achieved by the supply current is 0.01919A, whereas the terminal load current reachs 0.01412A after being initially for 0.3298 seconds. Further, the system response is over damped as $\zeta >> 1$, with no oscillations on the supply current or terminal load current.

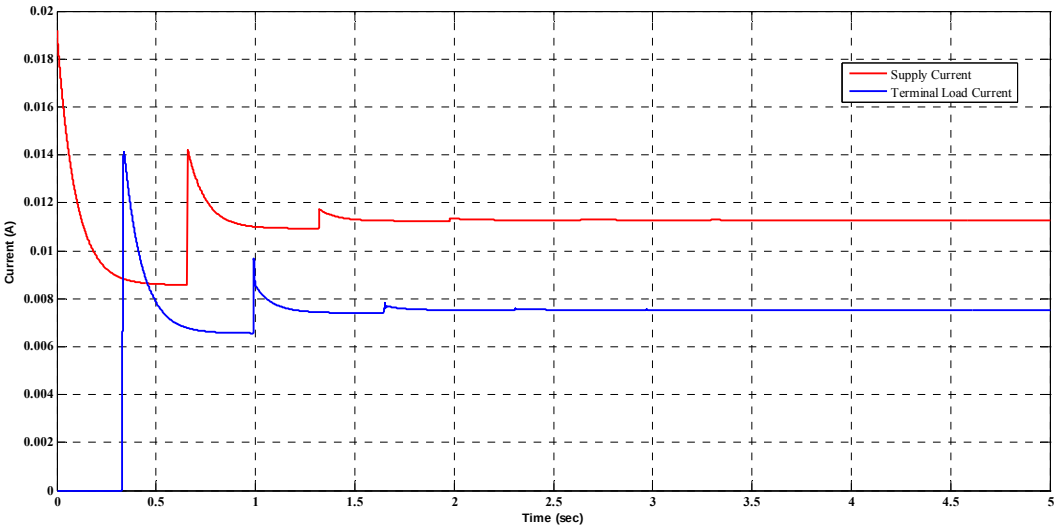

Figure-4.18: TLM: 400kV Cables transmission line response to step input - DC voltage
(Excluding Fan's effect and including line losses)

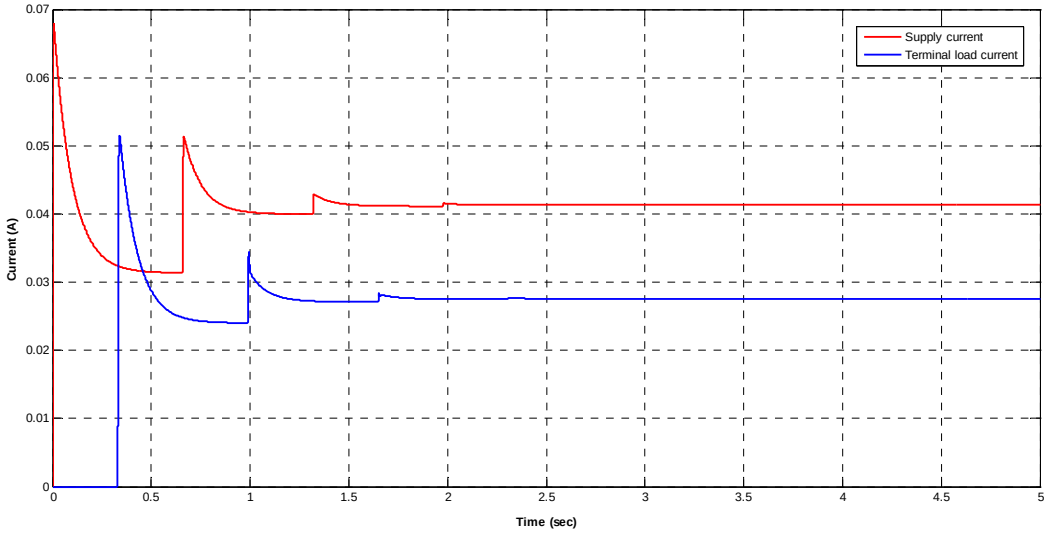

Figure-4.19: TLM: 400kV Cables transmission line response to step input - DC voltage
(Including Fan's effect and line losses)

Figure - 4.19 shows the 400kV cable transmission line's response when subjected to a step or a unity DC voltage signal, while including the effect of the disturbance. It can be seen in the resulted response that both the supply and the terminal load currents reach the steady state phase simultaneously within 2.881 and 3.068 seconds respectively, with, both currents settling at 0.04131A and 0.02758A in steady state. The maximum overshoot achieved by the supply current is 0.0679A, whereas the terminal load current reaches 0.05149A after being initially zero for 0.3298 seconds. Further, the system response is over damped as $\zeta >> 1$, with no oscillations on the supply or terminal load current.

4.3.2.3. AC Input

Figure - 4.20 shows the 400kV cable transmission line's response when subjected to a sine wave or AC voltage signal of 400kV amplitude, while ignoring the effect of the disturbances. The system takes 0.02 seconds to complete one cycle based on the set frequency, which is in this case 50 Hz. Within a time of 5 seconds, 250 cycles propagate representing the performance of both; the supply and the terminal load currents with reference to the applied 400kV AC voltage acting as the system input. The maximum value or the amplitude reached by supply current as a response to the applied 400kV AC voltage is 10.3kA in 5 seconds, whereas, the minimum value achieved is -10.3kA in zero seconds. In a similar way, the maximum value or the amplitude reached by terminal load current as a response to the applied 400kV AC voltage is 6.374kA in 5 seconds, whereas, the minimum value is -6.374kA in zero seconds. Further, it is to be noted that there are no oscillations on the system responses.

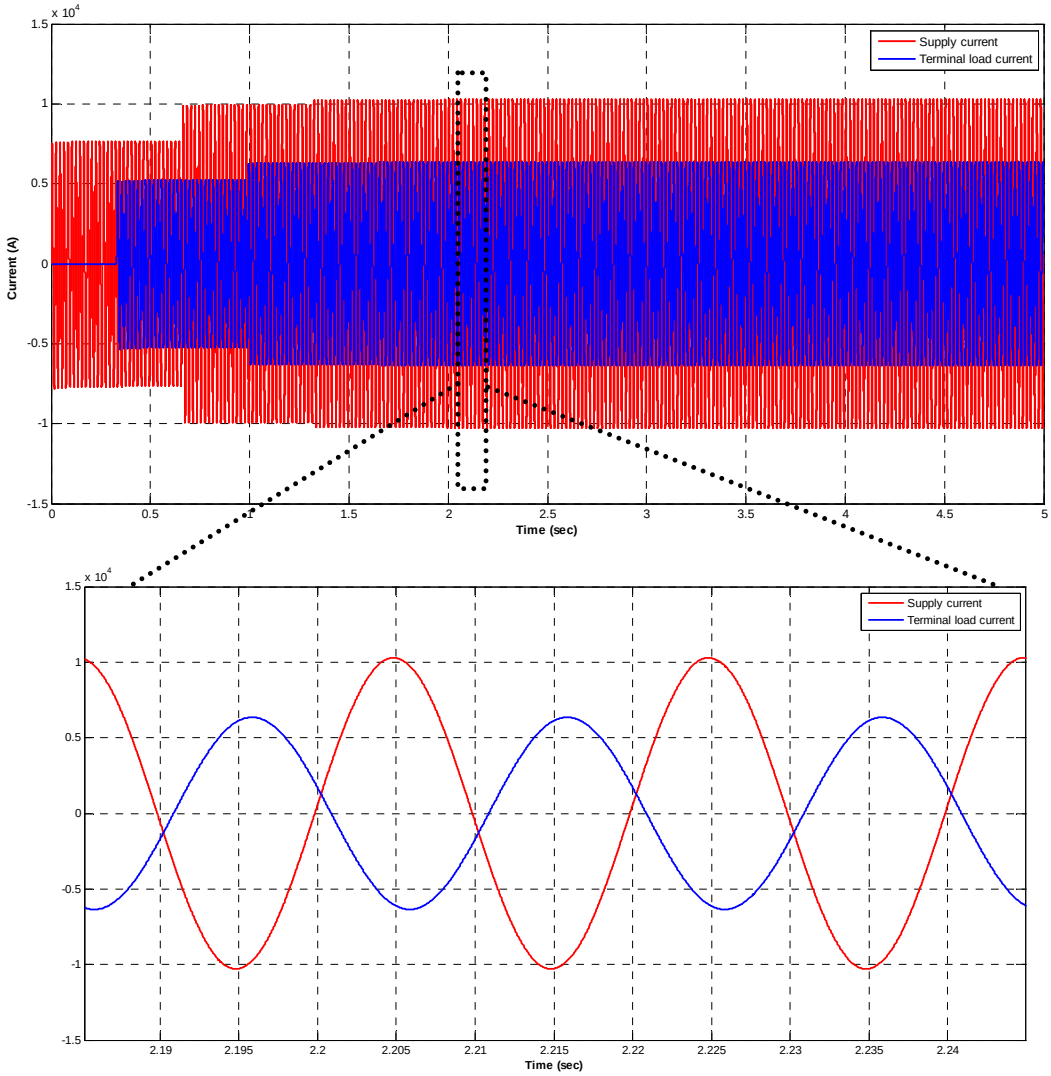

Figure-4.20: TLM: 400kV Cables transmission line response to sine wave input - AC voltage (excluding Fan's effect and including line losses)

Figure - 4.21 shows the 400kV cable transmission line's response when subjected to a sine wave or AC voltage signal of 400kV amplitude, while including the effect of the disturbances. The system takes 0.02 seconds to complete one cycle based on the set frequency, which is in this case 50 Hz. Within 5 seconds, 250 cycles propagate representing the performance of both; the supply and the terminal load currents with reference to the applied 400kV AC voltage acting as the system input.

The maximum value or the amplitude reached by supply current as a response to the applied 400kV AC voltage is 35.52kA in 5 seconds, whereas, the minimum value achieved is -35.52kA in zero seconds. In similar way, the maximum value or the amplitude reached by terminal load current as a response to the applied 400kV AC voltage is 21.99kA in 5 seconds, whereas, the minimum value is -21.99kA in zero seconds. Further, it is to be noted that there are no oscillations in the system responses.

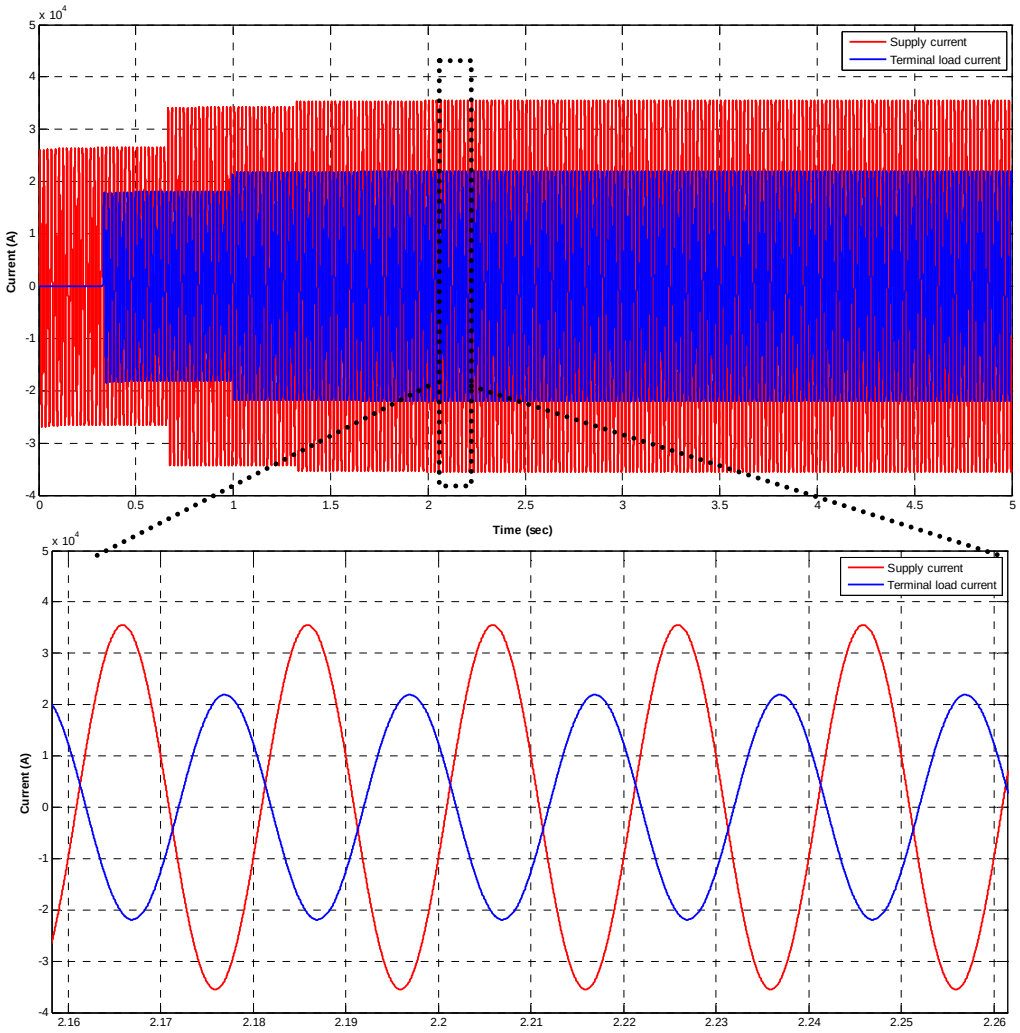

Figure-4.21: TLM: 400kV Cables transmission line response to sine wave input - AC voltage (including Fan's effect and line losses)

4.4. Comparison Study

The strategy is adapted to carryout the comparison between the findings of FEM and TLM is built on the four main areas described below. This starts from the mathematical derivation and ends with investigation of the effect of the shunt conductance variable values, on the performance of the long transmission line model.

4.4.1. Mathematical Model Derivation

It is observed that, in carrying out the long transmission line's mathematical derivation by using the Finite Element Method, the degree of complexity increases with the number of segments considered and components added. Not only that, the derived long transmission line's mathematical model needs to be re-derived in case of addition or deletion of any item to or from the model and in case of changing the number of divided sections. This leads to increasing computational time and increases the chances of making errors. For instance, the size of the impedance matrix increases with the number of divided sections. Computation of the impedance inverse in this case to simulate the system demands high mathematical skills or alternatively software tools. It also needs enlarged storage memory to simulate the derived mathematical model. Nevertheless, despite doing all this, the concept of wave propagation is not reflected in the FEM as the system is dimensionless.

In the case of Transmission Line Modelling technique, the long transmission line's mathematical derivation was lengthy but it reflects the wave propagation since the length of the line is included, as part of the model. Further, the distributed mathematical model for the transmission line proposed by Whalley in 1998 can be used as a reference in modelling any long transmission line. No major re-derivation is necessary except minor calculation and adjustment to determine $\omega(s)$ and $\Gamma(s)$.

4.4.2. Simulated Models

As stated in Section – 4.4.1, any changes in the number of divided segments or the addition or removal of components in the FEM model has an impact on the mathematical model and subsequently on the simulation model. This is due to its impact of the system's transfer function, which needs to be revised every time to be able to simulate and obtain the desired system responses. The assistance of the Maple software contributed in reducing the calculation time, but it was a very lengthy process. Moreover, chances of making mistakes were high and causing substantial reworking.

Besides, to run the FEM modelled system considering line losses, the availability of data storage area in the computer, was an obstacle and the step time was required to be set very small. Even with these considerations, the FEM showed numerical instability and, therefore, it could not obtain the desired results for further examination and comparison.

In short, FEM is limited by the available computer resources, which affect the simulation of the derived model.

With the TLM model, simulation was easier and faster with and without considering the line losses. Once the simulation model is established, only the parameter values need updating to accommodate changes. Faster execute speeds are also obtained when compared with FEM model.

4.4.3. Simulation Results

With reference to the no line losses, the responses of the model of FEM when subjected to DC input illustrated high oscillations in the supply current when the model of the fan was not included. After adding the fan model, the oscillations reduced but were not eliminated. The inclusion of the fan model has a positive impact on the swiftness of the system with regard to reaching the steady state. In this case, it shows a lesser time by 0.908 seconds taken when the fan not included with cable model. Additionally, due to the gain added from the fan motor, both the currents; the supply current and the terminal load current at the steady state are amplified from 4.295A to 4.96A and from 4.085A to 4.95A respectively. As a matter of fact, the supply and terminal load currents will be ultimately affected in steady state only by the terminal load resistance when applying a unit voltage ($I_{Lss.s} = I_{ss.s} = V / R_L = 1/0.2448 = 4.08496A$). However, it is noted that the supply current is shows higher steady state values with 5.14% error from the desired value. Moreover, due to the addition of the fan, the oscillation on the supply current was

enormously decreased showing a satisfactory enhancement of the cable performance when the temperature within the tunnel reduced.

On the other hand, when the same model is subjected to an AC input, the supply current oscillates specifically when the fan model is not included. After adding the fan model, the oscillation was negligible. Additionally, due to the gain added from the fan motor, both the currents; the supply current and the terminal load current maximum amplitudes, were drastically amplified by approximates four times; from 28.44kA to 100.2kA and from 28.3kA to 100.6kA respectively. On the other side, the minimum values achieved at which both currents are stabilized was significantly reduced from -14.54kA to -49.1kA in the case of supply current, and from -14.35kA to -49.48kA in the case of terminal load current, which shows asymmetrical with the maximum amplitude values. Theoretically and as per project's requirement, the 400kV cable should carryout and supply 2.165kA current throughout the transmission line to the terminal load end, at which, the terminal load current is supposed to be 5.201kA. Refer Appendix-A2. A large difference can be noticed when comparing the values achieved from simulation and calculation. Further, this impacts on the capability of 400kV cables to transmit full rated power, under the cable rating, with the availability of the ventilation as from these simulated values, it shows the cable is exceeding its specified capacity (1500MVA). This needs further examination to establish the reasons for such differences.

Pertaining to the FEM model considering line losses, the simulation was very sensitive when the shunt conductance and series resistance were considered as part of the model. It is noticed that upon simulating the above model in MATLAB, the

fundamental sampling time required to be set as (e^{-13}) seconds against (e^{-6}) used in the model, in which the line losses were ignored. This is in order to be able to simulate the system and obtain its results. Nevertheless, despite the long running time taken by MATLAB software to compute system response, FEM shows numerical instability in addition to the lack of storage area required to process the huge data generated. As stated earlier, the storage memory of the digital computer used to run the FEM model is 4GB DDR3 Memory. At the end, the desired output was not achievable when using FEM and including line losses. Hence, system results considering R and G were not achieved.

With reference to the no line losses, the responses of the model of TLM when subjected to DC input illustrated minor oscillation in the supply current when the model of the fan was not included. After adding the fan model, the oscillation reduced but was not eliminated. The inclusion of the fan model has positive impact on the swiftness of the system with regard to reaching the steady state. In this case, it shows lesser time by 0.477 seconds than the time taken by the system when the fan was not included. Additionally, due to the gain added from the fan motor, both the currents; the supply current and the terminal load current at steady state were drastically amplified from 4.085A and from 14.95A respectively. As a matter of fact, the supply and terminal load currents would be ultimately affected in the steady state only by the terminal load resistance when applying a unit voltage ($I_{Lss.s} = I_{ss.s} = V / R_L = 1/0.2448 = 4.08496A$). The accuracy of TLM model shows 0% error in achieving the desired value.

When the above referred TLM model is subjected to AC input, it illustrates minor oscillation in the supply current when the model of the fan was not included. After adding the fan model, the oscillation was negligible. Additionally, due to the gain added from the fan motor, both the currents; the supply current and the terminal load current maximum amplitudes were drastically amplified from 26.77kA to 94.37kA and from 26.89kA to 95.53kA respectively. Also, the minimum values achieved at which both currents are stabilized was significantly increased from 13.3kA to 45.86kA in the case of supply current, and hugely increased from 13.65kA to 46.99kA in the case of terminal load current, which shows, similar with the FEM results, asymmetrical with the maximum amplitudes values. Theoretically and as per project's requirement, the 400kV cable should carryout and supply 2.165kA current throughout the transmission line until the terminal load end, at which, the terminal load current is supposed to be 5.201kA. Refer Appendix-A2. A large difference can be noticed when comparing the values achieved from simulation and calculation. Further, this impacts on the capability of 400kV cables to transmit full rated power under the cable rating with the availability of the ventilation as from these simulated values, it shows the cable is exceeding its specified capacity (1500MVA). This needs further examination to determine the reasons for such difference.

Pertaining to the TLM line losses model, several attempts were carried out to obtain the approximated transfer function based on trail and error while using Bode diagram in order to get rid of the generated rational functions linked mainly with $\zeta(s)$ and $\Gamma(s)$. However, it is noticed that based on the provided line parameters,

the impedance with the ratio between the inductance and series resistance (L/R) is decreasing with the increases of the frequency, and on other side, increasing with the decreases in the frequency with the ratio between the capacitance and the shunt conductance (C/G). This raises some concerns about the degree of accuracy of the provided line parameters data used in the simulation, since the frequency, as per physical laws, increases when the impedance rises for the inductance (ωL) and decreases for the capacitance ($1/\omega C$). Due to this, it ends by having a damping ratio ζ extremely high which logically is not acceptable. This is not part of the objective of this research but is recommended to be further reviewed and studied.

Based on the outcome of the Bode diagram shown in Figure - 4.17, the responses of the model of TLM when subjected to DC input did not illustrated any oscillation in the supply or terminal load currents either with the model of the fan included or not. Only, it shows some overshoots foreseen when the fan model is added. Despite the time taken to reach the steady state by both currents are differing, the inclusion of the fan model made a positive impact on system speed of response. The time taken by the supply current was improved slightly by 0.02 seconds, whereas the time taken by the terminal load current was improved by 0.178 seconds. The supply current and the terminal load current at steady state significantly amplified from 0.01129A to 0.04131A and from 0.007535A to 0.02758A respectively. Further, the maximum overshoot achieved by supply current increased from 0.01919A to 0.0679A, and for the terminal load current increased from 0.01412A to 0.05149A after being initially delayed by 0.3298 seconds, due to the finite time delay being included a part of the simulated model of $w(s)$ and $\zeta(w^2(s)-1)^{1/2}$.

When the above referred TLM model is subjected to AC input, no oscillation was recorded in both currents either the model is including or not including the fan model. Additionally, due to the gain added from the fan motor, both the currents; the supply current and the terminal load current maximum amplitudes are amplified from 10.3kA to 35.52kA and from 6.374kA to 35.52kA respectively. Theoretically and as, per project's requirement, the 400kV cable should carryout and supply 2.165kA throughout the transmission line until the terminal load end, at which, the terminal load current is 5.201kA. Refer Appendix-A2. It can be noticed that the values of both current responses are approaching the desired values when compared to earlier values obtained, but these are still not in line with specified cable capacity.

It can be concluded from the derived mathematical models and the various simulation system responses comparisons that the TEM gives more accurate results compared to the FEM when both are used to model long transmission lines. However, some concerns were raised pertaining to the accuracy of the achieved current values, which as a result affected the cable full power rating capacity. By looking to the provided line parameters, there are no doubts on the provided values of series resistance and shunt capacitance as physically these two parameters are actually measured at the factory. The necessity in measuring these two parameters is due to their direct link to cable power losses. Hence, actual values are important to verify the compliance of cable "ampacity" calculation submitted by the cable manufacturer. Additionally, no major difference also expected in the inductance value. The main concerns arises on the accuracy of the shunt conductance provided

value as it is noticed from the Guarantee Particular Parameter Document submitted by the manufacture that the insulation resistance varies hugely with the changes in conductor temperature. For instant, from 20°C to 90°C, the shunt conductance changes 1000 times its value.

In this regard, and despite this, this is not part of the objectives of this research. Two different values for the shunt conductance are further simulated, in the next section, to observe its effect on the system response.

4.4.4. Effect of Shunt Conductance on Transmission Line

Returning to the results obtained from Bode diagram (Figure 4.22) and the concerns raised with respect to the effect of the shunt conductance value on system response, two attempts are carried out in this section to investigate further this concern. Two values are selected for the shunt conductance; one is higher than the original provided value by 10 times 7.14×10^{-6} Mohs/km and the other one is less than the original provided value by 10 times 7.14×10^{-8} Mohs/km.

Similar processes, as described in Sections 4.3.2.1, 4.3.2.2 and 4.3.2.3 are followed to obtain system responses considering the two selected values for the shunt conductance of the line followed by a brief discussion and comparison.

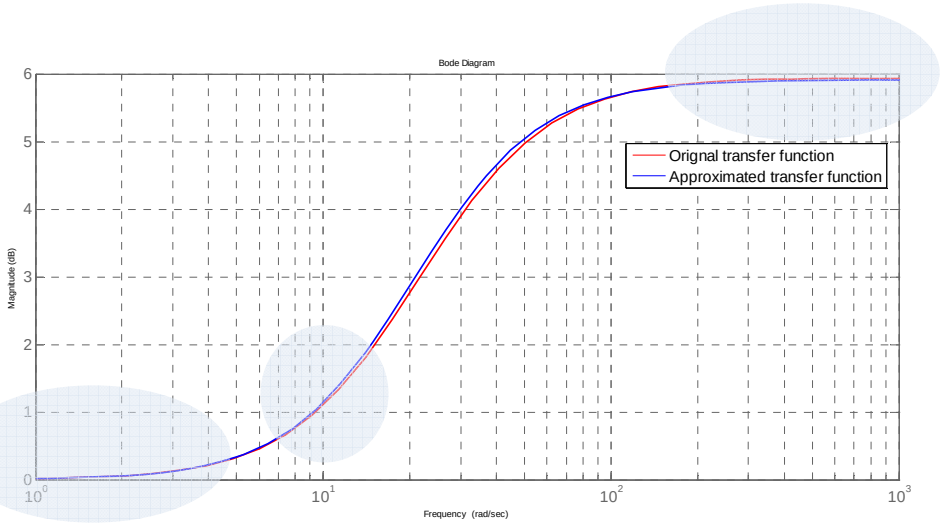

Figure-4.22: Bode diagram showing the original and approximated transfer functions with respect to the change in the shunt conductance value.

Figures – 4.23 and 4.24 show the 400kV cable transmission line's response when subjected to a step or a unity DC voltage signal, while excluding and excluding the effect of disturbance when the shunt conductance is increased from 7.14×10^{-7} to 7.14×10^{-6} Mhos/km. Its impact will be mainly on $\zeta(s)$, $\Gamma(s)$ and on the impedance characteristic, which will increase with the increases of the frequency. With this scenario, the time taken by the supply current to reach the steady state is slowdown from 1.292 seconds to 1.531 seconds and for the terminal load current from 1.486 seconds to 2.158 seconds. The supply current and the terminal load current at steady state are amplified from 0.02719A to 0.09952A and from 0.002602A to 0.009522A respectively, though the values are almost near to zero. Further, the system response remains over damped as ζ still much greater than one but less compared to the earlier calculated value. No oscillations are indicated in the supply current or terminal load current. The terminal load current is delayed by 0.3701 seconds with and without the inclusion of the fan model.

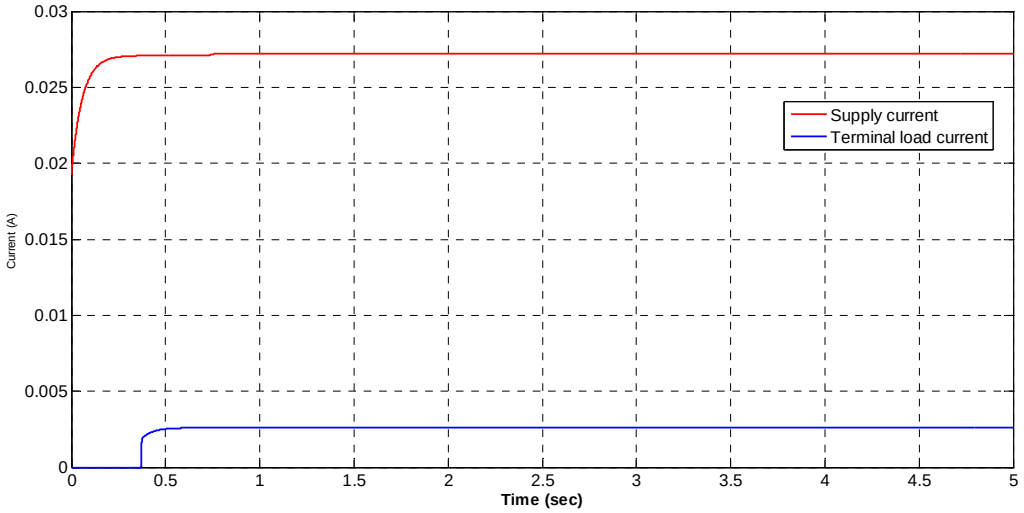

Figure-4.23: TLM: 400kV Cables transmission line response to step input - DC voltage when the value of shunt conductance changed from $7.14e^{-7}$ to $7.14e^{-6}$ (excluding Fan's effect and including line losses)

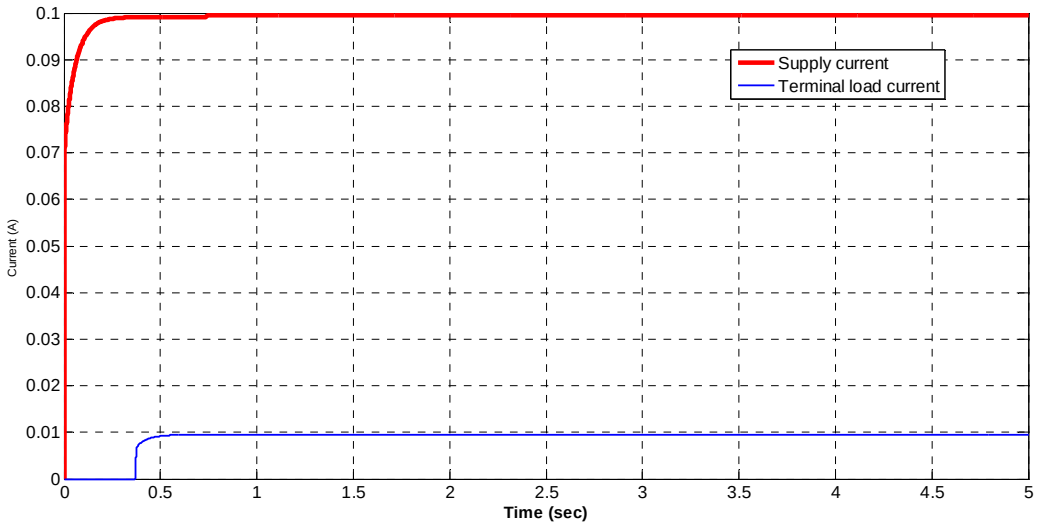

Figure-4.24: TLM: 400kV Cables transmission line response to step input - DC voltage when the value of shunt conductance changed from $7.14e^{-7}$ to $7.14e^{-6}$ (including Fan's effect and line losses)

Figures – 4.25 and 4.26 show the 400kV cable transmission line's response when subjected to a sine wave or AC voltage signal the value of shunt conductance changed from $7.14e^{-7}$ to $7.14e^{-6}$. Similar descriptions as given in Section – 4.3.2.3 except the differences in the values achieved can be considered.

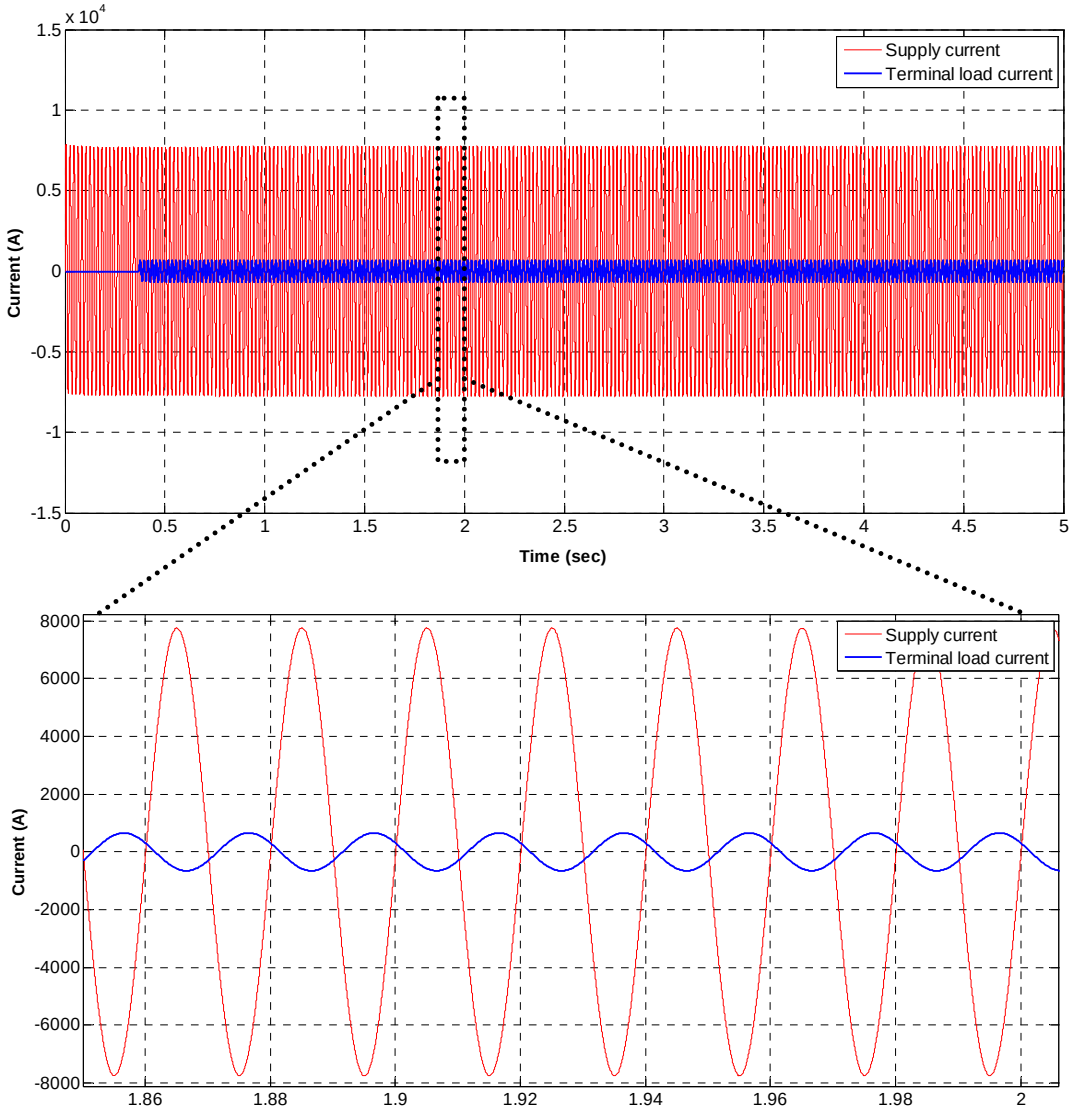

Figure-4.25: TLM: 400kV Cables transmission line response to sine wave input - AC voltage when the value of shunt conductance changed from $7.14e^{-7}$ to $7.14e^{-6}$ (Excluding Fan's effect and including line losses)

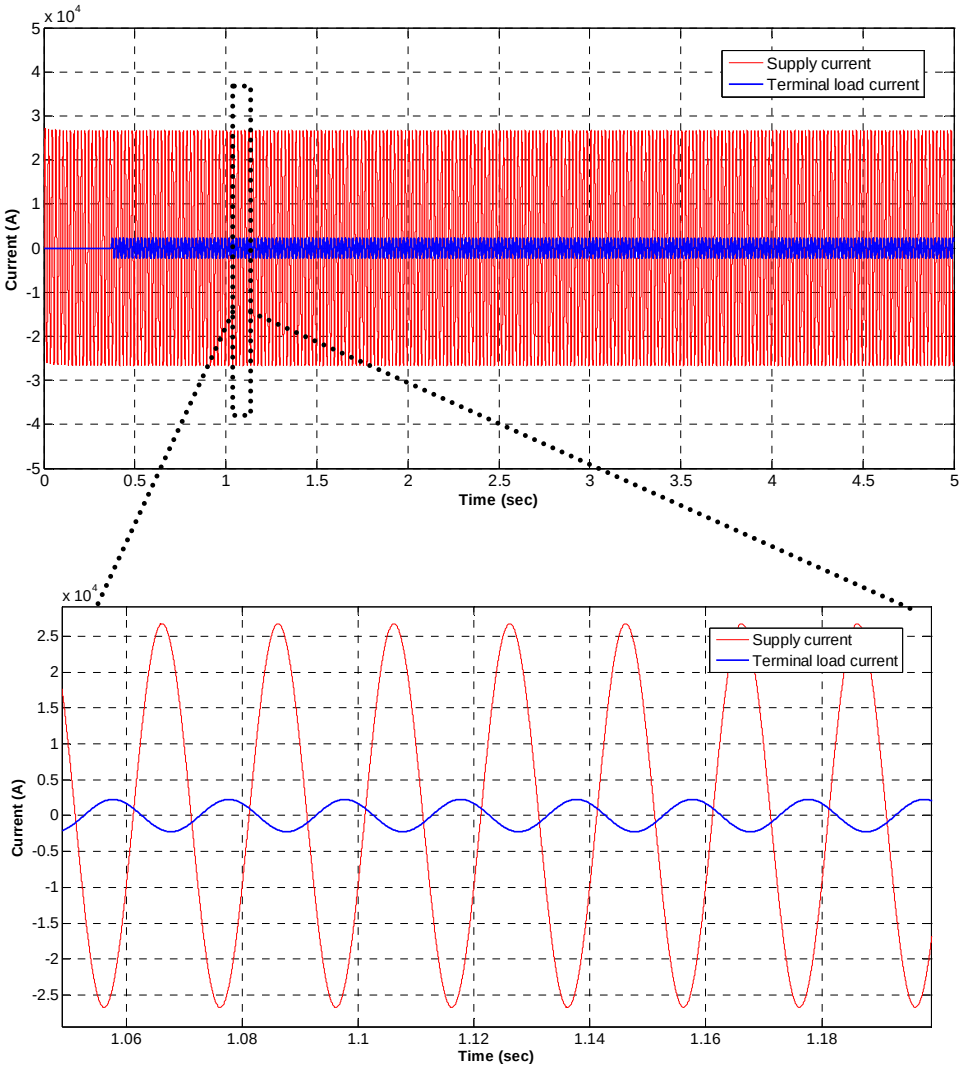

Figure-4.26: TLM: 400kV Cables transmission line response to sine wave input - AC voltage when the value of shunt conductance changed from $7.14e^{-7}$ to $7.14e^{-6}$ (including Fan's effect and line losses)

Figures – 4.27 to 4.31 show the Bode diagram and the 400kV cable transmission line's response when subjected to DC and AC voltage signals while including and excluding the effect of the disturbance when the series resistance is reduced shunt conductance is decreased from 7.14×10^{-7} to 7.14×10^{-8} Siemens/km.

Similar descriptions as given in Sections – 4.3.2.1 to 4.3.2.3 except the differences in the values achieved can be considered

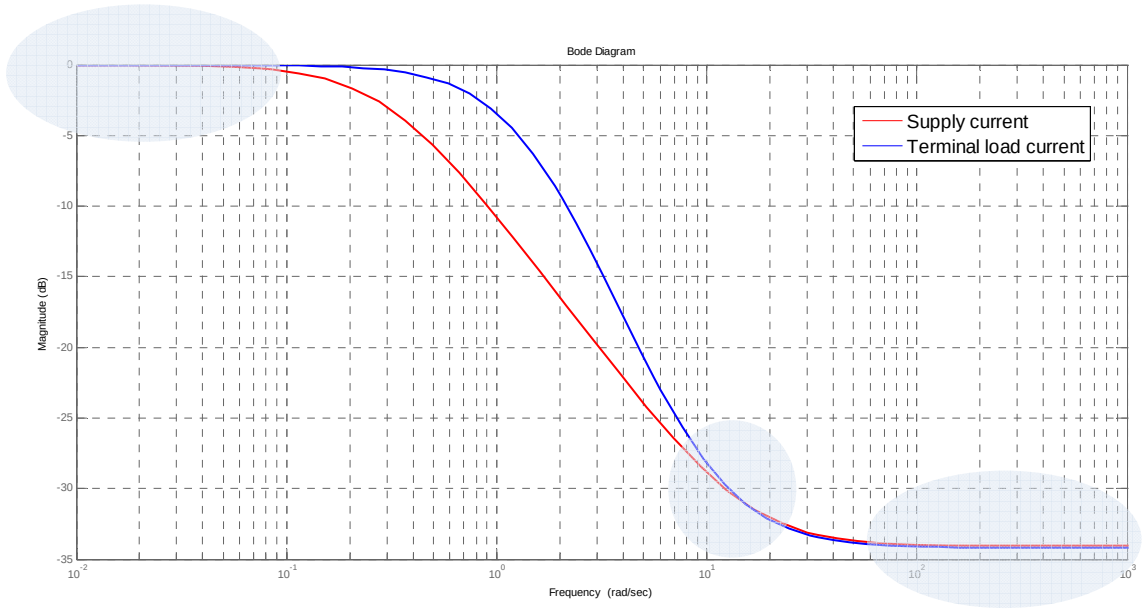

Figure-4.27: Bode diagram showing the original and approximated transfer functions when the value of shunt conductance changed from $7.14e^{-7}$ to $7.14e^{-8}$

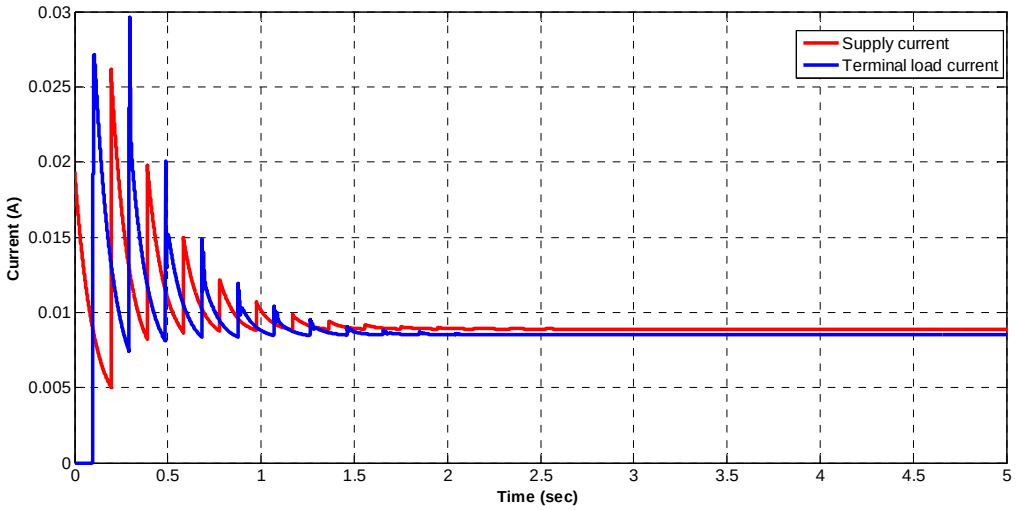

Figure-4.28: TLM: 400kV Cables transmission line response to step input - DC voltage when the value of shunt conductance changed from $7.14e^{-7}$ to $7.14e^{-8}$ (excluding Fan's effect and including line losses)

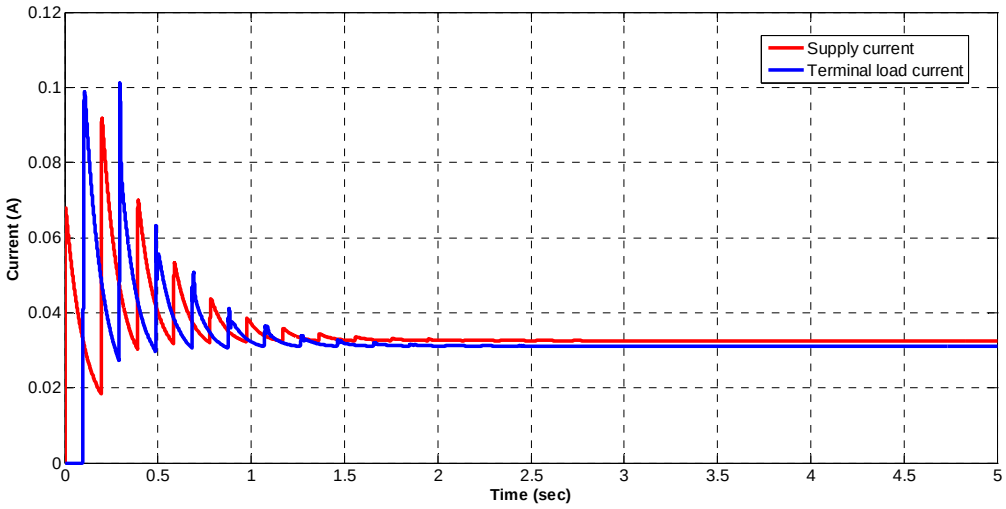

Figure-4.29: TLM: 400kV Cables transmission line response to step input - DC voltage when the value of shunt conductance changed from $7.14e^{-7}$ to $7.14e^{-8}$ (including Fan's effect and line losses)

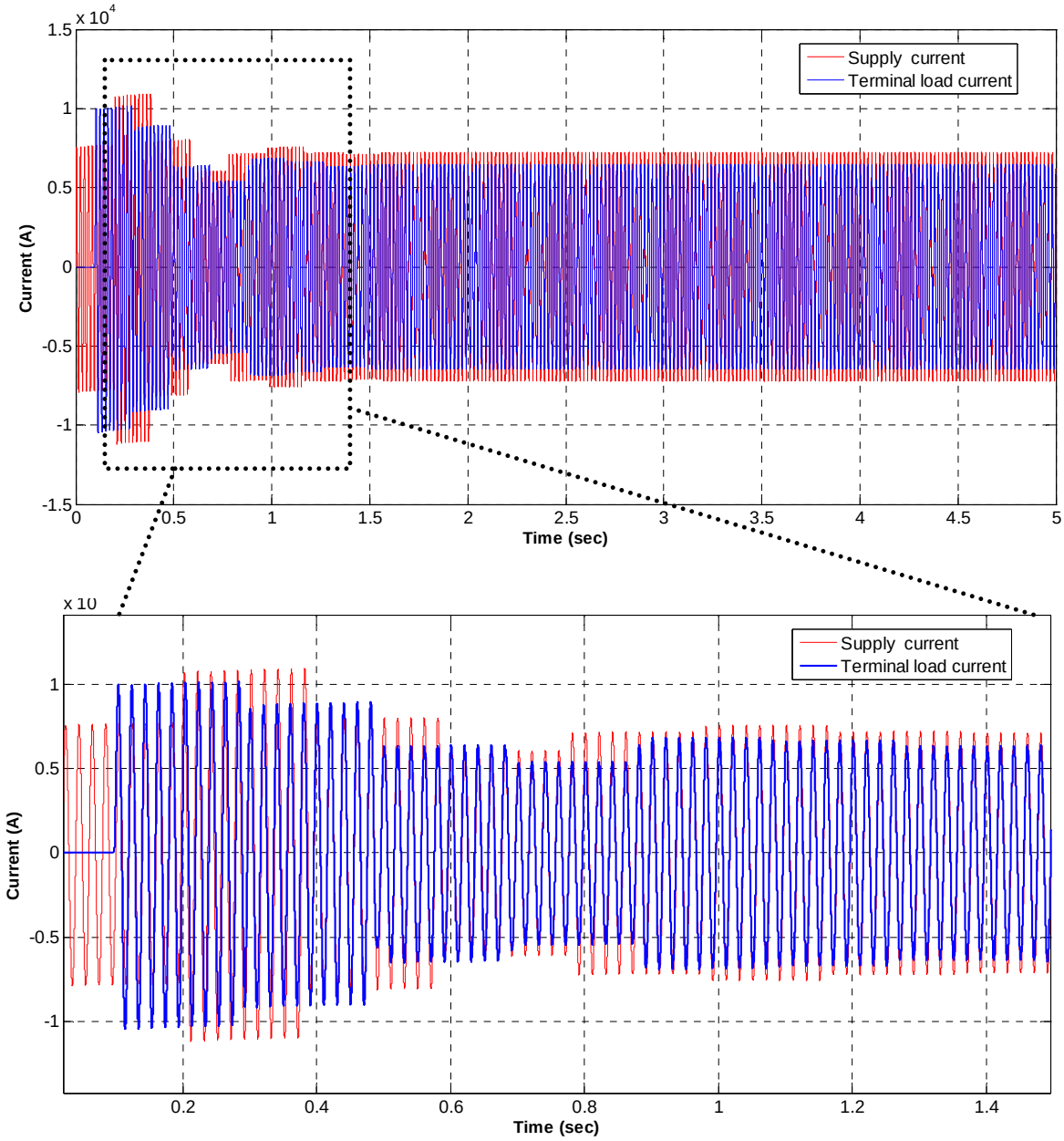

Figure-4.30: TLM: 400kV Cables transmission line response to sine wave input - AC voltage when the value of shunt conductance changed from $7.14e^{-7}$ to $7.14e^{-8}$ (Excluding Fan's effect and including line losses)

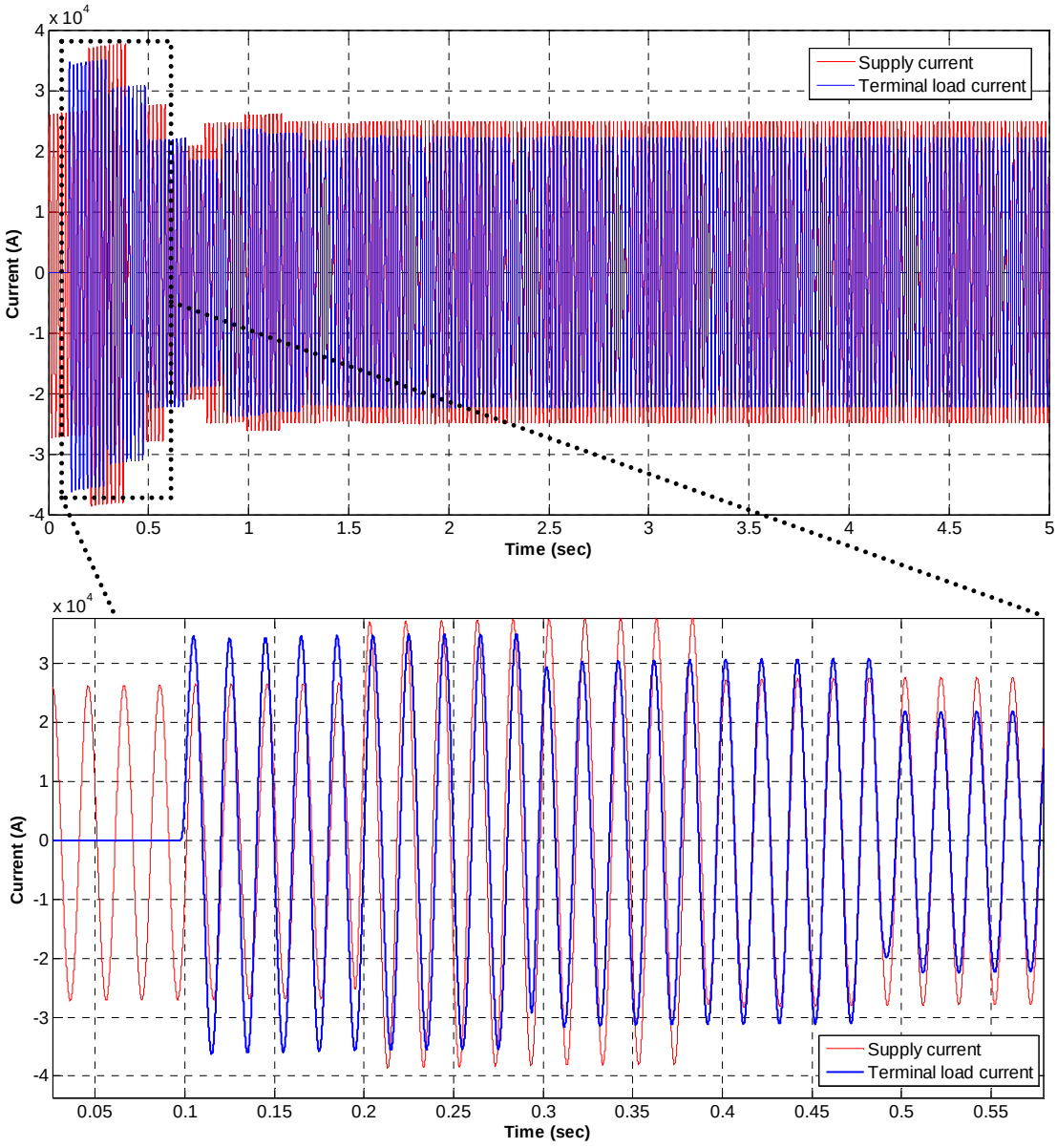

Figure-4.31: TLM: 400kV Cables transmission line response to sine wave input - AC voltage when the value of shunt conductance changed from $7.14e^{-7}$ to $7.14e^{-8}$ (including Fan's effect and line losses)

It can be seen from the above demonstrated various responses that the characteristic impedance is very sensitive to the shunt conductance changes in the low frequency range while the voltage and current propagation continue despite their illustrated steady state values being almost near to zero. As per manufacturer's provided parameters, the shunt conductance value varies enormously with the temperature (7.14×10^{-7} at 90°C and 7.14×10^{-10} at 20°C). The simulation results show that a small absolute change in the shunt conductance value can give different results when simulated in the time domain (Fernandes, Neves and Cavalcanti, 2004).

As a summary, the shunt conductance is sensitive and effected by temperature, ageing and pollution. It is also important to indicate that as the voltage case goes higher, the values of the shunt conductance should be set to a smaller value to control line losses.

Similar results regarding the effect of the shunt conductor on the transmission line were achieved also by Fernandes, Neves and Cavalcanti in their technical paper presented in 2004 (Fernandes, Neves and Cavalcanti, 2004).

Chapter-V

Conclusion and Recommendations

5.1. Conclusion

To sum up, the Transmission Line Modelling as stated earlier in this research was introduced in the beginning of seventies by Johns and Beurle. Since then, this technique was subjected to substantial development until it became a very powerful and progressively accepted numerical modelling tools (Duffy, 1995).

TLM has various areas where it is popularly used, but the main areas are in simulation of high frequencies and modelling long transmission lines. This is because it offers wide ranges of features and flexibility in modelling material properties and arbitrary geometries, in additions to its accuracy (Duffy, 1995).

As comprehensively discussed in the previous chapters, Transmission Line Modelling technique identifies the problem in the form of a set of continuous elements and boundary conditions. This is presented in 2-D or 3-D Cartesian network with initial excitation signals to reflect the wave propagation in the form of voltage and current in the network. The attractive advantage about this technique is its insurance of the availability of all spatial field elements within the centre of each node allocated in the network. Further, for transient analysis, it ensures also the

availability of all the related information to the frequency responses (Gothard and German, 1997).

Moreover, Transmission Line Modelling offers a time domain solution for various engineering applications. This cut the cost needed to be paid in case of usage of other methods which provide the solution vide going from frequency domain to the time domain such as Fourier Transform (Christopoulos, 2006).

This research focused in investigating the possibility of modelling the 400kV electrical cable transmission line considering its four line parameters against its no line losses. Accordingly, a hybrid system consisting of electrical and mechanical elements was modelled mathematically by using Finite Element and Distributed – Lumped Parameter techniques. The modelling of the transmission line was considered with no line resistance losses (R and G = 0) and with line resistance losses (R and G $\neq$ 0).

The derived mathematical models of Finite Element Method – FEM and Transmission Line Modelling – TLM were simulated using Mat-lap software and the achieved results were verified. The verification of the results focused on checking the system time domain responses while considering and not considering resistance line losses, the capability of 400kV cables to transmit full rated power for the cable rating, and finally, the effectiveness of the ventilation system which is provided inside the tunnel to enhance cable performance.

Detailed comparisons between the findings of Finite Element and Distributed – Lumped Parameter techniques were made. The comparisons covered the

mathematical model derivations, the simulated models, the simulation results and the effect of the shunt conductance variable values, on the performance of the long transmission line model.

It is concluded that from above, inaccuracy results were foreseen when the distributed element was lumped by length as shown in the Finite Element Method. In this regard, no benefits were added when the number of parameters increased. Instead, it increased the complexity in computation and difficulties in simulation. This confirm what stated earlier by Watton and Tadmori in 1988, where they explained that lumping by length, similar to the way followed by the traditional matrix method, will definitely increase the percentage of errors with the increases in the number of lumped elements. As an example, with five finite element sections, eleven eigenvalues will be generated and the order of equations will inflate to 21 with an equal number of eigenvalues and corresponding eigenvectors.

Hence, the increase in the number of finite elements for the purpose of enhancing the accuracy when it is linked with modelling a long transmission line will not add any value. Instead, it increases the complexity in computation. It also, not reflects the concept of wave propagation since FEM model is a dimensionless.

It is important to indicate, that the accuracy of the Transmission Line Modelling is observed clearly from the achieved system responses when compared with the Finite Element Method's results. This was specifically observed when the series resistance and the shunt conductance added in the hybrid modelled system. Not

only that, it shows applicability in simulating the cable model with its four line parameters.

In practice, attempts are normally made to achieve nearly lossless transmission lines. However, this is not achievable due to the line losses introduced through the series resistance and the shunt conductance throughout the line. Manufacturers and researchers normally ignore the effect of shunt conductance due to its negligible value or rational functions generated while carrying out the mathematical derivation. However, in this research, the possibility in modelling long transmission lines considering its four line parameters were successfully demonstrated.

Utilization of the Bode diagram to eliminate the rational functions generated for wave propagation $\Gamma(s)$ and damping ratio $\zeta(s)$ as part of the mathematical derivation, was a newly effective technique employed to achieve the main objective of this research. It assists in providing, from the frequency domain, an approximate transfer function to the original transfer function and uses this approximated transfer function in the time domain. This is in order to simulate $\Gamma(s)$ and $\zeta(s)$.

Below are the recommendations made as an outcome of this study.

5.2. Recommendations

The best to consider in the case of Finite Element Method, but in the same time shall not be treated as a working rule, is obtaining the results from two lump sections only. This will assist in minimizing the change of the time step size

(Watton and Tadmori, 1988). This was noticed when series resistance and shunt conductance were added a part of the model and led to setting the time step size to a value almost near to zero to be able to run the system. Despite this attempt, the model shown numerically instability and simulation results could not be obtained. Hence, Finite Element Method, from the author point of view, is not recommended to be adopted in modeling long transmission line due to the limitations and drawbacks discussed. However, judgment in this regard is left to the designer to choose the most suitable method to model the selected system.

For building more confident on the results of Transmission Line Modelling - TLM, it is recommended to carryout further verification by comparing the simulated results with the experimental results. Christopoulos stated in one of his published papers that experiments were carried out in a range of applications, from which, the accuracy of this method was confirmed (Chistopoulos, 1991). As such, the experimental methods along with numerical modelling are applicable to be utilized for the purpose of enhancing the understanding of the system responses. In addition, it assists in predicting the measurement in various environments (Christopoulos, Mallik, Naylor and Johns, 1988). This was also suggested by A.P. Duffy, T.M. Benson and C. Christopoulos (Duffy, Benson and Christopoulos). The author is of the opinion that the experimental method will assist in clearing the concern pertaining the provided values, specifically the value of the shunt conductance.

It is recommended to adopt the Distributed Lumped Parameter Model proposed by Whalley to model and analyze long transmission lines.

Based on the assessment highlighted in this research pertaining to the effect of the shunt conductance on the cable performance, it is strongly recommended to further study its effects and not to ignore it at the design stage, bearing in mind that this will have cost impact. However, it will add a value since the shunt conductance is related to line losses and therefore, has impact on system reliability and can also dealt with as unforeseen cost losses.

A further study is recommended to identify the reasons why the calculated and simulated values for supply and terminal load currents are not matching. This mismatching can be noticed clearly as an impact on the cable power transmission capacity, as it shows beyond its full rated power under the cable rating despite considering the given cable parameters in the simulated model. In addition, the inclusion of fan was meant to enable the cable achieve its full power rating. However, the simulation results show the values exceeding the requirement.

Finally, it is recommended to review the current simulated values in comparison with the international standard IEC-60287 used normally to calculate the maximum continuous current carrying capacity of transmission lines. It is important to highlight that based on the IEC-60287, the maximum continuous current carrying capacity is affected mainly by the conductor temperature rise above the ambient temperature, the dielectric loss per unit length for the insulation surrounding the conductor, the thermal resistance per unit length between the conductor and the sheath, the thermal resistance per unit length of the external serving of the cable, the thermal resistance per unit length of the surrounding medium, the alternating current resistance per unit length of the conductor at maximum operation

temperature, and the ratio of losses in the metallic screens to total losses in the conductor (DEWA/EDF/Nexan, 2011). Hence, such comparison will be useful to verify the accuracy of the modelled cable against the method used to calculate its maximum continuous current carrying capacity.

References

1. Akhtarzad S and Johns P.B, *"Transmission line-matrix solution of waveguides with wall losses"*, Electronics Letters, Vol.9, No. 15, pp 335-336, 1973.

2. Akhtarzad S and Johns P.B, *"Numerical Solution of Lossy Waveguides: T.L.M. Computer Program"*, Electronics Letters, Vol.10, No. 15, pp 309-311, 1974.

3. Akhtarzad S and Johns P.B, *"Generalised elements for t.l.m. method of numerical Analysis",* Proc. IEE, Vol. 122, No. 12, pp 1349-1352, 1975.

4. Akhtarzad S and Johns P.B, *"Solution of Maxwell's equations in three space dimensions and time by the t.l.m. method of numerical analysis"*, Proc. IEE, Vol. 122, No. 12, pp 1344-1348, 1975.

5. Akhtarzad S and Johns P.B, *"Three-Dimensional Transmission-Line Matrix Computer Analysis of Microstrip Resonators"*, IEEE Transactions on microwave theory and techniques, Vol. MTT-23 No. 12, pp 990-997, 1975.

6. Adam S and Huang W.G, *"Corona Modelling for the Calculation of Transients on Transmission Lines"*, IEEE Transactions on Power Delivery, Vol. PWRD-1, No. 3, pp 228–239, 1986.

7. Aleyaasin M and Ebrahimi M, *"Hybrid modelling for analysis and identification of rotors"*, Elsevier Science S.A, pp 163-176, 2000.

8. Al-Arainy A, Qureshi M and Malik N, *"Fundamentals of High Voltage Engineering"*, Academic Publishing and Press, KSA, 2005.

9. Al-Arainy A, Qureshi M and Malik N, *"Fundamentals of High Voltage Engineering"*, Academic Publishing and Press, KSA, 2007.

10. Abdul-Ameer A, "*Modelling of Fluid Power Transmission Systems*", International Symposium on Innovation in Intelligent Systems and Applications, 15-18 June, 2011, Istanbul – Turkey, pp 205-211, 2011.

11. Bandler J. W, *"Transmission- Line Modeling and Sensitivity Evaluation for-Lumped Network Simulation and Design in the Time Domain"*, Journal of The Franklin Institute, pp 15-32, 1977.

12. Bartlett H and Whalley R, *"Modelling and analysis of variable geometry exhaust gas systems"*, Elsevier Science Inc, pp 545–567, 1998.

13. Barati E and Esfahani J.A, *"Mathematical modeling of convective drying Lumped temperature and spatially distributed mositure in slab"*, Elsevier Ltd, pp 2294-2301, 2010.

14. Bartlett H, Whalley R and Rizvi S.S.I, *"Hybrid modelling of marine power transmission systems",* pp 97-108, 1998.

15. Choi D.H and Hoefer W.J.R, *"The Finite-Difference–Time-Domain Method and its Application to Eigenvalue Problems"*, IEEE Transaction Microwave Theory and Techniques, Vol. MTT-34, pp 1464-1470, 1986.

16. Christopoulos C, Mallik A, Naylor, P and Johns P.B, *"Computer modelling for vehicle electromagnetic compatibility",* IET conferences, pp 5/1- 5/2, 1988.

17. Christopoulos C, *"The Historical Development of TLM"*, IEEE, pp 1/1–1/4, 1991.

18. Christopoulos C, Herring J. L and Scaramuzza R.A, *"Electromagnetic simulation using transmission line modelling"*, IEEE, pp 5/1–5/4, 1991.

19. Chen Z, Ney M.M and Hoefer W. J. R, *"A New Finite-Difference Time-Domain Formulation and its Equivalence with the TLM Symmetrical Condensed Node"*, IEEE Transactions on Microwave Theory and Techniques, Vol. 39, No. 12, pp 2160-2169, 1991.

20. Chistopoulos C, *"Transmission-Line Modelling (TLM): A brief introduction and recent advance"*, IEEE, pp 1/1-1/6, 1993.

21. Close C.M and Frederick D.K, *"Modeling and analysis of dynamic systems"*, Houghton Mifflin, 2nd Edition, USA, 1993.

22. Cascio L and Hoefer W.J.R, *"Modification of the 3D-TLM Scattering matrix to model nonlinear devices in graded and heterogeneous regions"*, IEEE, pp 897-900, 1998.

23. Christopoulos C, *"Electromagnetic-Ancient and Modern"*, Asia Pacific Conference on Applied Electromagnetic, pp 1-4, 2003.

24. Christopoulos C, *"The Transmission-Line Modeling (TLM) Method in Electromagnetics"*, Morgan and Claypool Publishers, USA, 1st Edition, 2006.

25. Douglas C.G, *"Physics for Scientists and Engineers"*, Prentice-Hall International Editions, USA, 2nd Edition, 1988.

26. Duncan G.J and Sarma M, *"Power System Analysis and Design"*, PWS Publishing Company, Boston, 2nd Edition, 1994.

27. Duffy A.P, *"Transmission-Line Modelling (TLM) as High Frequency Numerical Modelling Tool"* IET Conferences, pp 4/1 4/5, 1995.

28. Duffy A.P, Heming, J.L, Benson T.M and Christopoulos, C, *"Comparison of TLM Simulations and Experiments in EMC Problems"*, pp 4/1-4/3, 2003.

29. Dorf R.C and Bishop R.H, *"Modern Control Systems"*, Pearson Prentice Hall, 11th edition, New Delhi, India, 2009.

30. Dynamic Models Distributed parameter systems, Chapter 7.

31. DEWA/EDF, CNE/0069/09, "*Requirements for Design and installation of Power Cables and their Accessories"*, Supply, Installation, Testing and Commissioning of 400kV Cables Work for Mushriff – Mamzar Beach – Nahda 400/132kV Substations, Tender documents, Technical specification, Volume-III, Section-1, Clause 3.2, pp 17, 2009.

32. DEWA/EDF, CNE/0069/09, Tender documents, Volume-IV, Section-1, pp 3-9, 2009.

33. DEW/Nexan, CNE/0069/09, "*2500 mm2 copper XLPE cable 230/400 (420) kV"*, HTC 2918-2, Revision 5, pp 1-7, 2010.

34. DEWA/EDF/Nexan, CNE/0069/09, *"Current rating calculation for 400kV Cable"*, E/05/40257, Rev.6, pp 1-46, 2011.

35. DEWA/EDF/Nexan, CNE/0069/09, *"Document Transmittal Sheet: Technical particulars and guarantees of 400kV cable",* E/05/40255, DTS-ref: CNE/0069/MBCH/0297, pp, 1-5, 2011.

36. DEWA/Nexan, CNE/0069/09, *"Natural and forced ventilation Nahda / Mamzar and Mushrif / Mamzar"* pp 3-13, 2011.

37. DEWA/Nexan, CNE/0069/09, Pictures, 2011.

38. Eswarappa C.G.I and Hoefer W. J. R, *"Transmission Line Matrix Modeling of Dispersive Wide-Band Absorbing Boundaries with Time-Domain Diakoptics for S-Parameter Extraction"*, IEEE Transactions on Microwave Theory and Techniques, Vol. 38, No. 4, pp 379-386, 1990.

39. EDF letter, ref: EDF-DEWA-306A-11-008, dated 12/01/2011

40. Flack T.J and Knight R.E, *"On the Domain Decomposition and Transmission Line Modelling Finite Element Met hod for Time-Domain Induction Motor Analysis"*, IEEE, pp 1290–1293, 1999.

41. Fernandes A.B, Neves W.L.A and Cavalcanti N, *"The Effect of the Shunt Conductance on Transmission Line Models"*, Vol 19, Issue-2, pp 722-728, 2004.

42. Gui X, Webb P.W and Gao G, *"Use of the Three-Dimensional TLM Method in the Thermal Simulation and Design of Semiconductor Devices"*, IEEE Transactions of Electron Devices, Vol. 39, No. 6, pp 2295-1302, 1992.

43. Groppi G, Belloli A, Tronconi E and Forzatti P, *"A Comparison of lumped and distributed models of monolith catalytic combustors"*, Elsevier Science Ltd, Vol. 50, No. 17, pp 2705-2715, 1995.

44. Gothard G.K, and German F.J, *"Transmission Line Modelling Method"*, Chapter 7, Harris Corporation, Raytheon Systems Company, 1997.

45. Garciaa G.A.R, M.R.R and Kevrekidis I.G, *"Identification of distributed parameter systems: A neural net based approach"*, Elsevier Science Ltd, Printed in Great Britain, Vol. 22, pp S965-S968, 1998.

46. Heydweiller J.C, Sincovec R.F and Fan L, *"Dynamic Simulation of Chemical Processes Described by Distributed and Lumped Parameter Models"*, Pergamon Press, Printed in Great Britain, Vol. I, pp 125-131, 1977.

47. Hendrickx M, Engels C, Tobback P and Johns P, *"Transmission Line Modelling (TLM) of Water Diffusion in White Rice"*, Journal of Food Engineering 5, pp 269-285, 1986.

48. Hoefer W.J.R, *"New Horizons in Numerical Time Domain Modelling of Microwave Structures"*, pp 7-20, 1990.

49. Hui S.Y.R, and Christopoulos C, *"The use of TLM-Based Discrete Transforms for General Numerical Analysis"*, pp 6/1 – 6/2, 1991.

50. Hoefer W.J.R, *"Huygens and the Computer-A Powerful Alliance in Numerical Electromagnetics"*, Proceedings of the IEEE, Vol. 79, No 11, pp 1459-1471, 1991.

51. Hein S, *"TLM numerical solution of Bloch's equations for magnetized gyrotropic media"*. Elsevier Science Inc, pp 221-229, 1997.

52. Hansen T. B and Kaiser G, *"Huygens' Principle for Complex Spheres"*, IEEE Transactions on Antennas and Propagation, Vol. 59, No. 10, pp 3835-3847, 2011.

53. Johns P.B, *"Numerical calculation for scattering in waveguides using a transmission line matrix"*, Volume 2, IEEE conference, pp D 1/2, 1971.

54. Johns P.B and Beurle R.L, *"Numerical solution of 2-dimensional scattering problems using a transmission-line matrix"*, Proc. IEE, Vol. 118, No. 9, pp 1203-1208, 1971.

55. Johns P.B, *"Application of the transmission-line-matrix method to homogeneous waveguides of arbitrary cross-section"*, Proc. IEE, Vol. 119, No. 8, pp 1086-1091, 1972.

56. Johns P.B, *"The Solution of Inhomogeneous Waveguide Problems Using a Transmission-Line Matrix"*, IEEE Transactions on Microwave Techniques, Vol. MTT-22, No. 3, pp 209 – 215, 1974.

57. Johns P.B, *"A new mathematical model to describe the physics of propagation"*, Vol. 44, No. 12, IEC Journal, pp 657-666, 1974.

58. Johns P.B, *"New Symmetrical Condensed Node for Three-Dimensional Solution of Electromagnetic-wave Problems by TLM"*, Electronics Letters, Vol. 22, No. 3, pp 162-164, 1986.

59. Johns P. B, *"Use of condensed and symmetrical TLM nodes in computer-aided electromagnetic design"*, IEE PROCEEDINGS, Vol. 133, Pt. H, No. 5, pp 368-374, 1986.

60. Johns P.B, *"On the Relationship Between TLM and Finite-Difference Methods for Maxwell's Equation"*, IEEE Transactions on Microwave Theory and Techniques, Vol. MTT-35, No. 1, pp 60-61, 1987.

61. Johns, P. B. (13 May 1988). *Simulation of electromagnetic wave interactions by using transmission line modelling.* Elsevier Science Publishers B.V. pp. 597-610.

62. Johns D.P, Wlodarczyk A.J, Mallik A and Scaramuua R, *"The Application of TLM to Electromagnetic Problems Over a Wide Range of Frequencies",* Kimberiey Communications Consultants Ltd, pp 3/1-3/5, 1993.

63. Jih H and Vahldieck R, *"Full-Wave Analysis of Guiding Structures Using a 2-D Array of 3-D TLM Nodes"*, IEEE Transactions on Microwave Theory and Techniques, Vol. 41, No. 3, pp 472-477, 1993.

64. Jonathan L.H and Hoefer, W.J.R, *"Developments in the Transmission-Line Modelling (TLM) of Microwave Components"*, YUMTT Chapter Informer, pp 15-19, 1996.

65. Johns D.P, *"Development of the TLM Method for EMC EMI analysis"*, International Symposium on Electromagnetic Theory, IEEE, pp 279-282, 2010

66. Kosar V, Gomzi Z and Sintic K, *"Modelling and simulation of the continuous power cable processing"*, Elsevier B.V, pp 83–88, 2006.

67. Leonard M, and Hoefer, W.J.R, *"Modeling of General Constitutive Relationships in SCN TLM"*, IEEE Transactions on Microwave Theory and Techniques, Vol. 44, No. 6, pp 854-861, 1996.

68. Li J and Liu C, *"A Three-Dimensional Transmission Line Matrix Method (TLM) for Simulations of Logging Tools"*, IEEE Transactions on Geoscience and Remote Sensing, Vol. 38, No. 4, pp 1522-1529, 2000.

69. Moore G.F, *"Electric Cables Hand Book"*, 3rd Edition, Blackwell publishing, 1997.

70. Michael F, Juergen V, Liliana O and Corneliu V, *"Modelling and simulation of high-voltage transmission lines with frequency dependent parameters"*, Elsevier Science B.V, pp 323 – 326, 1998.

71. Matthew N.O.S and Clarence N.O, *"A Comparison of Time-Domain Finite Difference (FDTD) and Transmission-Line Modeling (TLM) Methods"*, IEEE, pp, 19 – 22, 2000.

72. McClure G and Lapointe M, *"Modeling the structural dynamic response of overhead transmission line"*, pp 825 – 834, 2003.

73. Matsumura M, Fukuda K, Fujiwara E, Shiro T, Watanabe M, Sakaguchi Y and Ooimo T, *"Transmission Capacity Design of Underground Power Cables installed in Deep Tunnel"*, IEEE, The Kansai Electric Power Co.Inc, J-Power Systems Corp., Osaka, Japan, pp 1-7, 2006.

74. Mimouni S, Saidane A and Feradji A, *"Transmission-line-matrix (TLM) modeling of self-heating in AlGaN/GaN transistor structures"*. Microelectronics Journal 39, pp 1167–1172, 2008.

75. Mohan N, *"Electric Power Systems",* John Wiley & Sons, Inc, 2012.

76. Naylor P and Ait-Sadi R, *"Simple method for determining 3-D TLM nodal scattering in nonscalar problems"*, Electronics letters, Vol. 28, NO. 25, pp 2353-2354, 1992.

77. Ogata K, *"Modern Control Engineering",* 5th edition, Pearson Prentice Hall, New Delhi, India, 2010.

78. Oprea L and Velicescu C, *"Modelling Nonlinear Frequency Dependent Transmission Line for Electromagnetic Transients Studies in Power Systems"*, IEEE, pp 798 – 801, 1996.

79. Pulko S.H and Phizacklea C.P, *"Numerical aspects of modelling glass pressing processes using the TLM technique",* Pergamon Press plc, Proc. 7th Int. Conf. on Mathematical and Computer Modelling, Math1 Comput. Modelling, Vol. 14, pp 1061-1066, 1990.

80. Pomeroy S.C, *"Introduction to the modeling of wave propagation using TLM"* pp 2/1–2/3, 1991.

81. Pilgrim J.A, Swaffield D.J, Lewint P.L and Payne D, *"An Investigation of Thermal Ratings for High Voltage Cable Joints through the use of 2D and 3D Finite Element Analysis"*, IEEE, pp 543 – 546, 2008.

82. Rowbotham T.R and Johns P.B, *"Waveguide Analysis by Random Walks"*, Electronics Letters, Vol.8, No. 10, pp 251-253, 1972.

83. Ray W. H, *"Some Recent Applications of Distributed Parameter Systems Theory-A Survey",* Pergamon Press Ltd, Printed in Great Britain, Vol. 14, pp 281 – 287, 1978.

84. Ruddle A, Ward D, Scaramuzza R and Trenkic V, *"Development of Thin Wire Models in TLM",* IEEE, pp 196-201, 1998.

85. Rak M, Gui X and Cogan D, *"Transient analysis of surface supersaturation after crystal face submersion using the analytical and transmission-line matrix (TLM) methods",* Journal of Crystal Growth 197, Elsevier Science B.V, pp 944-954, 1999.

86. Schierwagen A.K, *"Identification Problems in Distributed Parameter Neuron Models"*, Printed in Great Britain, International Federation of Automatic Control, Vol.26, No.4, pp 739 – 755, 1990.

87. Selhi H, Hui Y.R.C, Christopoulos C and Howe A.F, *"The Application of Transmission-Line Modelling to the Simulation of an Induction Motor Drive"*, IEEE, pp 287 – 297, 1995.

88. Smart C.J and Christopoulos C, *"Modelling nonlinear and dispersive propagation problems biy using the TLM method",* IEE Proc.-Microw. Antennas Propag, Vol. 145, No. 3, pp 193-200, 1998.

89. Shehata A.Y, El Damatty A.A and Savory E, *"Finite element modeling of transmission line under downburst wind loading"*, Elsevier B.V, pp 71-89, 2005.

90. Trenkic V, Christopoulos C and Benson T.M, *"A Graded Symmetrical Super-condensed Node for the TLM method",* IEEE, pp 1106-1109, 1994.

91. Trenkic V, Christopoulos C and Benson T.M, *"Advanced Node Formulations in TLM-The Adaptable Symmetrical Condensed Node"*, IEEE Transactions on microwave theory and techniques, Vol. 44, No.12, pp 2473-2478, 1996.

92. Trenkic V, Christopoulos C and Benson T.M, *"Development of a General Symmetrical Condensed Node for the TLM Method"*, IEEE Transactions on microwave theory and techniques, Vol. 44, No.12, pp 2129-2135, 1996.

93. Trenkic V, Christopoulos C and Benson T.M, *"Optimization of TLM Schemes Based on the General Symmetrical Condensed Node"*, IEEE Transactions on antennas and propagation, Vol. 45, No. 3, pp 457-465, 1997.

94. Ting C.M and Jennings P.A, *"A novel Application of Transmission Line Theory in EMC Assessment"*, University of Warwick, UK, 10th International Conference on Electromagnetic Compatibility, 1-3, Conference Publication No 445, IEE, pp 181-186, 1997.

95. Venkatramana T and Jenkins L, *"Transient stability analysis using Diakoptics"*, IEE-IERE Proceeding, India, pp 135-143, 1978.

96. Van Deen J.K and Reintsema S.R, *"Modelling of high-pressure gas transmission line"*, The Netherlands, Appl. Math. Modelling, Vol. 7, pp 268-273, 1983.

97. Vukovic A, Sewell P, Styan C and Benson T.M, *"Modelling Non-Linear Photonic Structures Using the Transmission Line Modelling Method"*, pp 118-119, 2008.

98. Villegas J.A, Duncan S.R, Wang H.G, Yang W.Q and Raghavan R.S, *"Distributed parameter control of a batch fluidised bed dryer"*, pp 1096–1106, 2009.

99. Watton J and Tadmori M. J, *"A comparison of techniques for the analysis of transmission line dynamics in electrohydraulic control systems"*, Appl. Math. Modelling, Butterworth Publishers, pp 457-466, Vol. 12, 1988.

100. Whalley R, *"The response of distributed-lumped parameter system"*, Roc Instn Mech Engrs, Vol. 202, No C6, pp 421-429, 1988.

101. Whalley R; Abdul-Ameer A and Ebrahimi K.M, *"Hybrid modelling of machine tool axis drives"*, International Journal of Machine Tools and Manufacture 45, pp 1560–1576, 2005.

102. Whalley R and Abdul-Ameer A, *"Heating, ventilation and air conditioning system modelling"*, Elsevier Ltd, pp 644–656, 2010.

103. Whalley R, Abdul-Ameer A and Ebrahimi K.M, *"The axes response and resonance identification for a machine tool"*, Elsevier Ltd, pp 1171–1192, 2011.

104. Whalley, R and Abdul-Ameer, A. (2011). *The dynamics of cyclic ventilation systems*. Elsevier Inc. pp. 93–108.

105. Xu J, Chen Z and Chuang J, *"Numerical Implementations of PML Boundary Conditions in the TLM-Based SCN FDTD Grid",* IEEE Transactions on microwave and techniques, Vol. 45, No. 8, pp 1263-1267, 1997.

106. Yunus A.C, Michael A.B, *"Thermodynamics and Engineering Approach",* McGRAW-HILL, New York, 1989.

107. Zitron, Spain catalogues, CNE/0069/09, 2012.

Appendix

Appendix-A1:

Defined parameter values for the system (DEWA/EDF/Nexan, 2011)

Description	Symbol	Unit	Selected Value
Cable Specification:			
Cable mass	m	kg	38.4
Cable diameter	d	km	0.152×10^{-3}
Cable radius	r	km	0.076×10^{-3}
Cable length	l	km	11.5
Number of Joints	-	#	26
Conductor Resistance per unit length*	R_c	Ohm/km	9.73×10^{-3}
Conductor Inductance per unit length*	L_c	Henry/km	0.637×10^{-3}
Conductor Capacitance per unit length*	C_c	Farad/km	0.236×10^{-6}
Insulation resistance per unit length*	R_I	Ohm/km	1.4×10^{6}
Leakage conductance per unit length*	G_I	Siemens/km	0.714×10^{-6}
Damping ratio (zeta)**	ζ	Ratio	51.953
Time Delay**	T_1	sec	2.82×10^{-4}
AC Voltage Input			
Voltage	V_s	kV	400
Frequency	f	Hz or Cycles/sec	50
Angular Velocity of the coil**	ω	Rad/sec	314.159
Period of sinusoidal waveform**	T_2	sec	0.02
Terminal Load Impedance for one power transformer * **			
Resistance	R_L	Ohm	0.979
Inductance	L_L	Henry	0.345
Terminal Load Impedance for four power transformers connected in parallel * **			
Resistance	R_L	Ohm	0.2448
Inductance	L_L	Henry	0.08622
Fan AC Motor Specification:			
Motor Constant	K_m	Nm/A	3.66
Motor Resistance **	R_m	Ω	0.62
Motor Inductance **	L_m	H	0.7×10^{-3}

* Values measured at 90˚C

** Calculated Values. Refer Appendix-A2.

*** Terminal load is variable.

Appendix-A2:

Calculated Values

$$\omega = 2\pi f = 2\pi(50) = 314.159 rad/\sec \quad (1)$$

$$T_2 = \frac{1}{f} = \frac{1}{50} = 0.02\sec \quad (2)$$

Considering no line losses for TLM model:

$$\zeta = \sqrt{\frac{L}{C}} = \sqrt{\frac{0.637\times10^{-3}}{0.236\times10^{-6}}} = 51.95336892 \quad (3)$$

$$L = 0.637\times10^{-3}/km = 0.637\times10^{-6} \quad (4)$$

$$C = 0.236\times10^{-6}0/km = .236\times10^{-9} \quad (5)$$

$$T = 2l\sqrt{LC} = 2\times11.5\times10^{3}\times\sqrt{0.637\times10^{-6}\times0.236\times10^{-9}} = 2.820028865\times10^{-4}\ \sec \quad (6)$$

Considering line losses for TLM model:

A. Original and Approximated Transfer Functions: -

$$(\frac{Cs}{G}+1)\frac{(Ts+1)^2}{(\tau s+1)^2} \cong \frac{Ls}{R}+1 \quad (7)$$

$$\frac{\frac{L}{R}s+1}{\frac{C}{G}s+1} \cong \frac{(Ts+1)^2}{(\tau s+1)^2} \quad (8)$$

$$\frac{\frac{0.637\times10^{-3}}{9.73\times10^{-3}}s+1}{\frac{0.236\times10^{-6}}{0.714\times10^{-6}}s+1} \cong \frac{(0.0915s+1)^2}{(0.205s+1)^2} \quad (9)$$

$$\frac{0.0655s+1}{0.3305s+1} \cong \frac{(0.0915s+1)^2}{(0.205s+1)^2} \quad (10)$$

$$\zeta(s) = \sqrt{\frac{R}{G}}\sqrt{\frac{(Ts+1)^2}{(\tau s+1)^2}} = \bar{\alpha}\frac{(Ts+1)}{(\tau s+1)} \quad (11)$$

$$\zeta(s)=\sqrt{\frac{9.73\times10^{-3}}{0.714\times10^{-6}}}\frac{(0.0915s+1)}{(0.205s+1)} \tag{12}$$

$$\zeta(s)=116.7366737\frac{(0.0915s+1)}{(0.205s+1)} \tag{13}$$

$$w(s)=\frac{1+e^{-2l\alpha(as+b)}}{1-e^{-2l\alpha(as+b)}}=\frac{1+e^{-2l\alpha b}e^{-2l\alpha as}}{1-e^{-2l\alpha b}e^{-2l\alpha as}} \tag{14}$$

$$a=\left[\frac{C}{G}+T-\tau\right] \tag{15}$$

$$a=\left[\frac{0.236\times10^{-6}}{0.714\times10^{-6}}+(0.0915)-(0.205)\right]=0.217032212 \tag{16}$$

b=1 (17)

$$\alpha=\sqrt{RG}=\sqrt{(9.73\times10^{-3})(0.714\times10^{-6}}=8.3349985\times10^{-5} \tag{18}$$

$$e^{-2l\alpha b}=e^{-2(11.5\times10^{3})(8.3349985\times10^{-5})(1)}=e^{-1.917049655}=0.147040141 \tag{19}$$

$$e^{-2l\alpha a}=e^{-2(11.5\times10^{3})(8.3349985\times10^{-5})(0.217032212)}$$
$$=e^{-0.416061502}=0.6596397 \tag{20}$$

$$w(s)=\frac{1+e^{-2l\alpha b}e^{-2l\alpha as}}{1-e^{-2l\alpha b}e^{-2l\alpha as}}=\frac{1+0.147040141e^{-0.416061502s}}{1-0.147040141e^{-0.416061502s}} \tag{21}$$

B. When changing shunt conductance value from 7.14×10^{-7} to 7.14×10^{-6} and Approximated Transfer Functions: -

$$(\frac{Cs}{G}+1)\frac{(Ts+1)^2}{(\tau s+1)^2}\cong\frac{Ls}{R}+1 \tag{22}$$

$$\frac{\frac{L}{R}s+1}{\frac{C}{G}s+1}\cong\frac{(Ts+1)^2}{(\tau s+1)^2} \tag{23}$$

$$\frac{\frac{0.637\times10^{-3}}{9.73\times10^{-3}}s+1}{\frac{0.236\times10^{-6}}{7.14\times10^{-6}}s+1}\cong\frac{(0.0575s+1)^2}{(0.0409s+1)^2} \quad (24)$$

$$\frac{0.0655s+1}{0.03305s+1}\cong\frac{(0.0575s+1)^2}{(0.0409s+1)^2} \quad (25)$$

$$\zeta(s)=\sqrt{\frac{R}{G}}\sqrt{\frac{(Ts+1)^2}{(\tau s+1)^2}}=\alpha\frac{(Ts+1)}{(\tau s+1)} \quad (26)$$

$$\zeta(s)=\sqrt{\frac{9.73\times10^{-3}}{7.14\times10^{-6}}}\frac{(0.0575s+1)}{(0.0409s+1)} \quad (27)$$

$$\zeta(s)=36.91537753\frac{(0.0575s+1)}{(0.0409s+1)} \quad (28)$$

$$w(s)=\frac{1+e^{-2l\alpha(as+b)}}{1-e^{-2l\alpha(as+b)}}=\frac{1+e^{-2l\alpha b}e^{-2l\alpha as}}{1-e^{-2l\alpha b}e^{-2l\alpha as}} \quad (29)$$

$$a=\left[\frac{C}{G}+T-\tau\right] \quad (30)$$

$$a=\left[\frac{0.236\times10^{-6}}{7.14\times10^{-6}}+(0.0575)-(0.0409)\right]=0.0496 \quad (31)$$

b=1 (32)

$$\alpha=\sqrt{RG}=\sqrt{(9.73\times10^{-3})(7.14\times10^{-6}}=2.63576\times10^{-4} \quad (33)$$

$$e^{-2l\alpha b}=e^{-2(11.5\times10^{3})(2.63576\times10^{-4})(1)}=e^{-6.062248}=2.329159048\times10^{-3} \quad (34)$$

$$e^{-2l\alpha a}=e^{-2(11.5\times10^{3})(2.63576\times10^{-4})(0.0496)} \quad (35)$$
$$=e^{-0.300680656}=0.740314149$$

$$w(s)=\frac{1+e^{-2l\alpha b}e^{-2l\alpha as}}{1-e^{-2l\alpha b}e^{-2l\alpha as}}=\frac{1+2.329159048\times10^{-3}e^{-0.300680656s}}{1-2.329159048\times10^{-3}e^{-0.300680656s}} \quad (36)$$

C. When changing shunt conductance value from 7.14×10^{-7} to 7.14×10^{-8} and Approximated Transfer Functions: -

$$(\frac{Cs}{G}+1)\frac{(Ts+1)^2}{(\tau s+1)^2}\cong\frac{Ls}{R}+1 \tag{37}$$

$$\frac{\frac{L}{R}s+1}{\frac{C}{G}s+1}\cong\frac{(Ts+1)^2}{(\tau s+1)^2} \tag{38}$$

$$\frac{\frac{0.637\times10^{-3}}{9.73\times10^{-3}}s+1}{\frac{0.236\times10^{-6}}{7.14\times10^{-8}}s+1}\cong\frac{(0.0985s+1)^2}{(0.705s+1)^2} \tag{39}$$

$$\frac{0.0655s+1}{3.31s+1}\cong\frac{(0.0985s+1)^2}{(0.705s+1)^2} \tag{40}$$

$$\zeta(s)=\sqrt{\frac{R}{G}}\sqrt{\frac{(Ts+1)^2}{(\tau s+1)^2}}=\bar{\alpha}\frac{(Ts+1)}{(\tau s+1)} \tag{41}$$

$$\zeta(s)=\sqrt{\frac{9.73\times10^{-3}}{7.14\times10^{-8}}}\frac{(0.0985s+1)}{(0.705s+1)} \tag{42}$$

$$\zeta(s)=369.1537753\frac{(0.0985s+1)}{(0.705s+1)} \tag{43}$$

$$w(s)=\frac{1+e^{-2l\alpha(as+b)}}{1-e^{-2l\alpha(as+b)}}=\frac{1+e^{-2l\alpha b}e^{-2l\alpha as}}{1-e^{-2l\alpha b}e^{-2l\alpha as}} \tag{44}$$

$$a=\left[\frac{C}{G}+T-\tau\right] \tag{45}$$

$$a=\left[\frac{0.236\times10^{-6}}{7.14\times10^{-8}}+(0.0985)-(0.705)\right]=2.69882212 \tag{46}$$

b=1 (47)

$$\alpha=\sqrt{RG}=\sqrt{(9.73\times10^{-3})(7.14\times10^{-8}}=2.63576\times10^{-5} \tag{48}$$

$$e^{-2l\alpha b} = e^{-2(11.5\times10^{3})(2.63576\times10^{-5})(1)} = e^{-0.6062248} = 0.545406004 \quad (49)$$

$$e^{-2l\alpha a} = e^{-2(11.5\times10^{3})(2.63576\times10^{-5})(2.69882212)} = e^{-1.636029} = 0.194739424 \quad (50)$$

$$w(s) = \frac{1+e^{-2l\alpha b}e^{-2l\alpha as}}{1-e^{-2l\alpha b}e^{-2l\alpha as}} = \frac{1+0.545406004e^{-1.636029s}}{1-0.545406004e^{-1.636029s}} \quad (51)$$

Calculating Terminal impedance in terms of resistance and inductance for one Power Transformer connected as load to the system:

Power Transformer data:

Voltage rate (V): 400/132kV, Power Capacity (P): 505MVA, Impedance (U_k): 34.1982%, copper losses (P_{losses}): 1560kW (52)

$$I_{phase} = \frac{P}{\sqrt{3}\times V} = \frac{505\times10^{6}}{\sqrt{3}\times400\times10^{3}} = 728.9A \quad (53)$$

$$P_{losses} = 3\times X_R \times (I_{phase})^2 \quad (54)$$

$$R_L = X_R = \frac{P_{losses}}{3\times(I_{phase})^2} = \frac{1560\times10^{3}}{3\times(728.9)^2} = 0.979\Omega \quad (55)$$

$$U_k = \frac{I_{phase}\times Z}{\sqrt{3}\times V} \quad (56)$$

$$Z = \frac{V_{phase}\times U_k}{I_{phase}} = \frac{(400\times10^{3})/\sqrt{3}\times0.341982}{728.9} = 108.351 \quad (57)$$

$$Z = X_R + jX_L \quad (58)$$

$$X_L = \sqrt{Z^2 - X_R{}^2} = \sqrt{(108.351)^2 - (0.979)^2} = 108.347 \quad (59)$$

$$X_L = \omega L = 2\pi f L_L \quad (60)$$

$$L_L = \frac{X_L}{2\pi f} = \frac{108.237}{2\pi(50)} = 0.345H \quad (61)$$

Calculating Terminal impedance in terms of resistance and inductance for four Power Transformers connected in parallel as load to the system:

$$Z = Z_1 = Z_2 = Z_3 = Z_4 = X_R + jX_L = 0.979 + j108.385 \quad (62)$$

$$\frac{1}{Z_{equivalent}} = \frac{1}{Z_1} + \frac{1}{Z_2} + \frac{1}{Z_3} + \frac{1}{Z_4} \quad (63)$$

$$Z_{equivalent} = \frac{Z_1 Z_2 Z_3 Z_4}{Z_2 Z_3 Z_4 + Z_1 Z_3 Z_4 + Z_1 Z_2 Z_4 + Z_1 Z_2 Z_3} \quad (64)$$

$$Z_{equivalent} = \frac{1.3774\times10^{8} - j4.9803\times10^{6}}{-1.3791\times10^{5} - j5.0863\times10^{6}} \quad (65)$$

$$Z_{equivalent} = 0.2448 + j27.0867 \quad (66)$$

$$R_L = 0.2448\Omega \quad (67)$$

$$L_L = \frac{X_L}{2\pi f} = \frac{27.0867}{2\pi(50)} = 0.08622H \quad (68)$$

Supply Current and Terminal Load Current Calculation: -

$$I_s = \frac{P_s}{\sqrt{3}V_s} = \frac{1500\times10^{6}}{\sqrt{3}(400\times10^{3})} = 2.167kA \quad (69)$$

$$I_L = \frac{V_L}{L_L s + R_L} = \frac{400\times10^{3}}{0.2448 j\omega + 0.08622} \quad (70)$$

$$I_{LM} = \frac{400\times10^{3}}{\sqrt{(0.2448\omega)^2 + (0.08622)^2}} = \frac{400\times10^{3}}{\sqrt{(0.2448\times2\pi f)^2 + (0.08622)^2}} \quad (71)$$

$$= \frac{400\times10^{3}}{\sqrt{(0.2448\times2\pi(50))^2 + (0.08622)^2}} = \frac{400\times10^{3}}{\sqrt{5914.561777 + 7.4338884\times10^{-3}}} \quad (72)$$

$$= \frac{400 \times 10^3}{\sqrt{5914.569211}} = 5201.138663A \quad (73)$$

$$I_{LM} = 5.201kA \quad (74)$$

Appendix-A3:

Calculation of impedance inverse symbolically with no losses using Maple

Finite Element system impedance inverse symbolic computation using Maple software for Transmission Line Modeling consists of Inductance and Capacitance. All are per unit length.

- LDPS_FE_TLM_System_Impedance_LC_4Sections_V1_17_12_2011;

  LDPS_FE_TLM_System_Impedance_LC_4Sections_V1_17_12_2011

- a11:=L1*s+1/(C1*s);a12:=-1/(C1*s);a13:=0;a14:=0;a15:=0;a21:=-1/(C1*s);a22:=L2*s+1/(C2*s)+1/(C1*s);a23:=-1/(C2*s);a24:=0;a25:=0;a31:=0;a32:=-1/(C2*s);a33:=L3*s+1/(C3*s)+1/(C2*s);a34:=-1/(C3*s);a35:=0;a41:=0;a42:=0;a43:=-1/(C3*s);a44:=L4*s+1/(C4*s)+1/(C3*s);a45:=-1/(C4*s);a51:=0;a52:=0;a53:=0;a54:=-1/(C4*s);a55:=L*s+R+1/(C4*s);

$$a11 := L1\,s + \frac{1}{C1\,s}$$

$$a12 := -\frac{1}{C1\,s}$$

$$a13 := 0$$

$$a14 := 0$$

$$a15 := 0$$

$$a21 := -\frac{1}{C1\,s}$$

$$a22 := L2\,s + \frac{1}{C2\,s} + \frac{1}{C1\,s}$$

$$a23 := -\frac{1}{C2\,s}$$

$$a24 := 0$$

$$a25 := 0$$

$$a31 := 0$$

$$a32 := -\frac{1}{C2\ s}$$

$$a33 := L3\ s + \frac{1}{C3\ s} + \frac{1}{C2\ s}$$

$$a34 := -\frac{1}{C3\ s}$$

$$a35 := 0$$

$$a41 := 0$$

$$a42 := 0$$

$$a43 := -\frac{1}{C3\ s}$$

$$a44 := L4\ s + \frac{1}{C4\ s} + \frac{1}{C3\ s}$$

$$a45 := -\frac{1}{C4\ s}$$

$$a51 := 0$$

$$a52 := 0$$

$$a53 := 0$$

$$a54 := -\frac{1}{C4\ s}$$

$$a55 := L\ s + R + \frac{1}{C4\ s}$$

- Z(s):=matrix(5,5,[a11,a12,a13,a14,a15,a21,a22,a23,a24,a25,a31,a32,a33,a34,a35,a41,a42,a43,a44,a45,a51,a52,a53,a54,a55]);

$$Z(s) := \begin{bmatrix} L1\ s + \frac{1}{C1\ s}, & -\frac{1}{C1\ s}, & 0, & 0, & 0 \\ -\frac{1}{C1\ s}, & L2\ s + \frac{1}{C2\ s} + \frac{1}{C1\ s}, & -\frac{1}{C2\ s}, & 0, & 0 \\ 0, & -\frac{1}{C2\ s}, & L3\ s + \frac{1}{C3\ s} + \frac{1}{C2\ s}, & -\frac{1}{C3\ s}, & 0 \\ 0, & 0, & -\frac{1}{C3\ s}, & L4\ s + \frac{1}{C4\ s} + \frac{1}{C3\ s}, & -\frac{1}{C4\ s} \\ 0, & 0, & 0, & -\frac{1}{C4\ s}, & L\ s + R + \frac{1}{C4\ s} \end{bmatrix}$$

- > with(linalg):Zinv:=inverse(Z(s));

- ZZ11:=[Zinv[1,1]];

$$
\begin{aligned}
ZZ11 := [\,(\,&1 + R\,C4\,s + L\,s^2\,C4 + L4\,s^3\,C4\,C3\,R + L3\,s^4\,C3\,C2\,L \\
&+ L2\,s^7\,C2\,C1\,L3\,C3\,L4\,C4\,R + L4\,s^4\,C4\,C3\,L + L2\,s^8\,C2\,C1\,L3\,C3\,L4\,C4\,L \\
&+ L4\,s^2\,C3 + L3\,s^6\,C3\,C2\,L4\,C4\,L + L3\,s^5\,C3\,C2\,L4\,C4\,R + L3\,s^4\,C3\,C2\,L4 \\
&+ C2\,L4\,s^4\,C4\,L + L3\,s^4\,C2\,L\,C4 + L3\,s^3\,C2\,R\,C4 + C2\,L4\,s^3\,C4\,R \\
&+ L2\,s^4\,C2\,C1\,L4 + L2\,s^4\,C2\,C1\,L3 + L2\,s^3\,C2\,C1\,R + L2\,s^4\,C2\,C1\,L + C3\,R\,s \\
&+ C3\,L\,s^2 + L2\,s^5\,C2\,C1\,L3\,C3\,R + L2\,s^6\,C2\,C1\,L3\,C3\,L + L2\,s^6\,C2\,C1\,L3\,C3\,L4 \\
&+ L2\,s^5\,C2\,C1\,L4\,C4\,R + L2\,s^5\,C2\,C1\,L3\,R\,C4 + L2\,s^6\,C2\,C1\,L3\,L\,C4 \\
&+ L2\,s^6\,C2\,C1\,L4\,C4\,L + C2\,L4\,s^2 + C2\,R\,s + L3\,s^2\,C2 + C2\,L\,s^2 \\
&+ L2\,s^5\,C1\,L4\,C4\,C3\,R + L2\,s^3\,C1\,C3\,R + L2\,s^4\,C1\,C3\,L + L2\,s^4\,C1\,L4\,C3 \\
&+ C1\,L3\,s^2 + C1\,R\,s + C1\,L\,s^2 + L2\,s^2\,C1 + C1\,L4\,s^2 + L2\,s^6\,C1\,L4\,C4\,C3\,L \\
&+ C1\,L3\,s^3\,C3\,R + C1\,L3\,s^4\,C3\,L + C1\,L3\,s^4\,C3\,L4 + C1\,L3\,s^6\,C3\,L4\,C4\,L \\
&+ L2\,s^3\,C1\,R\,C4 + L2\,s^4\,C1\,L\,C4 + C1\,L4\,s^4\,C4\,L + C1\,L3\,s^3\,R\,C4 + C1\,L3\,s^4\,L\,C4 \\
&+ C1\,L3\,s^5\,C3\,L4\,C4\,R + C1\,L4\,s^3\,C4\,R + L3\,s^3\,C3\,C2\,R\,)\,/\,(\\
&L1\,s^8\,C1\,L2\,C2\,L3\,C3\,L4\,C4\,R + L1\,s^2\,C1\,R + L1\,s^9\,C1\,L2\,C2\,L3\,C3\,L4\,C4\,L \\
&+ L1\,s^3\,C1\,L3 + L1\,s^7\,L3\,C3\,C2\,L4\,C4\,L + L1\,s^6\,L3\,C3\,C2\,L4\,C4\,R \\
&+ L2\,s^7\,C2\,L3\,C3\,L4\,C4\,L + L2\,s^6\,C2\,L3\,C3\,L4\,C4\,R + L4\,s^2\,C4\,R + L3\,s^3\,L\,C4 \\
&+ L3\,s^2\,R\,C4 + L4\,s^3\,C4\,L + L2\,s^3\,L\,C4 + L2\,s^2\,R\,C4 + L3\,s^3\,C3\,L4 + L3\,s^3\,C3\,L \\
&+ L3\,s^2\,C3\,R + L2\,s^3\,L4\,C3 + L2\,s^3\,C3\,L + L2\,s^2\,C3\,R + L2\,s^3\,C2\,L + L2\,s^2\,C2\,R \\
&+ L2\,s^3\,C2\,L3 + L2\,s^3\,C2\,L4 + L1\,s^2\,R\,C4 + L1\,s^3\,L\,C4 + L1\,s^3\,L4\,C3 + L1\,s^2\,C3\,R \\
&+ L1\,s^3\,C3\,L + L1\,s^3\,C2\,L + L2\,s^5\,C2\,L3\,L\,C4 + L2\,s^4\,C2\,L3\,R\,C4 \\
&+ L2\,s^4\,C2\,L4\,C4\,R + L2\,s^5\,C2\,L3\,C3\,L4 + L2\,s^5\,C2\,L3\,C3\,L + L2\,s^4\,C2\,L3\,C3\,R \\
&+ L2\,s^5\,L4\,C4\,C3\,L + L2\,s^4\,L4\,C4\,C3\,R + L1\,s^5\,L4\,C4\,C3\,L + L1\,s^5\,L3\,C3\,C2\,L4 \\
&+ L1\,s^5\,C2\,L4\,C4\,L + L1\,s^5\,L3\,C2\,L\,C4 + L1\,s^4\,L3\,C2\,R\,C4 + L1\,s^4\,C2\,L4\,C4\,R \\
&+ L1\,s^4\,L3\,C3\,C2\,R + L1\,s^4\,L4\,C4\,C3\,R + L1\,s^5\,L3\,C3\,C2\,L + L2\,s^5\,C2\,L4\,C4\,L \\
&+ L3\,s^4\,C3\,L4\,C4\,R + L3\,s^5\,C3\,L4\,C4\,L + L1\,s^3\,C2\,L4 + L1\,s^3\,C1\,L + L1\,s^3\,C1\,L2 \\
&+ L1\,s^3\,C1\,L4 + L2\,s + L1\,s^3\,L3\,C2 + R + L3\,s + L1\,s^2\,C2\,R + L1\,s + L4\,s + L\,s \\
&+ L1\,s^5\,C1\,L2\,C2\,L4 + L1\,s^6\,C1\,L2\,C2\,L3\,C3\,R + L1\,s^5\,C1\,L2\,C2\,L3 \\
&+ L1\,s^4\,C1\,L2\,C2\,R + L1\,s^5\,C1\,L2\,C2\,L + L1\,s^7\,C1\,L2\,C2\,L3\,L\,C4 \\
&+ L1\,s^7\,C1\,L2\,C2\,L4\,C4\,L + L1\,s^6\,C1\,L2\,C2\,L4\,C4\,R + L1\,s^7\,C1\,L2\,C2\,L3\,C3\,L \\
&+ L1\,s^7\,C1\,L2\,C2\,L3\,C3\,L4 + L1\,s^5\,C1\,L2\,L4\,C3 + L1\,s^4\,C1\,L3\,C3\,R \\
&+ L1\,s^6\,C1\,L2\,L4\,C4\,C3\,R + L1\,s^6\,C1\,L2\,C2\,L3\,R\,C4 + L1\,s^6\,C1\,L3\,C3\,L4\,C4\,R \\
&+ L1\,s^4\,C1\,L3\,R\,C4 + L1\,s^5\,C1\,L3\,L\,C4 + L1\,s^4\,C1\,L4\,C4\,R + L1\,s^5\,C1\,L3\,C3\,L \\
&+ L1\,s^7\,C1\,L2\,L4\,C4\,C3\,L + L1\,s^4\,C1\,L2\,C3\,R + L1\,s^5\,C1\,L2\,C3\,L \\
&+ L1\,s^5\,C1\,L3\,C3\,L4 + L1\,s^4\,C1\,L2\,R\,C4 + L1\,s^5\,C1\,L2\,L\,C4 + L1\,s^5\,C1\,L4\,C4\,L \\
&+ L1\,s^7\,C1\,L3\,C3\,L4\,C4\,L\,)\,]
\end{aligned}
$$

- *Num1=*

$L_2C_2C_1L_3C_3L_4C_4L_Ls^8+L_2C_2C_1L_3C_3L_4C_4R_Ls^7+(L_3C_3C_2L_4C_4L_L+L_2C_2C_1L_3C_3L_L+L_2C_2C_1L_3C_3L_4+L_2C_2C_1L_4C_4L_L+L_2C_2C_1L_3L_LC_4+L_2C_1L_4C_4C_3L_L+C_1L_3C_3L_4C_4L_L)s^6+(L_3C_3C_2L_4C_4R_L+L_2C_2C_1L_3C_3R_L+L_2C_2C_1L_4C_4R_L+L_2C_2C_1L_3R_LC_4+L_2C_1L_4C_4C_3R_L+C_1L_3C_3L_4C_4R_L)s^5+(L_4C_4C_3L_L+L_3C_3C_2L_4+L_3C_3C_2L_L+L_3C_2L_LC_4+C_2L_LC_4L_4+L_2C_2C_1L_3+L_2C_2C_1L_L+L_2C_2C_1L_4+C_1L_3C_3L_4+L_2C_1C_3L_L+L_2C_1L_4C_3+L_2C_1L_LC_4+C_1L_3C_3L_L+C_1L_4C_4L_L+C_1L_3LC_4)s^4+(L_4C_4C_3R_L+L_3C_3C_2R_L+L_3C_2R_LC_4+C_2L_4C_4R_L+L_2C_2C_1R_L+L_2C_1R_LC_4+L_2C_1C_3R_L+C_1L_3R_LC_4+C_1L_3C_3R_L+C_1L_4C_4R_L)s^3+(L_LC_4+C_1L_L+C_1L_3+C_3L_L+C_2L_L+L_3C_2+L_2C_1+L_4C_3+C_1L_4+C_2L_4)s^2+(R_LC_4+C_3R_L+C_1R_L+C_2R_L)s+1$

$=L^3C^4L_Ls^8+L^3C^4R_Ls^7+(L^2C^3L_L+L^2C^3L_L+L^3C^3+L^2C^3L_L+L^2C^3L_L+L^2C^3L_L+L^2C^3L_L)s^6+(L^2C^3R_L+L^2C^3R_L+L^2C^3R_L+L^2C^3R_L+L^2C^3R_L+L^2C^3R_L)s^5+(LC^2L_L+L^2C^2+LC^2L_L+LC^2L_L+LC^2L_L+L^2C^2+LC^2_L+L^2C^2+L^2C^2+LC^2L_L+L^2C^2+LC^2L_L+LC^2L_L+LC^2L_L+LC^2L_L)s^4+(LC^2R_L+LC^2R_L+LC^2R_L+LC^2R_L+LC^2R_L+LC^2R_L+LC^2R_L+LC^2R_L+LC^2R_L+LC^2R_L)s^3+(L_LC+CL_L+CL+CL_L+CL_L+LC+LC+LC+CL+CL)s^2+(CR_L+CR_L+CR_L+CR_L)s+1$

$= L^3C^4L_Ls^8+L^3C^4R_Ls^7+(6L^2C^3L_L+L^3C^3)s^6+6L^2C^3R_Ls^5+(10LC^2L_L+5L^2C^2)s^4+10LC^2R_Ls^3+10CL_Ls^2+4CR_Ls+1$

- ZZ51:=[Zinv[5,1]];

$$
\begin{aligned}
ZZ51 := [\,1/(\,& L1\,s^8\,C1\,L2\,C2\,L3\,C3\,L4\,C4\,R + L1\,s^2\,C1\,R \\
& + L1\,s^9\,C1\,L2\,C2\,L3\,C3\,L4\,C4\,L + L1\,s^3\,C1\,L3 + L1\,s^7\,L3\,C3\,C2\,L4\,C4\,L \\
& + L1\,s^6\,L3\,C3\,C2\,L4\,C4\,R + L2\,s^7\,C2\,L3\,C3\,L4\,C4\,L + L2\,s^6\,C2\,L3\,C3\,L4\,C4\,R \\
& + L4\,s^2\,C4\,R + L3\,s^3\,L\,C4 + L3\,s^2\,R\,C4 + L4\,s^3\,C4\,L + L2\,s^3\,L\,C4 + L2\,s^2\,R\,C4 \\
& + L3\,s^3\,C3\,L4 + L3\,s^3\,C3\,L + L3\,s^2\,C3\,R + L2\,s^3\,L4\,C3 + L2\,s^3\,C3\,L + L2\,s^2\,C3\,R \\
& + L2\,s^3\,C2\,L + L2\,s^2\,C2\,R + L2\,s^3\,C2\,L3 + L2\,s^3\,C2\,L4 + L1\,s^2\,R\,C4 + L1\,s^3\,L\,C4 \\
& + L1\,s^3\,L4\,C3 + L1\,s^2\,C3\,R + L1\,s^3\,C3\,L + L1\,s^3\,C2\,L + L2\,s^5\,C2\,L3\,L\,C4 \\
& + L2\,s^4\,C2\,L3\,R\,C4 + L2\,s^4\,C2\,L4\,C4\,R + L2\,s^5\,C2\,L3\,C3\,L4 + L2\,s^5\,C2\,L3\,C3\,L \\
& + L2\,s^4\,C2\,L3\,C3\,R + L2\,s^5\,L4\,C4\,C3\,L + L2\,s^4\,L4\,C4\,C3\,R + L1\,s^5\,L4\,C4\,C3\,L \\
& + L1\,s^5\,L3\,C3\,C2\,L4 + L1\,s^5\,C2\,L4\,C4\,L + L1\,s^5\,L3\,C2\,L\,C4 + L1\,s^4\,L3\,C2\,R\,C4 \\
& + L1\,s^4\,C2\,L4\,C4\,R + L1\,s^4\,L3\,C3\,C2\,R + L1\,s^4\,L4\,C4\,C3\,R + L1\,s^5\,L3\,C3\,C2\,L \\
& + L2\,s^5\,C2\,L4\,C4\,L + L3\,s^4\,C3\,L4\,C4\,R + L3\,s^5\,C3\,L4\,C4\,L + L1\,s^3\,C2\,L4 \\
& + L1\,s^3\,C1\,L + L1\,s^3\,C1\,L2 + L1\,s^3\,C1\,L4 + L2\,s + L1\,s^3\,L3\,C2 + R + L3\,s \\
& + L1\,s^2\,C2\,R + L1\,s + L4\,s + L\,s + L1\,s^5\,C1\,L2\,C2\,L4 + L1\,s^6\,C1\,L2\,C2\,L3\,C3\,R \\
& + L1\,s^5\,C1\,L2\,C2\,L3 + L1\,s^4\,C1\,L2\,C2\,R + L1\,s^5\,C1\,L2\,C2\,L \\
& + L1\,s^7\,C1\,L2\,C2\,L3\,L\,C4 + L1\,s^7\,C1\,L2\,C2\,L4\,C4\,L + L1\,s^6\,C1\,L2\,C2\,L4\,C4\,R \\
& + L1\,s^7\,C1\,L2\,C2\,L3\,C3\,L + L1\,s^7\,C1\,L2\,C2\,L3\,C3\,L4 + L1\,s^5\,C1\,L2\,L4\,C3 \\
& + L1\,s^4\,C1\,L3\,C3\,R + L1\,s^6\,C1\,L2\,L4\,C4\,C3\,R + L1\,s^6\,C1\,L2\,C2\,L3\,R\,C4 \\
& + L1\,s^6\,C1\,L3\,C3\,L4\,C4\,R + L1\,s^4\,C1\,L3\,R\,C4 + L1\,s^5\,C1\,L3\,L\,C4 \\
& + L1\,s^4\,C1\,L4\,C4\,R + L1\,s^5\,C1\,L3\,C3\,L + L1\,s^7\,C1\,L2\,L4\,C4\,C3\,L \\
& + L1\,s^4\,C1\,L2\,C3\,R + L1\,s^5\,C1\,L2\,C3\,L + L1\,s^5\,C1\,L3\,C3\,L4 + L1\,s^4\,C1\,L2\,R\,C4 \\
& + L1\,s^5\,C1\,L2\,L\,C4 + L1\,s^5\,C1\,L4\,C4\,L + L1\,s^7\,C1\,L3\,C3\,L4\,C4\,L\,)\,]
\end{aligned}
$$

Appendix-A4:

Calculation of impedance inverse numerically without losses using Maple

Finite Element system impedance inverse numerical computation using Maple software for Transmission Line Modeling consists of Inductance and Capacitance. All are per unit length.

- LDPS_FE_TLM_System_Impedance_LC_4Sections_V1_28_03_2012;

  LDPS_FE_TLM_System_Impedance_LC_4Sections_V1_28_03_2012

- L1:=0.637e-3;L2:=L1;L3:=L1;L4:=L1;C1:=0.236E-6;C2:=C1;C3:=C1;C4:=C1;L:=0.08622;R:=0.2448;

$$L1 := .000637$$

$$L2 := .000637$$

$$L3 := .000637$$

$$L4 := .000637$$

$$C1 := .236\ 10^{-6}$$

$$C2 := .236\ 10^{-6}$$

$$C3 := .236\ 10^{-6}$$

$$C4 := .236\ 10^{-6}$$

$$L := .08622$$

$$R := .2448$$

- a11:=L1*s+1/(C1*s);a12:=-1/(C1*s);a13:=0;a14:=0;a15:=0;a21:=-1/(C1*s);a22:=L2*s+1/(C2*s)+1/(C1*s);a23:=-1/(C2*s);a24:=0;a25:=0;a31:=0;a32:=-1/(C2*s);a33:=L3*s+1/(C3*s)+1/(C2*s);a34:=-1/(C3*s);a35:=0;a41:=0;a42:=0;a43:=-1/(C3*s);a44:=L4*s+1/(C4*s)+1/(C3*s);a45:=-1/(C4*s);a51:=0;a52:=0;a53:=0;a54:=-1/(C4*s);a55:=L*s+R+1/(C4*s);

$$a11 := .000637\ s + \frac{.4237288136\ \ 10^7}{s}$$

$$a12 := -.4237288136\ \ 10^7 \frac{1}{s}$$

$$a13 := 0$$

$$a14 := 0$$

$$a15 := 0$$

$$a21 := -.4237288136\ \ 10^7 \frac{1}{s}$$

$$a22 := .000637\ s + \frac{.8474576272\ \ 10^7}{s}$$

$$a23 := -.4237288136\ \ 10^7 \frac{1}{s}$$

$$a24 := 0$$

$$a25 := 0$$

$$a31 := 0$$

$$a32 := -.4237288136\ \ 10^7 \frac{1}{s}$$

$$a33 := .000637\ s + \frac{.8474576272\ \ 10^7}{s}$$

$$a34 := -.4237288136\ \ 10^7 \frac{1}{s}$$

$$a35 := 0$$

$$a41 := 0$$

$$a42 := 0$$

$$a43 := -.4237288136\ \ 10^7 \frac{1}{s}$$

$$a44 := .000637\ s + \frac{.8474576272\ \ 10^7}{s}$$

$$a45 := -.4237288136\ \ 10^7 \frac{1}{s}$$

$$a51 := 0$$

$$a52 := 0$$

$$a53 := 0$$

$$a54 := -.4237288136\ \ 10^{7}\ \frac{1}{s}$$

$$a55 := .08622\ s + .2448 + \frac{.4237288136\ \ 10^{7}}{s}$$

- Z(s):=matrix(5,5,[a11,a12,a13,a14,a15,a21,a22,a23,a24,a25,a31,a32,a33,a34,a35,a41,a42,a43,a44,a45,a51,a52,a53,a54,a55]);

$$Z(s) := \begin{bmatrix} .000637\ s + \frac{.4237288136\ \ 10^{7}}{s}, & -.4237288136\ \ 10^{7}\ \frac{1}{s}, & 0, & 0, & 0 \\ -.4237288136\ \ 10^{7}\ \frac{1}{s}, & .000637\ s + \frac{.8474576272\ \ 10^{7}}{s}, & -.4237288136\ \ 10^{7}\ \frac{1}{s}, & 0, & 0 \\ 0, & -.4237288136\ \ 10^{7}\ \frac{1}{s}, & .000637\ s + \frac{.8474576272\ \ 10^{7}}{s}, & -.4237288136\ \ 10^{7}\ \frac{1}{s}, & 0 \\ 0, & 0, & -.4237288136\ \ 10^{7}\ \frac{1}{s}, & .000637\ s + \frac{.8474576272\ \ 10^{7}}{s}, & -.4237288136\ \ 10^{7}\ \frac{1}{s} \\ 0, & 0, & 0, & -.4237288136\ \ 10^{7}\ \frac{1}{s}, & .08622\ s + .2448 + \frac{.4237288136\ \ 10^{7}}{s} \end{bmatrix}$$

- with(linalg):Zinv:=inverse(Z(s));

$$Zinv :=$$

$$\begin{aligned} &[(.2228570183\ \ 10^{-10}\ s^{8} + .6327464401\ \ 10^{-10}\ s^{7} + .8905546355\ \ s^{6} \\ &+ .9897483575\ \ 10^{10}\ s^{4} + 2.525396217\ \ s^{5} + .2652885032\ \ 10^{20}\ s^{2} \\ &+ .2799798909\ \ 10^{11}\ s^{3} + .3223680470\ \ 10^{27} + .7449641878\ \ 10^{20}\ s) \,/\, (\\ &.1419599207\ \ 10^{-13}\ s^{9} + .4030594823\ \ 10^{-13}\ s^{8} + .0006617142428\ \ s^{7} \\ &+ .9450084334\ \ 10^{7}\ s^{5} + .001876790288\ \ s^{6} + .4209284193\ \ 10^{17}\ s^{3} \\ &+ .2675207858\ \ 10^{8}\ s^{4} + .2861596669\ \ 10^{26}\ s + .1186355470\ \ 10^{18}\ s^{2} \\ &+ .7891569770\ \ 10^{26}), .4237288136\ \ 10^{7}\ (.3498540318\ \ 10^{-7}\ s^{6} \\ &+ .9933225120\ \ 10^{-7}\ s^{5} + 932.6030891\ \ s^{4} + .4678450877\ \ 10^{13}\ s^{2} + 2643.010170\ \ s^{3} \\ &+ .7607885908\ \ 10^{20} + .1318586613\ \ 10^{14}\ s) \,/\, (.1419599207\ \ 10^{-13}\ s^{9} \\ &+ .4030594823\ \ 10^{-13}\ s^{8} + .0006617142428\ \ s^{7} + .9450084334\ \ 10^{7}\ s^{5} \\ &+ .001876790288\ \ s^{6} + .4209284193\ \ 10^{17}\ s^{3} + .2675207858\ \ 10^{8}\ s^{4} \\ &+ .2861596669\ \ 10^{26}\ s + .1186355470\ \ 10^{18}\ s^{2} + .7891569770\ \ 10^{26}), \\ &.1795461075\ \ 10^{14}\ (.00005492214000\ \ s^{4} + .0001559376000\ \ s^{3} + 733377.1187\ \ s^{2} \\ &+ .1795461074\ \ 10^{14} + .2074576271\ \ 10^{7}\ s) \,/\, (.1419599207\ \ 10^{-13}\ s^{9} \\ &+ .4030594823\ \ 10^{-13}\ s^{8} + .0006617142428\ \ s^{7} + .9450084334\ \ 10^{7}\ s^{5} \end{aligned}$$

$$+ .001876790288\ s^6 + .4209284193\ 10^{17} s^3 + .2675207858\ 10^8 s^4$$
$$+ .2861596669\ 10^{26} s + .1186355470\ 10^{18} s^2 + .7891569770\ 10^{26}),$$
$$.7607885912\ 10^{20} (.08622000000\ s^2 + .2448000000\ s + .4237288136\ 10^7) \Big/ ($$
$$.1419599207\ 10^{-13} s^9 + .4030594823\ 10^{-13} s^8 + .0006617142428\ s^7$$
$$+ .9450084334\ 10^7 s^5 + .001876790288\ s^6 + .4209284193\ 10^{17} s^3$$
$$+ .2675207858\ 10^8 s^4 + .2861596669\ 10^{26} s + .1186355470\ 10^{18} s^2$$
$$+ .7891569770\ 10^{26}), .3223680471\ 10^{27}\ 1/(.1419599207\ 10^{-13} s^9$$
$$+ .4030594823\ 10^{-13} s^8 + .0006617142428\ s^7 + .9450084334\ 10^7 s^5$$
$$+ .001876790288\ s^6 + .4209284193\ 10^{17} s^3 + .2675207858\ 10^8 s^4$$
$$+ .2861596669\ 10^{26} s + .1186355470\ 10^{18} s^2 + .789156977\ 10^{26})]$$
$$[.4237288136\ 10^7 (.3498540318\ 10^{-7} s^6 + .9933225120\ 10^{-7} s^5 + 932.6030891\ s^4$$
$$+ .4678450877\ 10^{13} s^2 + 2643.010170\ s^3 + .7607885908\ 10^{20}$$
$$+ .1318586613\ 10^{14} s) \Big/ (.1419599207\ 10^{-13} s^9 + .4030594823\ 10^{-13} s^8$$
$$+ .0006617142428\ s^7 + .9450084334\ 10^7 s^5 + .001876790288\ s^6$$
$$+ .4209284193\ 10^{17} s^3 + .2675207858\ 10^8 s^4 + .2861596669\ 10^{26} s$$
$$+ .1186355470\ 10^{18} s^2 + .7891569770\ 10^{26}), ((.3498540318\ 10^{-7} s^6$$
$$+ .9933225120\ 10^{-7} s^5 + 932.6030891\ s^4 + .4678450877\ 10^{13} s^2 + 2643.010170\ s^3$$
$$+ .7607885908\ 10^{20} + .1318586613\ 10^{14} s)$$
$$(.0006370000000\ s^2 + .4237288136\ 10^7)) \Big/ (.1419599207\ 10^{-13} s^9$$
$$+ .4030594823\ 10^{-13} s^8 + .0006617142428\ s^7 + .9450084334\ 10^7 s^5$$
$$+ .001876790288\ s^6 + .4209284193\ 10^{17} s^3 + .2675207858\ 10^8 s^4$$
$$+ .2861596669\ 10^{26} s + .1186355470\ 10^{18} s^2 + .7891569770\ 10^{26}),$$
$$.4237288136\ 10^7 ((.00005492214000\ s^4 + .0001559376000\ s^3 + 733377.1187\ s^2$$
$$+ .1795461074\ 10^{14} + .2074576271\ 10^7 s)$$
$$(.0006370000000\ s^2 + .4237288136\ 10^7)) \Big/ (.1419599207\ 10^{-13} s^9$$
$$+ .4030594823\ 10^{-13} s^8 + .0006617142428\ s^7 + .9450084334\ 10^7 s^5$$
$$+ .001876790288\ s^6 + .4209284193\ 10^{17} s^3 + .2675207858\ 10^8 s^4$$
$$+ .2861596669\ 10^{26} s + .1186355470\ 10^{18} s^2 + .7891569770\ 10^{26}),$$
$$.1795461075\ 10^{14} ((.08622000000\ s^2 + .2448000000\ s + .4237288136\ 10^7)$$
$$(.0006370000000\ s^2 + .4237288136\ 10^7)) \Big/ (.1419599207\ 10^{-13} s^9$$
$$+ .4030594823\ 10^{-13} s^8 + .0006617142428\ s^7 + .9450084334\ 10^7 s^5$$
$$+ .001876790288\ s^6 + .4209284193\ 10^{17} s^3 + .2675207858\ 10^8 s^4$$
$$+ .2861596669\ 10^{26} s + .1186355470\ 10^{18} s^2 + .7891569770\ 10^{26}),$$
$$.7607885912\ 10^{20} (.0006370000000\ s^2 + .4237288136\ 10^7) \Big/ ($$
$$.1419599207\ 10^{-13} s^9 + .4030594823\ 10^{-13} s^8 + .0006617142428\ s^7$$
$$+ .9450084334\ 10^7 s^5 + .001876790288\ s^6 + .4209284193\ 10^{17} s^3$$

$$+ .2675207858\ 10^{8} s^4 + .2861596669\ 10^{26} s + .1186355470\ 10^{18} s^2$$
$$+ .7891569770\ 10^{26})]$$
$$[.1795461075\ 10^{14} (.00005492214000\ s^4 + .0001559376000\ s^3 + 733377.1187\ s^2$$
$$+ .1795461074\ 10^{14} + .2074576271\ 10^{7} s) \Big/ (.1419599207\ 10^{-13} s^9$$
$$+ .4030594823\ 10^{-13} s^8 + .0006617142428\ s^7 + .9450084334\ 10^{7} s^5$$
$$+ .001876790288\ s^6 + .4209284193\ 10^{17} s^3 + .2675207858\ 10^{8} s^4$$
$$+ .2861596669\ 10^{26} s + .1186355470\ 10^{18} s^2 + .7891569770\ 10^{26}),$$
$$.4237288136\ 10^{7} ((.00005492214000\ s^4 + .0001559376000\ s^3 + 733377.1187\ s^2$$
$$+ .1795461074\ 10^{14} + .2074576271\ 10^{7} s)$$
$$(.0006370000000\ s^2 + .4237288136\ 10^{7})) \Big/ (.1419599207\ 10^{-13} s^9$$
$$+ .4030594823\ 10^{-13} s^8 + .0006617142428\ s^7 + .9450084334\ 10^{7} s^5$$
$$+ .001876790288\ s^6 + .4209284193\ 10^{17} s^3 + .2675207858\ 10^{8} s^4$$
$$+ .2861596669\ 10^{26} s + .1186355470\ 10^{18} s^2 + .7891569770\ 10^{26}), ($$
$$.2228570183\ 10^{-10} s^8 + .6327464401\ 10^{-10} s^7 + .7423114016\ s^6$$
$$+ .6931881213\ 10^{10} s^4 + 2.104496848\ s^5 + .3223680468\ 10^{27}$$
$$+ .1331288739\ 10^{20} s^2 + .1959859236\ 10^{11} s^3 + .3724820939\ 10^{20} s) \Big/ ($$
$$.1419599207\ 10^{-13} s^9 + .4030594823\ 10^{-13} s^8 + .0006617142428\ s^7$$
$$+ .9450084334\ 10^{7} s^5 + .001876790288\ s^6 + .4209284193\ 10^{17} s^3$$
$$+ .2675207858\ 10^{8} s^4 + .2861596669\ 10^{26} s + .1186355470\ 10^{18} s^2$$
$$+ .7891569770\ 10^{26}), (.1482432338\ s^6 + .4208993695\ s^5 + .2965602360\ 10^{10} s^4$$
$$+ .3223680470\ 10^{27} + .8399396725\ 10^{10} s^3 + .6704905927\ 10^{19} s^2$$
$$+ .1862410470\ 10^{20} s) \Big/ (.1419599207\ 10^{-13} s^9 + .4030594823\ 10^{-13} s^8$$
$$+ .0006617142428\ s^7 + .9450084334\ 10^{7} s^5 + .001876790288\ s^6$$
$$+ .4209284193\ 10^{17} s^3 + .2675207858\ 10^{8} s^4 + .2861596669\ 10^{26} s$$
$$+ .1186355470\ 10^{18} s^2 + .7891569770\ 10^{26}), ($$
$$.7285424449\ 10^{7} s^4 + .1453866998\ 10^{18} s^2 + .3223680471\ 10^{27}) \Big/ ($$
$$.1419599207\ 10^{-13} s^9 + .4030594823\ 10^{-13} s^8 + .0006617142428\ s^7$$
$$+ .9450084334\ 10^{7} s^5 + .001876790288\ s^6 + .4209284193\ 10^{17} s^3$$
$$+ .2675207858\ 10^{8} s^4 + .2861596669\ 10^{26} s + .1186355470\ 10^{18} s^2$$
$$+ .7891569770\ 10^{26})]$$
$$[.7607885912\ 10^{20} (.08622000000\ s^2 + .2448000000\ s + .4237288136\ 10^{7}) \Big/ ($$
$$.1419599207\ 10^{-13} s^9 + .4030594823\ 10^{-13} s^8 + .0006617142428\ s^7$$
$$+ .9450084334\ 10^{7} s^5 + .001876790288\ s^6 + .4209284193\ 10^{17} s^3$$
$$+ .2675207858\ 10^{8} s^4 + .2861596669\ 10^{26} s + .1186355470\ 10^{18} s^2$$
$$+ .7891569770\ 10^{26}), .1795461075\ 10^{14} ($$
$$(.08622000000\ s^2 + .2448000000\ s + .4237288136\ 10^{7})$$

$$(.0006370000000\ s^2 + .4237288136\ 10^7)) \Big/ (.1419599207\ 10^{-13}\ s^9 + .4030594823\ 10^{-13}\ s^8 + .0006617142428\ s^7 + .9450084334\ 10^7\ s^5 + .001876790288\ s^6 + .4209284193\ 10^{17}\ s^3 + .2675207858\ 10^8\ s^4 + .2861596669\ 10^{26}\ s + .1186355470\ 10^{18}\ s^2 + .7891569770\ 10^{26}) , (.1482432338\ s^6 + .4208993695\ s^5 + .2965602360\ 10^{10}\ s^4 + .3223680470\ 10^{27} + .8399396725\ 10^{10}\ s^3 + .6704905927\ 10^{19}\ s^2 + .1862410470\ 10^{20}\ s) \Big/ (.1419599207\ 10^{-13}\ s^9 + .4030594823\ 10^{-13}\ s^8 + .0006617142428\ s^7 + .9450084334\ 10^7\ s^5 + .001876790288\ s^6 + .4209284193\ 10^{17}\ s^3 + .2675207858\ 10^8\ s^4 + .2861596669\ 10^{26}\ s + .1186355470\ 10^{18}\ s^2 + .7891569770\ 10^{26}) , (.2228570183\ 10^{-10}\ s^8 + .6327464401\ 10^{-10}\ s^7 + .7423114016\ s^6 + .6850292630\ 10^{19}\ s^2 + 2.104496848\ s^5 + .5953060993\ 10^{10}\ s^4 + .1679879345\ 10^{11}\ s^3 + .3223680470\ 10^{27} + .1862410470\ 10^{20}\ s) \Big/ (.1419599207\ 10^{-13}\ s^9 + .4030594823\ 10^{-13}\ s^8 + .0006617142428\ s^7 + .9450084334\ 10^7\ s^5 + .001876790288\ s^6 + .4209284193\ 10^{17}\ s^3 + .2675207858\ 10^8\ s^4 + .2861596669\ 10^{26}\ s + .1186355470\ 10^{18}\ s^2 + .7891569770\ 10^{26}) , (.001095232428\ s^6 + .3642712224\ 10^8\ s^4 + .2907733994\ 10^{18}\ s^2 + .3223680469\ 10^{27}) \Big/ (.1419599207\ 10^{-13}\ s^9 + .4030594823\ 10^{-13}\ s^8 + .0006617142428\ s^7 + .9450084334\ 10^7\ s^5 + .001876790288\ s^6 + .4209284193\ 10^{17}\ s^3 + .2675207858\ 10^8\ s^4 + .2861596669\ 10^{26}\ s + .1186355470\ 10^{18}\ s^2 + .7891569770\ 10^{26})]$$

$$[.3223680471\ 10^{27}\ 1/(.1419599207\ 10^{-13}\ s^9 + .4030594823\ 10^{-13}\ s^8 + .0006617142428\ s^7 + .9450084334\ 10^7\ s^5 + .001876790288\ s^6 + .4209284193\ 10^{17}\ s^3 + .2675207858\ 10^8\ s^4 + .2861596669\ 10^{26}\ s + .1186355470\ 10^{18}\ s^2 + .789156977\ 10^{26}) , .7607885912\ 10^{20}\ (.0006370000000\ s^2 + .4237288136\ 10^7) \Big/ (.1419599207\ 10^{-13}\ s^9 + .4030594823\ 10^{-13}\ s^8 + .0006617142428\ s^7 + .9450084334\ 10^7\ s^5 + .001876790288\ s^6 + .4209284193\ 10^{17}\ s^3 + .2675207858\ 10^8\ s^4 + .2861596669\ 10^{26}\ s + .1186355470\ 10^{18}\ s^2 + .7891569770\ 10^{26}) , (.7285424449\ 10^7\ s^4 + .1453866998\ 10^{18}\ s^2 + .3223680471\ 10^{27}) \Big/ (.1419599207\ 10^{-13}\ s^9 + .4030594823\ 10^{-13}\ s^8 + .0006617142428\ s^7 + .9450084334\ 10^7\ s^5 + .001876790288\ s^6 + .4209284193\ 10^{17}\ s^3 + .2675207858\ 10^8\ s^4 + .2861596669\ 10^{26}\ s + .1186355470\ 10^{18}\ s^2 + .7891569770\ 10^{26}) , (.001095232428\ s^6 + .3642712224\ 10^8\ s^4 + .2907733994\ 10^{18}\ s^2 + .3223680469\ 10^{27}) \Big/ (.1419599207\ 10^{-13}\ s^9 + .4030594823\ 10^{-13}\ s^8 + .0006617142428\ s^7 + .9450084334\ 10^7\ s^5 + .001876790288\ s^6 + .4209284193\ 10^{17}\ s^3 + .2675207858\ 10^8\ s^4$$

$$+ .2861596669\ 10^{26} s + .1186355470\ 10^{18} s^2 + .7891569770\ 10^{26}) , ($$
$$.1646484814\ 10^{-12} s^8 + .007666626998\ s^6 + .1092813667\ 10^{9} s^4$$
$$+ .4846223322\ 10^{18} s^2 + .3223680466\ 10^{27}) \,/\, (.1419599207\ 10^{-13} s^9$$
$$+ .4030594823\ 10^{-13} s^8 + .0006617142428\ s^7 + .9450084334\ 10^{7} s^5$$
$$+ .001876790288\ s^6 + .4209284193\ 10^{17} s^3 + .2675207858\ 10^{8} s^4$$
$$+ .2861596669\ 10^{26} s + .1186355470\ 10^{18} s^2 + .7891569770\ 10^{26})]$$

- ZZ11:=[Zinv[1,1]];

$$ZZ11 := [(.2228570183\ 10^{-10} s^8 + .6327464401\ 10^{-10} s^7 + .8905546355\ s^6$$
$$+ .9897483575\ 10^{10} s^4 + 2.525396217\ s^5 + .2652885032\ 10^{20} s^2$$
$$+ .2799798909\ 10^{11} s^3 + .3223680470\ 10^{27} + .7449641878\ 10^{20} s) \,/\, ($$
$$.1419599207\ 10^{-13} s^9 + .4030594823\ 10^{-13} s^8 + .0006617142428\ s^7$$
$$+ .9450084334\ 10^{7} s^5 + .001876790288\ s^6 + .4209284193\ 10^{17} s^3$$
$$+ .2675207858\ 10^{8} s^4 + .2861596669\ 10^{26} s + .1186355470\ 10^{18} s^2$$
$$+ .7891569770\ 10^{26})]$$

- ZZ51:=[Zinv[5,1]];

$$ZZ51 := [.3223680471\ 10^{27}\ 1/(.1419599207\ 10^{-13} s^9 + .4030594823\ 10^{-13} s^8$$
$$+ .0006617142428\ s^7 + .9450084334\ 10^{7} s^5 + .001876790288\ s^6$$
$$+ .4209284193\ 10^{17} s^3 + .2675207858\ 10^{8} s^4 + .2861596669\ 10^{26} s$$
$$+ .1186355470\ 10^{18} s^2 + .789156977\ 10^{26})]$$

Appendix-A5:

Calculation of impedance inverse symbolically with losses using Maple

Finite Element system impedance inverse symbolic computation using Maple software for Transmission Line Modeling consists of Inductance, Series Resistance, Capacitance, and Shunt Conductance. All are per unit length.

- LDPS_FE_TLM_System_Impedance_LRCG_4Sections_V1_17_02_2012;

  LDPS_FE_TLM_System_Impedance_LRCG_4Sections_V1_17_02_2012

- a11:=L1*s+R1+G1/(C1*s*G1+1);a12:=-G1/(C1*s*G1+1);a13:=0;a14:=0;a15:=0;a21:=-G1/(C1*s*G1+1);a22:=G1/(C1*s*G1+1)+L2*s+R2+G2/(C2*s*G2+1);a23:=-G2/(C2*s*G2+1);a24:=0;a25:=0;a31:=0;a32:=-G2/(C2*s*G2+1);a33:=G2/(C2*s*G2+1)+L3*s+R3+G3/(C3*s*G3+1);a34:=-G3/(C3*s*G3+1);a35:=0;a41:=0;a42:=0;a43:=-G3/(C3*s*G3+1);a44:=G3/(C3*s*G3+1)+L4*s+R4+G4/(C4*s*G4+1);a45:=-G4/(C4*s*G4+1);a51:=0;a52:=0;a53:=0;a54:=-G4/(C4*s*G4+1);a55:=L*s+R+G4/(C4*s*G4+1);

$$a11 := L1\,s + R1 + \frac{G1}{C1\,s\,G1 + 1}$$

$$a12 := -\frac{G1}{C1\,s\,G1 + 1}$$

$$a13 := 0$$

$$a14 := 0$$

$$a15 := 0$$

$$a21 := -\frac{G1}{C1\,s\,G1 + 1}$$

$$a22 := \frac{G1}{C1\,s\,G1 + 1} + L2\,s + R2 + \frac{G2}{C2\,s\,G2 + 1}$$

$$a23 := -\frac{G2}{C2\,s\,G2 + 1}$$

$$a24 := 0$$

$$a25 := 0$$

$$a31 := 0$$

$$a32 := -\frac{G2}{C2\ s\ G2 + 1}$$

$$a33 := \frac{G2}{C2\ s\ G2 + 1} + L3\ s + R3 + \frac{G3}{C3\ s\ G3 + 1}$$

$$a34 := -\frac{G3}{C3\ s\ G3 + 1}$$

$$a35 := 0$$

$$a41 := 0$$

$$a42 := 0$$

$$a43 := -\frac{G3}{C3\ s\ G3 + 1}$$

$$a44 := \frac{G3}{C3\ s\ G3 + 1} + L4\ s + R4 + \frac{G4}{C4\ s\ G4 + 1}$$

$$a45 := -\frac{G4}{C4\ s\ G4 + 1}$$

$$a51 := 0$$

$$a52 := 0$$

$$a53 := 0$$

$$a54 := -\frac{G4}{C4\ s\ G4 + 1}$$

$$a55 := L\ s + R + \frac{G4}{C4\ s\ G4 + 1}$$

- Z(s):=matrix(5,5,[a11,a12,a13,a14,a15,a21,a22,a23,a24,a25,a31,a32,a33,a34,a35,a41,a42,a43,a44,a45,a51,a52,a53,a54,a55]);

$$Z(s) := \begin{bmatrix} L1\,s + R1 + \frac{G1}{C1\,s\,G1 + 1}, & -\frac{G1}{C1\,s\,G1 + 1}, & 0, & 0, & 0 \\ -\frac{G1}{C1\,s\,G1 + 1}, & \frac{G1}{C1\,s\,G1 + 1} + L2\,s + R2 + \frac{G2}{C2\,s\,G2 + 1}, & -\frac{G2}{C2\,s\,G2 + 1}, & 0, & 0 \\ 0, & -\frac{G2}{C2\,s\,G2 + 1}, & \frac{G2}{C2\,s\,G2 + 1} + L3\,s + R3 + \frac{G3}{C3\,s\,G3 + 1}, & -\frac{G3}{C3\,s\,G3 + 1}, & 0 \\ 0, & 0, & -\frac{G3}{C3\,s\,G3 + 1}, & \frac{G3}{C3\,s\,G3 + 1} + L4\,s + R4 + \frac{G4}{C4\,s\,G4 + 1}, & -\frac{G4}{C4\,s\,G4 + 1} \\ 0, & 0, & 0, & -\frac{G4}{C4\,s\,G4 + 1}, & L\,s + R + \frac{G4}{C4\,s\,G4 + 1} \end{bmatrix}$$

- with(linalg):Zinv:=inverse(Z(s));
- ZZ11:=[Zinv[1,1]];
- ZZ51:=[Zinv[5,1]];

Appendix-A6:

Calculation of impedance inverse numerically with losses using Maple

Finite Element system impedance inverse numerical computation using Maple software for Transmission Line Modeling consists of Inductance, Series Resistance, Capacitance, and Shunt Conductance. All are per unit length.

- LDPS_FE_TLM_System_Impedance_LRCG_4Sections_V2_29_03_2012;

LDPS_FE_TLM_System_Impedance_LRCG_4Sections_V2_29_03_2012

- L1:=0.637e-3;L2:=L1;L3:=L1;L4:=L1;R1:=9.73e-3;R2:=R1;R3:=R1;R4:=R1;C1:=0.236E-6;C2:=C1;C3:=C1;C4:=C1;G1:=0.714E-6;G2:=G1;G3:=G1;G4:=G1;L:=0.08622;R:=0.2448;

$$L1 := .000637$$

$$L2 := .000637$$

$$L3 := .000637$$

$$L4 := .000637$$

$$R1 := .00973$$

$$R2 := .00973$$

$$R3 := .00973$$

$$R4 := .00973$$

$$C1 := .236\ 10^{-6}$$

$$C2 := .236\ 10^{-6}$$

$$C3 := .236\ 10^{-6}$$

$$C4 := .236\ 10^{-6}$$

$$G1 := .714\ 10^{-6}$$

$$G2 := .714\ 10^{-6}$$

$$G3 := .714\ 10^{-6}$$

$$G4 := .714\ 10^{-6}$$

$$L := .08622$$

$$R := .2448$$

- a11:=L1*s+R1+G1/(C1*s*G1+1);a12:=-G1/(C1*s*G1+1);a13:=0;a14:=0;a15:=0;a21:=-G1/(C1*s*G1+1);a22:=G1/(C1*s*G1+1)+L2*s+R2+G2/(C2*s*G2+1);a23:=-G2/(C2*s*G2+1);a24:=0;a25:=0;a31:=0;a32:=-G2/(C2*s*G2+1);a33:=G2/(C2*s*G2+1)+L3*s+R3+G3/(C3*s*G3+1);a34:=-G3/(C3*s*G3+1);a35:=0;a41:=0;a42:=0;a43:=-G3/(C3*s*G3+1);a44:=G3/(C3*s*G3+1)+L4*s+R4+G4/(C4*s*G4+1);a45:=-G4/(C4*s*G4+1);a51:=0;a52:=0;a53:=0;a54:=-G4/(C4*s*G4+1);a55:=L*s+R+G4/(C4*s*G4+1);

$$a11 := .000637\ s + .00973 + \frac{.714\ 10^{-6}}{.168504\ 10^{-12}\ s + 1}$$

$$a12 := -.714\ 10^{-6}\ \frac{1}{.168504\ 10^{-12}\ s + 1}$$

$$a13 := 0$$

$$a14 := 0$$

$$a15 := 0$$

$$a21 := -.714\ 10^{-6}\ \frac{1}{.168504\ 10^{-12}\ s + 1}$$

$$a22 := .1428\ 10^{-5}\ \frac{1}{.168504\ 10^{-12}\ s + 1} + .000637\ s + .00973$$

$$a23 := -.714\ 10^{-6}\ \frac{1}{.168504\ 10^{-12}\ s + 1}$$

$$a24 := 0$$

$$a25 := 0$$

$$a31 := 0$$

$$a32 := -.714\ 10^{-6}\ \frac{1}{.168504\ 10^{-12}\ s + 1}$$

$$a33 := .1428\ 10^{-5}\ \frac{1}{.168504\ 10^{-12}\ s + 1} + .000637\ s + .00973$$

$$a34 := -.714\ 10^{-6}\ \frac{1}{.168504\ 10^{-12}\ s + 1}$$

$$a35 := 0$$

$$a41 := 0$$

$$a42 := 0$$

$$a43 := -.714\ 10^{-6}\ \frac{1}{.168504\ 10^{-12}\ s + 1}$$

$$a44 := .1428\ 10^{-5}\ \frac{1}{.168504\ 10^{-12}\ s + 1} + .000637\ s + .00973$$

$$a45 := -.714\ 10^{-6}\ \frac{1}{.168504\ 10^{-12}\ s + 1}$$

$$a51 := 0$$

$$a52 := 0$$

$$a53 := 0$$

$$a54 := -.714\ 10^{-6}\ \frac{1}{.168504\ 10^{-12}\ s + 1}$$

$$a55 := .08622\ s + .2448 + \frac{.714\ 10^{-6}}{.168504\ 10^{-12}\ s + 1}$$

- Z(s):=matrix(5,5,[a11,a12,a13,a14,a15,a21,a22,a23,a24,a25,a31,a32,a33,a34,a35,a41,a42,a43,a44,a45,a51,a52,a53,a54,a55]);

$$Z(s) := \left[\begin{array}{ccccc} .000637\ s + .00973 + \frac{.714\ 10^{-6}}{.168504\ 10^{-12}\ s + 1} & -.714\ 10^{-6}\ \frac{1}{.168504\ 10^{-12}\ s + 1} & 0 & 0 & 0 \\ -.714\ 10^{-6}\ \frac{1}{.168504\ 10^{-12}\ s + 1} & .1428\ 10^{-5}\ \frac{1}{.168504\ 10^{-12}\ s + 1} + .000637\ s + .00973 & -.714\ 10^{-6}\ \frac{1}{.168504\ 10^{-12}\ s + 1} & 0 & 0 \\ 0 & -.714\ 10^{-6}\ \frac{1}{.168504\ 10^{-12}\ s + 1} & .1428\ 10^{-5}\ \frac{1}{.168504\ 10^{-12}\ s + 1} + .000637\ s + .00973 & -.714\ 10^{-6}\ \frac{1}{.168504\ 10^{-12}\ s + 1} & 0 \\ 0 & 0 & -.714\ 10^{-6}\ \frac{1}{.168504\ 10^{-12}\ s + 1} & \cdots & \end{array}\right.$$

$$.1428\ 10^{-5}\ \frac{1}{.168504\ 10^{-12}\ s+1}+.000637\ s+.00973\ ,$$

$$-.714\ 10^{-6}\ \frac{1}{.168504\ 10^{-12}\ s+1}\Bigg]$$

$$\left[0\ ,0\ ,0\ ,-.714\ 10^{-6}\ \frac{1}{.168504\ 10^{-12}\ s+1}\ ,.08622\ s+.2448+\frac{.714\ 10^{-6}}{.168504\ 10^{-12}\ s+1}\right]$$

- with(linalg):Zinv:=inverse(Z(s));

Zinv :=

$$[((.1685040000\ 10^{-12}\ s+1.)\ (.1850343617\ 10^{-7}\ s^2+.1237603439\ 10^{-6}\ s$$
$$+.2256017150\ 10^{-6}+.2228570183\ 10^{-10}\ s^4+.1084648625\ 10^{-8}\ s^3$$
$$+.3796627555\ 10^{-35}\ s^6+.1502091961\ 10^{-22}\ s^5+.1796665276\ 10^{-61}\ s^8$$
$$+.4264979530\ 10^{-48}\ s^7))\ /\ (.1196040724\ 10^{-25}\ s^6+.1419599207\ 10^{-13}\ s^5$$
$$+.2588869839\ 10^{-9}\ s^2+.4030752922\ 10^{-38}\ s^7+.6791979902\ 10^{-51}\ s^8$$
$$+.1347984798\ 10^{-8}\ s+.1928487470\ 10^{-77}\ s^{10}+.5722378906\ 10^{-64}\ s^9$$
$$+.2195265755\ 10^{-8}+.2234109438\ 10^{-10}\ s^3+.9077769649\ 10^{-12}\ s^4)\ ,\ .714\ 10^{-6}\ (($$
$$.1168274243\ 10^{-5}\ s^2+.00001120009344\ s+.00002318279663$$
$$+.1768554114\ 10^{-19}\ s^4+.3498540318\ 10^{-7}\ s^3+.1673853818\ 10^{-45}\ s^6$$
$$+.2980084423\ 10^{-32}\ s^5)\ (.1685040000\ 10^{-12}\ s+1.))\ /\ (.1196040724\ 10^{-25}\ s^6$$
$$+.1419599207\ 10^{-13}\ s^5+.2588869839\ 10^{-9}\ s^2+.4030752922\ 10^{-38}\ s^7$$
$$+.6791979902\ 10^{-51}\ s^8+.1347984798\ 10^{-8}\ s+.1928487470\ 10^{-77}\ s^{10}$$
$$+.5722378906\ 10^{-64}\ s^9+.2195265755\ 10^{-8}+.2234109438\ 10^{-10}\ s^3$$
$$+.9077769649\ 10^{-12}\ s^4)\ ,\ .509796\ 10^{-12}\ ((.00005492214000\ s^2$$
$$+.0009949817770\ s+.002382260522\ +.1559437165\ 10^{-29}\ s^4$$
$$+.1850920056\ 10^{-16}\ s^3)\ (.1685040000\ 10^{-12}\ s+1.))\ /\ (.1196040724\ 10^{-25}\ s^6$$
$$+.1419599207\ 10^{-13}\ s^5+.2588869839\ 10^{-9}\ s^2+.4030752922\ 10^{-38}\ s^7$$
$$+.6791979902\ 10^{-51}\ s^8+.1347984798\ 10^{-8}\ s+.1928487470\ 10^{-77}\ s^{10}$$
$$+.5722378906\ 10^{-64}\ s^9+.2195265755\ 10^{-8}+.2234109438\ 10^{-10}\ s^3$$
$$+.9077769649\ 10^{-12}\ s^4)\ ,\ .363994344\ 10^{-18}\ ((.1685040000\ 10^{-12}\ s+1.)$$
$$(.1452841488\ 10^{-13}\ s^2+.08622000000\ s+.2448007140\ ))\ /\ (.1196040724\ 10^{-25}\ s^6$$
$$+.1419599207\ 10^{-13}\ s^5+.2588869839\ 10^{-9}\ s^2+.4030752922\ 10^{-38}\ s^7$$
$$+.6791979902\ 10^{-51}\ s^8+.1347984798\ 10^{-8}\ s+.1928487470\ 10^{-77}\ s^{10}$$
$$+.5722378906\ 10^{-64}\ s^9+.2195265755\ 10^{-8}+.2234109438\ 10^{-10}\ s^3$$
$$+.9077769649\ 10^{-12}\ s^4)\ ,\ .2598919616\ 10^{-24}\ (.1685040000\ 10^{-12}\ s+1.)\ /\ ($$
$$.1196040724\ 10^{-25}\ s^6+.1419599207\ 10^{-13}\ s^5+.2588869839\ 10^{-9}\ s^2$$
$$+.4030752922\ 10^{-38}\ s^7+.6791979902\ 10^{-51}\ s^8+.1347984798\ 10^{-8}\ s$$

$$+ .1928487470\ 10^{-77} s^{10} + .5722378906\ 10^{-64} s^9 + .2195265755\ 10^{-8}$$
$$+ .2234109438\ 10^{-10} s^3 + .9077769649\ 10^{-12} s^4)]$$
$$[.714\ 10^{-6}((.1168274243\ 10^{-5} s^2 + .00001120009344\ s + .00002318279663$$
$$+ .1768554114\ 10^{-19} s^4 + .3498540318\ 10^{-7} s^3 + .1673853818\ 10^{-45} s^6$$
$$+ .2980084423\ 10^{-32} s^5)(.1685040000\ 10^{-12} s + 1.)) \Big/ (.1196040724\ 10^{-25} s^6$$
$$+ .1419599207\ 10^{-13} s^5 + .2588869839\ 10^{-9} s^2 + .4030752922\ 10^{-38} s^7$$
$$+ .6791979902\ 10^{-51} s^8 + .1347984798\ 10^{-8} s + .1928487470\ 10^{-77} s^{10}$$
$$+ .5722378906\ 10^{-64} s^9 + .2195265755\ 10^{-8} + .2234109438\ 10^{-10} s^3$$
$$+ .9077769649\ 10^{-12} s^4), (.168504\ 10^{-12} s + 1)^2 (.1168274243\ 10^{-5} s^2$$
$$+ .00001120009344\ s + .00002318279663 + .1768554114\ 10^{-19} s^4$$
$$+ .3498540318\ 10^{-7} s^3 + .1673853818\ 10^{-45} s^6 + .2980084423\ 10^{-32} s^5)$$
$$(.1073370480\ 10^{-15} s^2 + .0006370000000\ s + .009730714000) \Big/ ((.1196040724\ 10^{-25} s^6 + .1419599207\ 10^{-13} s^5 + .2588869839\ 10^{-9} s^2$$
$$+ .4030752922\ 10^{-38} s^7 + .6791979902\ 10^{-51} s^8 + .1347984798\ 10^{-8} s$$
$$+ .1928487470\ 10^{-77} s^{10} + .5722378906\ 10^{-64} s^9 + .2195265755\ 10^{-8}$$
$$+ .2234109438\ 10^{-10} s^3 + .9077769649\ 10^{-12} s^4)(.1685040000\ 10^{-12} s + 1.)),$$
$$.714\ 10^{-6}((.00005492214000\ s^2 + .0009949817770\ s + .002382260522$$
$$+ .1559437165\ 10^{-29} s^4 + .1850920056\ 10^{-16} s^3)(.168504\ 10^{-12} s + 1)^2$$
$$(.1073370480\ 10^{-15} s^2 + .0006370000000\ s + .009730714000)) \Big/ ((.1196040724\ 10^{-25} s^6 + .1419599207\ 10^{-13} s^5 + .2588869839\ 10^{-9} s^2$$
$$+ .4030752922\ 10^{-38} s^7 + .6791979902\ 10^{-51} s^8 + .1347984798\ 10^{-8} s$$
$$+ .1928487470\ 10^{-77} s^{10} + .5722378906\ 10^{-64} s^9 + .2195265755\ 10^{-8}$$
$$+ .2234109438\ 10^{-10} s^3 + .9077769649\ 10^{-12} s^4)(.1685040000\ 10^{-12} s + 1.)),$$
$$.509796\ 10^{-12}((.1073370480\ 10^{-15} s^2 + .0006370000000\ s + .009730714000)$$
$$(.1685040000\ 10^{-12} s + 1.)$$
$$(.1452841488\ 10^{-13} s^2 + .08622000000\ s + .2448007140)) \Big/ (.1196040724\ 10^{-25} s^6$$
$$+ .1419599207\ 10^{-13} s^5 + .2588869839\ 10^{-9} s^2 + .4030752922\ 10^{-38} s^7$$
$$+ .6791979902\ 10^{-51} s^8 + .1347984798\ 10^{-8} s + .1928487470\ 10^{-77} s^{10}$$
$$+ .5722378906\ 10^{-64} s^9 + .2195265755\ 10^{-8} + .2234109438\ 10^{-10} s^3$$
$$+ .9077769649\ 10^{-12} s^4), .363994344\ 10^{-18} (.168504\ 10^{-12} s + 1)^2$$
$$(.1073370480\ 10^{-15} s^2 + .0006370000000\ s + .009730714000) \Big/ ((.1196040724\ 10^{-25} s^6 + .1419599207\ 10^{-13} s^5 + .2588869839\ 10^{-9} s^2$$

$$+ .4030752922\ 10^{-38} s^7 + .6791979902\ 10^{-51} s^8 + .1347984798\ 10^{-8} s$$
$$+ .1928487470\ 10^{-77} s^{10} + .5722378906\ 10^{-64} s^9 + .2195265755\ 10^{-8}$$
$$+ .2234109438\ 10^{-10} s^3 + .9077769649\ 10^{-12} s^4)\,(.1685040000\ 10^{-12} s + 1.))]$$
$$[.509796\ 10^{-12}\,((.00005492214000\ s^2 + .0009949817770\ s + .002382260522$$
$$+ .1559437165\ 10^{-29} s^4 + .1850920056\ 10^{-16} s^3)\,(.1685040000\ 10^{-12} s + 1.)) \Big/ ($$
$$.1196040724\ 10^{-25} s^6 + .1419599207\ 10^{-13} s^5 + .2588869839\ 10^{-9} s^2$$
$$+ .4030752922\ 10^{-38} s^7 + .6791979902\ 10^{-51} s^8 + .1347984798\ 10^{-8} s$$
$$+ .1928487470\ 10^{-77} s^{10} + .5722378906\ 10^{-64} s^9 + .2195265755\ 10^{-8}$$
$$+ .2234109438\ 10^{-10} s^3 + .9077769649\ 10^{-12} s^4), .714\ 10^{-6}\,((.00005492214000\ s^2$$
$$+ .0009949817770\ s + .002382260522 + .1559437165\ 10^{-29} s^4$$
$$+ .1850920056\ 10^{-16} s^3)\,(.168504\ 10^{-12} s + 1)^2$$
$$(.1073370480\ 10^{-15} s^2 + .0006370000000\ s + .009730714000)) \Big/ ((.1196040724\ 10^{-25} s^6 + .1419599207\ 10^{-13} s^5 + .2588869839\ 10^{-9} s^2$$
$$+ .4030752922\ 10^{-38} s^7 + .6791979902\ 10^{-51} s^8 + .1347984798\ 10^{-8} s$$
$$+ .1928487470\ 10^{-77} s^{10} + .5722378906\ 10^{-64} s^9 + .2195265755\ 10^{-8}$$
$$+ .2234109438\ 10^{-10} s^3 + .9077769649\ 10^{-12} s^4)\,(.1685040000\ 10^{-12} s + 1.)), ($$
$$(.1685040000\ 10^{-12} s + 1.)\,(.3796627556\ 10^{-35} s^6 + .1502091960\ 10^{-22} s^5$$
$$+ .1850260204\ 10^{-7} s^2 + .4264979530\ 10^{-48} s^7 + .1796665276\ 10^{-61} s^8$$
$$+ .1237523474\ 10^{-6} s + .2255851637\ 10^{-6} + .1084623645\ 10^{-8} s^3$$
$$+ .2228570183\ 10^{-10} s^4)) \Big/ (.1196040724\ 10^{-25} s^6 + .1419599207\ 10^{-13} s^5$$
$$+ .2588869839\ 10^{-9} s^2 + .4030752922\ 10^{-38} s^7 + .6791979902\ 10^{-51} s^8$$
$$+ .1347984798\ 10^{-8} s + .1928487470\ 10^{-77} s^{10} + .5722378906\ 10^{-64} s^9$$
$$+ .2195265755\ 10^{-8} + .2234109438\ 10^{-10} s^3 + .9077769649\ 10^{-12} s^4), ($$
$$(.1685040000\ 10^{-12} s + 1.)\,(.1262747637\ 10^{-25} s^4 + .2497957787\ 10^{-13} s^3$$
$$+ .8341198100\ 10^{-12} s^2 + .1195131626\ 10^{-51} s^6 + .2127780278\ 10^{-38} s^5$$
$$+ .1655130233\ 10^{-10} + .7996359474\ 10^{-11} s)) \Big/ (.1196040724\ 10^{-25} s^6$$
$$+ .1419599207\ 10^{-13} s^5 + .2588869839\ 10^{-9} s^2 + .4030752922\ 10^{-38} s^7$$
$$+ .6791979902\ 10^{-51} s^8 + .1347984798\ 10^{-8} s + .1928487470\ 10^{-77} s^{10}$$
$$+ .5722378906\ 10^{-64} s^9 + .2195265755\ 10^{-8} + .2234109438\ 10^{-10} s^3$$
$$+ .9077769649\ 10^{-12} s^4), ((.1685040000\ 10^{-12} s + 1.)\,(.2068594131\ 10^{-18} s^2$$
$$+ .5873483020\ 10^{-44} s^4 + .6971327712\ 10^{-31} s^3 + .6320137003\ 10^{-17} s$$
$$+ .4827449098\ 10^{-16})) \Big/ (.1196040724\ 10^{-25} s^6 + .1419599207\ 10^{-13} s^5$$
$$+ .2588869839\ 10^{-9} s^2 + .4030752922\ 10^{-38} s^7 + .6791979902\ 10^{-51} s^8$$
$$+ .1347984798\ 10^{-8} s + .1928487470\ 10^{-77} s^{10} + .5722378906\ 10^{-64} s^9$$
$$+ .2195265755\ 10^{-8} + .2234109438\ 10^{-10} s^3 + .9077769649\ 10^{-12} s^4)]$$
$$[.363994344\ 10^{-18}\,((.1685040000\ 10^{-12} s + 1.)$$

$$(.1452841488\ 10^{-13} s^2 + .08622000000\ s + .2448007140\ )) \Big/ (.1196040724\ 10^{-25} s^6 + .1419599207\ 10^{-13} s^5 + .2588869839\ 10^{-9} s^2 + .4030752922\ 10^{-38} s^7 + .6791979902\ 10^{-51} s^8 + .1347984798\ 10^{-8} s + .1928487470\ 10^{-77} s^{10} + .5722378906\ 10^{-64} s^9 + .2195265755\ 10^{-8} + .2234109438\ 10^{-10} s^3 + .9077769649\ 10^{-12} s^4) , .509796\ 10^{-12} ($$

$$(.1073370480\ 10^{-15} s^2 + .0006370000000\ s + .009730714000\ )$$

$$(.1685040000\ 10^{-12} s + 1.)$$

$$(.1452841488\ 10^{-13} s^2 + .08622000000\ s + .2448007140\ )) \Big/ (.1196040724\ 10^{-25} s^6 + .1419599207\ 10^{-13} s^5 + .2588869839\ 10^{-9} s^2 + .4030752922\ 10^{-38} s^7 + .6791979902\ 10^{-51} s^8 + .1347984798\ 10^{-8} s + .1928487470\ 10^{-77} s^{10} + .5722378906\ 10^{-64} s^9 + .2195265755\ 10^{-8} + .2234109438\ 10^{-10} s^3 + .9077769649\ 10^{-12} s^4) , ((.1685040000\ 10^{-12} s + 1.) (.1262747637\ 10^{-25} s^4 + .2497957787\ 10^{-13} s^3 + .8341198100\ 10^{-12} s^2 + .1195131626\ 10^{-51} s^6 + .2127780278\ 10^{-38} s^5 + .1655130233\ 10^{-10} + .7996359474\ 10^{-11} s)) \Big/ ($$

$$.1196040724\ 10^{-25} s^6 + .1419599207\ 10^{-13} s^5 + .2588869839\ 10^{-9} s^2 + .4030752922\ 10^{-38} s^7 + .6791979902\ 10^{-51} s^8 + .1347984798\ 10^{-8} s + .1928487470\ 10^{-77} s^{10} + .5722378906\ 10^{-64} s^9 + .2195265755\ 10^{-8} + .2234109438\ 10^{-10} s^3 + .9077769649\ 10^{-12} s^4) , ((.1685040000\ 10^{-12} s + 1.) ($$

$$.2228570183\ 10^{-10} s^4 + .1084623645\ 10^{-8} s^3 + .1850260202\ 10^{-7} s^2 + .3796627555\ 10^{-35} s^6 + .1502091961\ 10^{-22} s^5 + .1796665276\ 10^{-61} s^8 + .4264979530\ 10^{-48} s^7 + .2255851625\ 10^{-6} + .1237523469\ 10^{-6} s)) \Big/ ($$

$$.1196040724\ 10^{-25} s^6 + .1419599207\ 10^{-13} s^5 + .2588869839\ 10^{-9} s^2 + .4030752922\ 10^{-38} s^7 + .6791979902\ 10^{-51} s^8 + .1347984798\ 10^{-8} s + .1928487470\ 10^{-77} s^{10} + .5722378906\ 10^{-64} s^9 + .2195265755\ 10^{-8} + .2234109438\ 10^{-10} s^3 + .9077769649\ 10^{-12} s^4) , ((.1685040000\ 10^{-12} s + 1.) ($$

$$.8457933833\ 10^{-14} s^2 + .9329276790\ 10^{-28} s^4 + .1845510450\ 10^{-15} s^3 + .8829724494\ 10^{-54} s^6 + .1572020456\ 10^{-40} s^5 + .1292084157\ 10^{-12} s + .6579548050\ 10^{-12})) \Big/ (.1196040724\ 10^{-25} s^6 + .1419599207\ 10^{-13} s^5 + .2588869839\ 10^{-9} s^2 + .4030752922\ 10^{-38} s^7 + .6791979902\ 10^{-51} s^8 + .1347984798\ 10^{-8} s + .1928487470\ 10^{-77} s^{10} + .5722378906\ 10^{-64} s^9 + .2195265755\ 10^{-8} + .2234109438\ 10^{-10} s^3 + .9077769649\ 10^{-12} s^4)]$$

$$[.2598919616\ 10^{-24} (.1685040000\ 10^{-12} s + 1.) \Big/ (.1196040724\ 10^{-25} s^6 + .1419599207\ 10^{-13} s^5 + .2588869839\ 10^{-9} s^2 + .4030752922\ 10^{-38} s^7 + .6791979902\ 10^{-51} s^8 + .1347984798\ 10^{-8} s + .1928487470\ 10^{-77} s^{10} + .5722378906\ 10^{-64} s^9 + .2195265755\ 10^{-8} + .2234109438\ 10^{-10} s^3 + .9077769649\ 10^{-12} s^4) , .363994344\ 10^{-18} (.168504\ 10^{-12} s + 1)^2$$

$$(.1073370480\ 10^{-15} s^2 + .0006370000000\ s + .009730714000\ ) \Big/ ((.1196040724\ 10^{-25} s^6 + .1419599207\ 10^{-13} s^5 + .2588869839\ 10^{-9} s^2 + .4030752922\ 10^{-38} s^7 + .6791979902\ 10^{-51} s^8 + .1347984798\ 10^{-8} s + .1928487470\ 10^{-77} s^{10} + .5722378906\ 10^{-64} s^9 + .2195265755\ 10^{-8} + .2234109438\ 10^{-10} s^3 + .9077769649\ 10^{-12} s^4)(.1685040000\ 10^{-12} s + 1.)), ((.1685040000\ 10^{-12} s + 1.)(.2068594131\ 10^{-18} s^2 + .5873483020\ 10^{-44} s^4 + .6971327712\ 10^{-31} s^3 + .6320137003\ 10^{-17} s + .4827449098\ 10^{-16})) \Big/ (.1196040724\ 10^{-25} s^6 + .1419599207\ 10^{-13} s^5 + .2588869839\ 10^{-9} s^2 + .4030752922\ 10^{-38} s^7 + .6791979902\ 10^{-51} s^8 + .1347984798\ 10^{-8} s + .1928487470\ 10^{-77} s^{10} + .5722378906\ 10^{-64} s^9 + .2195265755\ 10^{-8} + .2234109438\ 10^{-10} s^3 + .9077769649\ 10^{-12} s^4), ((.1685040000\ 10^{-12} s + 1.)(.8457933833\ 10^{-14} s^2 + .9329276790\ 10^{-28} s^4 + .1845510450\ 10^{-15} s^3 + .8829724494\ 10^{-54} s^6 + .1572020456\ 10^{-40} s^5 + .1292084157\ 10^{-12} s + .6579548050\ 10^{-12})) \Big/ (.1196040724\ 10^{-25} s^6 + .1419599207\ 10^{-13} s^5 + .2588869839\ 10^{-9} s^2 + .4030752922\ 10^{-38} s^7 + .6791979902\ 10^{-51} s^8 + .1347984798\ 10^{-8} s + .1928487470\ 10^{-77} s^{10} + .5722378906\ 10^{-64} s^9 + .2195265755\ 10^{-8} + .2234109438\ 10^{-10} s^3 + .9077769649\ 10^{-12} s^4), ((.1685040000\ 10^{-12} s + 1.)(.2305511691\ 10^{-9} s^2 + .1646484814\ 10^{-12} s^4 + .1006113313\ 10^{-10} s^3 + .2804977676\ 10^{-37} s^6 + .1109757108\ 10^{-24} s^5 + .1327390143\ 10^{-63} s^8 + .3150999723\ 10^{-50} s^7 + .2348038656\ 10^{-8} s + .8967562713\ 10^{-8})) \Big/ (.1196040724\ 10^{-25} s^6 + .1419599207\ 10^{-13} s^5 + .2588869839\ 10^{-9} s^2 + .4030752922\ 10^{-38} s^7 + .6791979902\ 10^{-51} s^8 + .1347984798\ 10^{-8} s + .1928487470\ 10^{-77} s^{10} + .5722378906\ 10^{-64} s^9 + .2195265755\ 10^{-8} + .2234109438\ 10^{-10} s^3 + .9077769649\ 10^{-12} s^4)]$$

- ZZ11:=[Zinv[1,1]];

$$ZZ11 := [((.1685040000\ 10^{-12} s + 1.)(.1850343617\ 10^{-7} s^2 + .1237603439\ 10^{-6} s + .2256017150\ 10^{-6} + .2228570183\ 10^{-10} s^4 + .1084648625\ 10^{-8} s^3 + .3796627555\ 10^{-35} s^6 + .1502091961\ 10^{-22} s^5 + .1796665276\ 10^{-61} s^8 + .4264979530\ 10^{-48} s^7)) \Big/ (.1196040724\ 10^{-25} s^6 + .1419599207\ 10^{-13} s^5 + .2588869839\ 10^{-9} s^2 + .4030752922\ 10^{-38} s^7 + .6791979902\ 10^{-51} s^8 + .1347984798\ 10^{-8} s + .1928487470\ 10^{-77} s^{10} + .5722378906\ 10^{-64} s^9 + .2195265755\ 10^{-8} + .2234109438\ 10^{-10} s^3 + .9077769649\ 10^{-12} s^4)]$$

- ZZ11:=[.1084648625e-8*s^3/(.1196040724e-25*s^6+.1419599207e-13*s^5+.2588869839e-9*s^2+.4030752922e-38*s^7+.6791979902e-51*s^8+.1347984798e-8*s+.1928487470e-77*s^10+.5722378906e-64*s^9+.2195265755e-8+.2234109438e-10*s^3+.9077769649e-12*s^4)+.1850343617e-7*s^2/(.1196040724e-25*s^6+.1419599207e-13*s^5+.2588869839e-9*s^2+.4030752922e-38*s^7+.6791979902e-51*s^8+.1347984798e-8*s+.1928487470e-77*s^10+.5722378906e-64*s^9+.2195265755e-8+.2234109438e-10*s^3+.9077769649e-12*s^4)+.1237603439e-6*s/(.1196040724e-25*s^6+.1419599207e-13*s^5+.2588869839e-9*s^2+.4030752922e-38*s^7+.6791979902e-51*s^8+.1347984798e-8*s+.1928487470e-77*s^10+.5722378906e-64*s^9+.2195265755e-8+.2234109438e-10*s^3+.9077769649e-12*s^4)+.1877614951e-22*s^5/(.1196040724e-25*s^6+.1419599207e-13*s^5+.2588869839e-9*s^2+.4030752922e-38*s^7+.6791979902e-51*s^8+.1347984798e-8*s+.1928487470e-77*s^10+.5722378906e-64*s^9+.2195265755e-8+.2234109438e-10*s^3+.9077769649e-12*s^4)+.2228570183e-10*s^4/(.1196040724e-25*s^6+.1419599207e-13*s^5+.2588869839e-9*s^2+.4030752922e-38*s^7+.6791979902e-51*s^8+.1347984798e-8*s+.1928487470e-77*s^10+.5722378906e-64*s^9+.2195265755e-8+.2234109438e-10*s^3+.9077769649e-12*s^4)+.1066244882e-47*s^7/(.1196040724e-25*s^6+.1419599207e-13*s^5+.2588869839e-9*s^2+.4030752922e-38*s^7+.6791979902e-51*s^8+.1347984798e-8*s+.1928487470e-77*s^10+.5722378906e-64*s^9+.2195265755e-8+.2234109438e-10*s^3+.9077769649e-12*s^4)+.6327712593e-35*s^6/(.1196040724e-25*s^6+.1419599207e-13*s^5+.2588869839e-9*s^2+.4030752922e-38*s^7+.6791979902e-51*s^8+.1347984798e-8*s+.1928487470e-77*s^10+.5722378906e-64*s^9+.2195265755e-8+.2234109438e-10*s^3+.9077769649e-12*s^4)+.3027452857e-74*s^9/(.1196040724e-25*s^6+.1419599207e-13*s^5+.2588869839e-9*s^2+.4030752922e-38*s^7+.6791979902e-51*s^8+.1347984798e-8*s+.1928487470e-77*s^10+.5722378906e-64*s^9+.2195265755e-8+.2234109438e-10*s^3+.9077769649e-12*s^4)+.8983326383e-61*s^8/(.1196040724e-25*s^6+.1419599207e-13*s^5+.2588869839e-9*s^2+.4030752922e-38*s^7+.6791979902e-51*s^8+.1347984798e-8*s+.1928487470e-77*s^10+.5722378906e-64*s^9+.2195265755e-8+.2234109438e-10*s^3+.9077769649e-12*s^4)+.2256017150e-6/(.1196040724e-25*s^6+.1419599207e-13*s^5+.2588869839e-9*s^2+.4030752922e-38*s^7+.6791979902e-51*s^8+.1347984798e-8*s+.1928487470e-77*s^10+.5722378906e-64*s^9+.2195265755e-8+.2234109438e-10*s^3+.9077769649e-12*s^4)];

$$ZZ11 := [.1084648625\ 10^{-8} s^3 / (.1196040724\ 10^{-25} s^6 + .1419599207\ 10^{-13} s^5 + .2588869839\ 10^{-9} s^2 + .4030752922\ 10^{-38} s^7 + .6791979902\ 10^{-51} s^8 + .1347984798\ 10^{-8} s + .1928487470\ 10^{-77} s^{10} + .5722378906\ 10^{-64} s^9 + .2195265755\ 10^{-8} + .2234109438\ 10^{-10} s^3 + .9077769649\ 10^{-12} s^4) + .1850343617\ 10^{-7} s^2 / (.1196040724\ 10^{-25} s^6 + .1419599207\ 10^{-13} s^5 + .2588869839\ 10^{-9} s^2 + .4030752922\ 10^{-38} s^7 + .6791979902\ 10^{-51} s^8 + .1347984798\ 10^{-8} s + .1928487470\ 10^{-77} s^{10} + .5722378906\ 10^{-64} s^9 + .2195265755\ 10^{-8} + .2234109438\ 10^{-10} s^3 + .9077769649\ 10^{-12} s^4) + .1237603439\ 10^{-6} s / (.1196040724\ 10^{-25} s^6 + .1419599207\ 10^{-13} s^5 + .2588869839\ 10^{-9} s^2 + .4030752922\ 10^{-38} s^7 + .6791979902\ 10^{-51} s^8 + .1347984798\ 10^{-8} s + .1928487470\ 10^{-77} s^{10} + .5722378906\ 10^{-64} s^9 + .2195265755\ 10^{-8} + .2234109438\ 10^{-10} s^3 + .9077769649\ 10^{-12} s^4) + .1877614951\ 10^{-22} s^5 / (.1196040724\ 10^{-25} s^6 + .1419599207\ 10^{-13} s^5 + .2588869839\ 10^{-9} s^2 + .4030752922\ 10^{-38} s^7 + .6791979902\ 10^{-51} s^8 + .1347984798\ 10^{-8} s + .1928487470\ 10^{-77} s^{10} + .5722378906\ 10^{-64} s^9 + .2195265755\ 10^{-8} + .2234109438\ 10^{-10} s^3 + .9077769649\ 10^{-12} s^4) + .2228570183\ 10^{-10} s^4 / (.1196040724\ 10^{-25} s^6 + .1419599207\ 10^{-13} s^5 + .2588869839\ 10^{-9} s^2 + .4030752922\ 10^{-38} s^7 + .6791979902\ 10^{-51} s^8 + .1347984798\ 10^{-8} s + .1928487470\ 10^{-77} s^{10} + .5722378906\ 10^{-64} s^9 + .2195265755\ 10^{-8} + .2234109438\ 10^{-10} s^3 + .9077769649\ 10^{-12} s^4) + .1066244882\ 10^{-47} s^7 / (.1196040724\ 10^{-25} s^6 + .1419599207\ 10^{-13} s^5 + .2588869839\ 10^{-9} s^2 + .4030752922\ 10^{-38} s^7 + .6791979902\ 10^{-51} s^8 + .1347984798\ 10^{-8} s + .1928487470\ 10^{-77} s^{10} + .5722378906\ 10^{-64} s^9 + .2195265755\ 10^{-8} + .2234109438\ 10^{-10} s^3 + .9077769649\ 10^{-12} s^4) + .6327712593\ 10^{-35} s^6 / (.1196040724\ 10^{-25} s^6 + .1419599207\ 10^{-13} s^5 + .2588869839\ 10^{-9} s^2 + .4030752922\ 10^{-38} s^7 + .6791979902\ 10^{-51} s^8 + .1347984798\ 10^{-8} s + .1928487470\ 10^{-77} s^{10} + .5722378906\ 10^{-64} s^9 + .2195265755\ 10^{-8} + .2234109438\ 10^{-10} s^3 + .9077769649\ 10^{-12} s^4) + .3027452857\ 10^{-74} s^9 / (.1196040724\ 10^{-25} s^6 + .1419599207\ 10^{-13} s^5 + .2588869839\ 10^{-9} s^2 + .4030752922\ 10^{-38} s^7 + .6791979902\ 10^{-51} s^8 + .1347984798\ 10^{-8} s + .1928487470\ 10^{-77} s^{10} + .5722378906\ 10^{-64} s^9 + .2195265755\ 10^{-8} + .2234109438\ 10^{-10} s^3 + .9077769649\ 10^{-12} s^4) +$$

$$.8983326383\ 10^{-61} s^8 \,/\, (.1196040724\ 10^{-25} s^6 + .1419599207\ 10^{-13} s^5 + .2588869839\ 10^{-9} s^2 + .4030752922\ 10^{-38} s^7 + .6791979902\ 10^{-51} s^8 + .1347984798\ 10^{-8} s + .1928487470\ 10^{-77} s^{10} + .5722378906\ 10^{-64} s^9 + .2195265755\ 10^{-8} + .2234109438\ 10^{-10} s^3 + .9077769649\ 10^{-12} s^4) + .2256017150\ 10^{-6} \,/\, (.1196040724\ 10^{-25} s^6 + .1419599207\ 10^{-13} s^5 + .2588869839\ 10^{-9} s^2 + .4030752922\ 10^{-38} s^7 + .6791979902\ 10^{-51} s^8 + .1347984798\ 10^{-8} s + .1928487470\ 10^{-77} s^{10} + .5722378906\ 10^{-64} s^9 + .2195265755\ 10^{-8} + .2234109438\ 10^{-10} s^3 + .9077769649\ 10^{-12} s^4)]$$

- ZZ51:=[Zinv[5,1]];

$$ZZ51 := [.2598919616\ 10^{-24} (.1685040000\ 10^{-12} s + 1.) \,/\, (.1196040724\ 10^{-25} s^6 + .1419599207\ 10^{-13} s^5 + .2588869839\ 10^{-9} s^2 + .4030752922\ 10^{-38} s^7 + .6791979902\ 10^{-51} s^8 + .1347984798\ 10^{-8} s + .1928487470\ 10^{-77} s^{10} + .5722378906\ 10^{-64} s^9 + .2195265755\ 10^{-8} + .2234109438\ 10^{-10} s^3 + .9077769649\ 10^{-12} s^4)]$$

- ZZ51:=[.4379283510e-37*s/(.1196040724e-25*s^6+.1419599207e-13*s^5+.2588869839e-9*s^2+.4030752922e-38*s^7+.6791979902e-51*s^8+.1347984798e-8*s+.1928487470e-77*s^10+.5722378906e-64*s^9+.2195265755e-8+.2234109438e-10*s^3+.9077769649e-12*s^4)+.2598919616e-24/(.1196040724e-25*s^6+.1419599207e-13*s^5+.2588869839e-9*s^2+.4030752922e-38*s^7+.6791979902e-51*s^8+.1347984798e-8*s+.1928487470e-77*s^10+.5722378906e-64*s^9+.2195265755e-8+.2234109438e-10*s^3+.9077769649e-12*s^4)];

$$ZZ51 := [.4379283510\ 10^{-37} s/(.1196040724\ 10^{-25} s^6 + .1419599207\ 10^{-13} s^5 + .2588869839\ 10^{-9} s^2 + .4030752922\ 10^{-38} s^7 + .6791979902\ 10^{-51} s^8 + .1347984798\ 10^{-8} s + .1928487470\ 10^{-77} s^{10} + .5722378906\ 10^{-64} s^9 + .2195265755\ 10^{-8} + .2234109438\ 10^{-10} s^3 + .9077769649\ 10^{-12} s^4) + .2598919616\ 10^{-24} \,/\, (.1196040724\ 10^{-25} s^6 + .1419599207\ 10^{-13} s^5 + .2588869839\ 10^{-9} s^2 + .4030752922\ 10^{-38} s^7 + .6791979902\ 10^{-51} s^8 + .1347984798\ 10^{-8} s + .1928487470\ 10^{-77} s^{10} + .5722378906\ 10^{-64} s^9 + .2195265755\ 10^{-8} + .2234109438\ 10^{-10} s^3 + .9077769649\ 10^{-12} s^4)]$$

Appendix-A7:

Simulation Model's Derivation in the form of Transfer Function

$$\Delta(s) = \zeta w(L_L s + R_L) + \zeta^2 \tag{1}$$

$$I_s(s) = \frac{\zeta w(s) + (L_L s + R_L)}{\Delta(s)} V_s(s) = \frac{\zeta w(s) + (L_L s + R_L)}{\zeta w(L_L s + R_L) + \zeta^2} V_s(s) \tag{2}$$

$$\frac{\zeta w + (L_L s + R_L)}{\zeta w(L_L s + R_L) + \zeta^2} = \frac{\zeta w + (L_L s + R_L)}{\zeta^2(\zeta^{-1} w(L_L s + R_L) + 1)} == \frac{\zeta^{-1} w + \zeta^{-2}(L_L s + R_L)}{1 + \zeta^{-1} w(L_L s + R_L)} \tag{3}$$

$$= \frac{\zeta^{-1} w + \zeta^{-2}(L_L s + R_L)}{\zeta^{-1} w(L_L s + R_L)\left[\frac{\zeta w^{-1}}{(L_L s + R_L)} + 1\right]} = \frac{\frac{1}{(L_L s + R_L)} + \zeta^{-1} w^{-1}}{1 + \left[\frac{\zeta w^{-1}}{(L_L s + R_L)}\right]} \tag{4}$$

$$I_s(s) = \frac{\frac{1}{(L_L s + R_L)} + \zeta^{-1} w^{-1}}{1 + \left[\frac{\zeta w^{-1}}{(L_L s + R_L)}\right]} V_s(s) \tag{5}$$

$$I_L(s) = \frac{\zeta(w^2(s) - 1)^{\frac{1}{2}}}{\Delta(s)} V_s(s) = \frac{\zeta(w^2(s) - 1)^{\frac{1}{2}}}{\zeta w(L_L s + R_L) + \zeta^2} V_s(s) \tag{6}$$

$$I_L(s) = \frac{\frac{1}{(L_L s + R_L)} + \zeta^{-1} w^{-1}}{1 + \left[\frac{\zeta w^{-1}}{(L_L s + R_L)}\right]} V_s(s) \times \frac{\zeta(w(s) - 1)^{\frac{1}{2}}}{1 + \frac{\zeta w(s)}{L_L s + R_L}} \tag{7}$$

$$I_L(s) = I_s(s) \times \frac{\zeta(w(s) - 1)^{\frac{1}{2}}}{1 + \frac{\zeta w(s)}{L_L s + R_L}} \tag{8}$$

Appendix-A8:

Project's Pictures

Picture -1: 400kV Cables – Transmission Lines
(DEWA/Nexan, 2011)

Picture -2: Tunnel
(DEWA/Nexan, 2011)

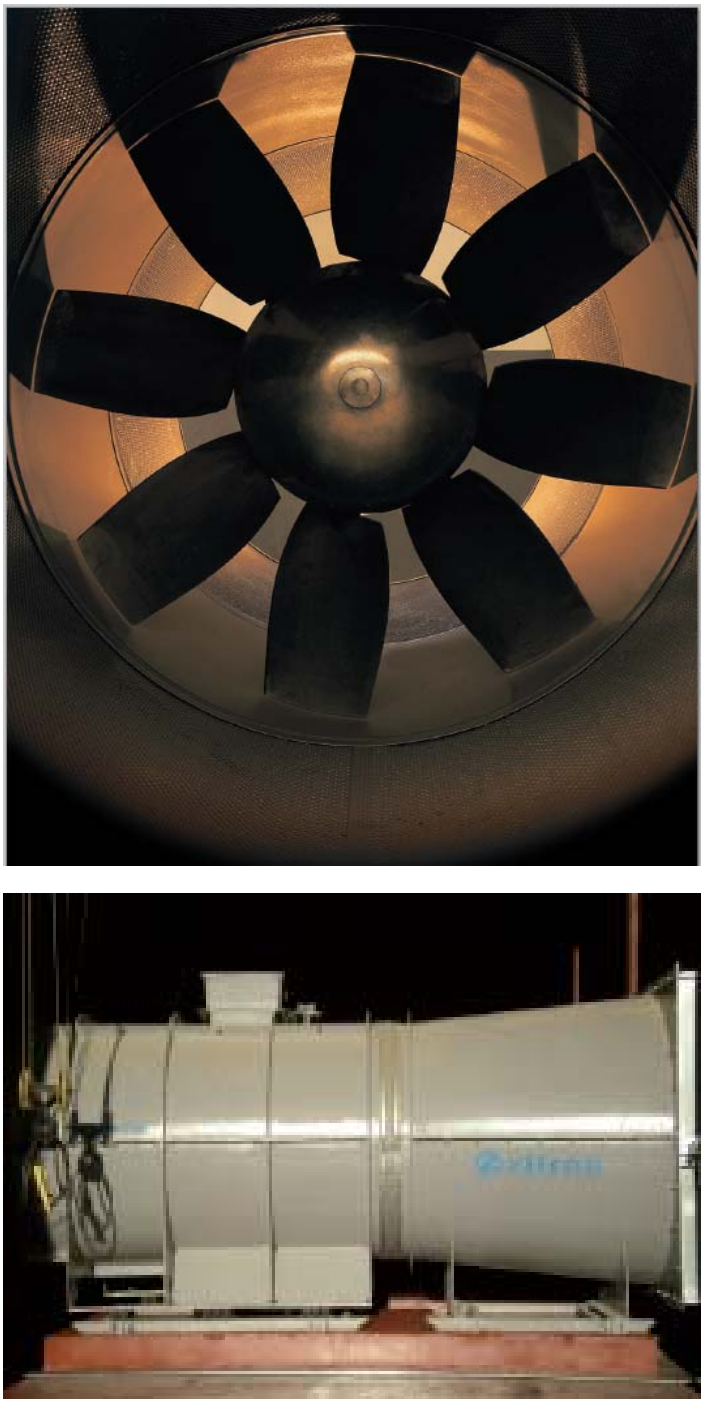

Picture -3: Fan
(DEWA/Zitron, 2012)